DEVELOPMENT OF ORCHESTRATED STEM CELL-BASED REGENERATION (OSCeR) -STRATEGIES TO RECRUIT AND DIFFERENTIATE AUTOLOGOUS STEM CELLS FOR TISSUE REGENERATION

by

ASHWIN NAIR

Presented to the Faculty of the Graduate School of
The University of Texas at Arlington in Partial Fulfillment
of the Requirements
for the Degree of

DOCTOR OF PHILOSOPHY

THE UNIVERSITY OF TEXAS AT ARLINGTON
December 2010

ACKNOWLEDGEMENTS

I have been influenced by so many people throughout my student life at UTA, that I hope I do some justice to the love, faith and respect that they have bestowed upon me. I don't need to think twice before thanking my mentor Dr. Liping Tang, for not just being a mentor but also a friend and a guide. I am truly thankful for having been provided the opportunity to work under his tutelage. I have seen my share of ups and downs and despite all that I am confident I could not have been at a better place and worked with a better scientist and more importantly a better human being than you. So, thank you sir!

I have had the opportunity to interact with my committee members on numerous occasions and would like to thank each one of them. Dr. Jian Yang has influenced my development as a researcher and was always available for any scientific discussion. I look forward to working closely with him in future as well. It is my privilege to have interacted with Dr. Chi-Chun Tsai, both as a student and as a researcher in Dr. Tang's lab. I often cite his example for his sincerity and dedication to one's profession and above all for his humility. I would like to thank Dr. Cheng Cheng (Alec) Zhang for his recommendations on my proposal and assistance with the flow cytometric analysis that helped not just me but paved the way for more work that can be done in this promising field. Dr. Ramesh Saxena's practical and insightful comments and recommendations went a long way in making this work more robust and I would like to whole-heartedly acknowledge him along with all my committee members here as well.

My co-workers, my friends you have been a constant source of inspiration and support for me. I can't thank Dr. Jinhui Shen enough for his patience when it came to teaching me the nuances of surgical techniques. I would also like to thank him for helping me at various stages of the *in vivo* experiments and flow cytometric analysis. A lot of work done in this study would not be completed on time if it had not been for the contributions made by Parisa Lotfi. Thank you Parisa

for being a great co-worker, but more importantly for becoming one of my best friends, who would quietly listen to my random ramblings when I was frustrated with something. Thank you Paul, for I have had a great time working with you and learnt a lot from you as well. I would also like to acknowledge Drs. Zou Ling and Hong Weng for their help with histology and Yi-Ting Tsai for assistance with *in vivo* imaging. I would also like to thank David, Shiuli, Cheng-Yu and Man-Wu for always being there whenever I needed any kind of support. I acknowledge Richard Tran for his efforts in the fabrication of the vascular graft. Another person that I would like to thank is Jagannath. An intelligent and hard working man, I have learnt a lot from him and I miss those long discussions we would have. There are so many people in the department and outside that I would like to thank, that in case I leave out a few names, it is just because I am getting old. Thank you Deepti, Srikanth, Vikrant, Nidhi, Sohaeb, Surendhar, Sihi, Hari, Swaroopa, Vijay, Dr. Wu. You have been my support system here and I can't thank you enough.

I could not have done anything in life if it were not for my family. I owe everything to my parents Mr. Mohan Nair and Mrs. Kamala Nair. I don't have words to thank them; the amount of gratitude, love and respect that I have for them is something I cannot express in words. Thank you to my sisters Kalpana, Kavita, my brothers-in law Raaj and Manoj and my dearest nephew Advaith. Another person, who cannot be left out under any circumstance is my fiancée Sapna. She has borne the brunt of my fluctuating mood especially during the final stages of my research. I have a lot to learn from her, especially when it comes to anger management.

I have always believed that god guides you and shows you the right path and I can't be thankful to anybody more than the almighty for having appeared before me as my parents, siblings, adviser and friends.

October 29, 2010

ABSTRACT

DEVELOPMENT OF ORCHESTRATED STEM CELL-BASED
REGENERATION (OSCeR) -STRATEGIES TO RECRUIT
AND DIFFERENTIATE AUTOLOGOUS STEM CELLS
FOR TISSUE REGENERATION

Ashwin Nair, PhD

The University of Texas at Arlington, 2010

Supervising Professor: Liping Tang

Stem cell therapy has shown great promise in curing diseases. However, clinical application of stem cell therapy is often hindered by the lack of reliable sources and convenient methods to recover stem cells. Our laboratory has recently discovered that adult stem cells can be actively recruited *via* inflammatory chemokines/growth factor. My research was aimed towards the development of a new technology - "*Orchestrated Stem Cell-based Regeneration*" or *OSCeR* - to induce stem cell-mediated tissue regeneration by blending stem cell therapy and tissue engineering technology. This work has led to a series of interesting findings as listed below.

Shortly after implantation, biomaterial implants are often accompanied by large numbers of mesenchymal stem cells (MSC) and hematopoietic stem cells (HSC) around the implantation sites. These spontaneously recruited multipotent stem cells could be differentiated into various lineages *in vitro*. Subsequent studies confirmed that there is a good relationship between the extent of inflammatory responses and stem cell recruitment. Very interestingly, by supplementing an osteogenic factor [bone morphogenetic protein-2 (BMP-2)] in scaffolds, the recruited

multipotent stem cells turned into an osteogenic type and formed mineralized tissue in the subcutaneous soft tissue space. To apply *OSCeR* for regenerating different tissue, one of the main challenges was to establish scaffold a fabrication technique that could incorporate a variety of cytokines and growth factors. This was imperative since almost all tissue engineering scaffolds are unable to load and release proteins in an active form. Based on our preliminary work, we established a microbubble scaffold fabrication technique which can easily load and release bioactive proteins over a period of time. The scaffolds were characterized in an *in vitro* and *in vivo* setting.

With the microbubble scaffold technique, we investigated the feasibility of applying *OSCeR* technology for bone and vascular graft regeneration. For bone application, a combination of BMP and erythropoietin prompted maximal cell infiltration and showed signs of bone formation. To regenerate vascular grafts, we used an intra-peritoneal implantation model to study the vascular tissue formation, especially endothelialization, of the inner lumen of biphasic vascular grafts – crosslinked urethane doped polyester (CUPE). Within a week of SDVG implantation, the lumen was quickly covered with endothelial progenitor cells and by week 2 there were signs of endothelial cells lining the lumen.

Through these studies we were able to develop a novel *OSCeR technology which* turns the normally unwanted foreign body reactions into an appreciable phenomenon of *in vivo* tissue regeneration. The results from this work prove that, by blending stem cell therapy and tissue engineering, *OSCeR* technology may have a bright future in regenerative medicine.

TABLE OF CONTENTS

LIST OF ILLUSTRATIONS

LIST OF TABLES

CHAPTER 1

INTRODUCTION

1.1 Tissue Engineering

The dream of regenerating tissues and organs has always existed, but it has shown signs of being a reality only over the past two decades or so. To some extent this dream has been partially realized by the use of a combination of cells, engineering principles and materials, along with various bio- and physico-chemical factors that improve or replace biological functions. This field we now call tissue engineering is defined as “an interdisciplinary field that applies the principles of engineering and life sciences to develop biological substitutes that restore, maintain, or improve the tissue function.”[3] However, radical steps have to be taken to make tissue engineering strategies effective as it can potentially impact a broad spectrum of healthcare related issues.

While the definition of tissue engineering does cover a broad range of applications, in practice it mainly deals with repair or replacement of portions of or whole tissues like bone, cartilage, blood vessels etc. When stem cells are used to produce tissues it is termed regenerative tissue engineering which forms the crux of this dissertation. Regenerative tissue engineering, as it stands today is symbolic of the exemplar progress made in tissue reconstruction and repair since the late 1980s and early 1990s. Tissue loss due to disease, trauma or even tumor removal necessitates its replacement and thereby lays a pressing emphasis on therapeutic strategies like regenerative tissue engineering.

The key components of a tissue engineered product are scaffolds, cells, signals and *in vitro* bioreactors. Scaffolds could be decellularized extra cellular matrix or a synthetic polymer which is usually cast onto a 3-D structure to resemble the actual tissue that is being engineered. Cells, ideally differentiated, are seeded on to the scaffolds. They adhere to the scaffold and

proliferate upon the right conditions. The right conditions are provided by the signaling molecules in the form of growth factors, proteins and/or mechanical/electrical signals etc., The *in vitro* bioreactor provides the right environment that proves conducive to the growth of cells in to the scaffolds and development of tissues. Regardless of the approach, scaffolds and cells have become the mainstays of regenerative tissue engineering. The underlying principle is the combination of a scaffold with cells under proper conditions for tissue repair.[4] Its fundamental aim to create a natural tissue that can restore organ or tissue function in organisms that have lost the ability to regenerate under normal conditions.

1.2 Barriers Facing Regenerative Tissue Engineering

For the past 30 years, substantial research efforts in tissue engineering have been placed on creating safer and better scaffolds. Tissue engineering scaffolds serve not only as a template for growing tissue but also as a system for delivering cytokines and growth factors. Degradable polymeric materials, such as poly (L-lactic acid) (PLLA) and poly (l-lactic-co-glycolic acid) (PLGA), are commonly used and have been extensively researched.[5, 6]

Polymeric tissue engineering scaffolds prepared by conventional techniques like salt leaching and phase separation are greatly limited by their poor biomolecule-delivery abilities and also small pore sizes as seen in conventional phase separation technique. Majority of these researches have uncovered that physical and chemical properties of scaffolds such as pore size, porosity, chemical and mechanical properties determine not only the behavior of cells seeded on it but also the response elicited from the body's immune system.[2]

Despite considerable efforts there are very limited clinical applications mainly due to uncontrollable tissue reactions to implants and also due to their poor cellularization and vascularization. In addition, the requirement of cell culture and preseeding in scaffold *in vitro* associated with conventional tissue engineering are very tedious.[7] To make the situation worse, a study showed that a large number of cells died after implantation for only 2 weeks.[8]

The residual cells may also undergo transformation by localized inflammatory responses which diminish or alter the specific cell activities required to generate functional tissues.[9]

To improve cell seeding and growth, substantial progress has been made in recent years by either coating the scaffold with different adhesive proteins like laminin, fibronectin, fibrin, collagen and vitronectin,[2, 10] or soaking the scaffold with various growth factors like insulin-like growth factor, transforming growth factor-β, platelet derived growth factor, fibroblast growth factor *via* spontaneous adsorption or covalent linking.[2, 10-12] These additional treatments improved cell growth, although such enhancements were often limited and short-lived. Despite impressive progress in growth factor loaded nanoparticle technology, the denaturation of the loaded agent by solvents and other fabrication conditions limits their use.[2] It is also possible that common growth factor: scaffold conjugation processes may alter the morphological and physical strength of the scaffold. Studies have also shown that scaffolds soaked in growth factors have a characteristic high burst release in the first 1-2 days. This occurs since most of the growth factor is bound to the surface, instead of being embedded inside the scaffold.[13] Hence a porous scaffold fabrication technique that can preserve the bioactivity of the loaded cytokine or growth factor and release them over a period of time is highly desirable.

Tissue engineering technology has achieved reasonable success in regenerating bone and skin tissues. However, the same technique has encountered with many difficulties in reproducing other types of tissues, like articular cartilage and cardiovascular tissues.[14] One of the main challenges is that cells including stem cells have to be extracted from various sources,[15-17] and then expanded *in vitro*. This cell culture and then seeding process is time consuming and could be harmful to many types of cells, including stem cells.[7] In addition, the transplantation of non-autologous cells has the risk of exerting immune reactions.[18, 19] Since the use of allogenic stem cells is associated with immune-rejection, autologous stem cells are highly desirable. This in turn poses the expensive and time-consuming dilemma of stem cell

extraction, isolation and expansion from the bone marrow or fat tissue of a donor. Since the solution to the challenge faced with stem cells brings one back to an earlier obstacle – laden cell source, a new strategy is mandated.

1.3 Role of Stem Cells in Regenerative Medicine

Stem cells are cells with the ability to divide for indefinite periods in culture and to give rise to specialized cells and have gained popularity in regenerative medicine.[20-22] Their unique pluripotency and regenerative properties has thrust stem cells into the forefront of regenerative orthopedic, chondrogenic and myogenic tissue engineering strategies.[23-25] There are numerous sources and based on it various types of stem cells.

- **Embryonic Stem Cells (ESC):** First identified as totipotent cells in embryos, they can give rise to all tissues in the human body. Embryonic stem (ES) cells have been used in the production of knockout mice, and can potentially be used to create genetically modified living beings.
- **Induced Pluripotent Stem Cells (iPSC):** In a major development, in the year 2006, Takahashi and Yamanaka reprogrammed mouse fibroblasts to a pluripotent state by viral transfection of various markers that maintain pluripotency.[26] Since then, iPSC lines have been generated from human,[27, 28] monkey,[29] porcine,[30] and rodent,[31, 32] somatic sources.
- **Adult Stem Cells:** Adult stem cells have various sources, like adipose, bone marrow, peritonea, umbilical vein etc., Since tissue damage is believed to be responsible for the homing of stem cells and differentiation into specific tissue types, studies have been conducted to identify these sources. Various sites in adult animals have been shown to be reservoirs of adult stem cells.[33] Stem cells derived from the human umbilical cord blood repopulate the bone marrow in children and adults with various diseases.[34-36] The bone marrow for one holds a heterogenous population of cells which have varied developmental capabilities.[37] It is known that bone marrow derived mesenchymal

stem cells can differentiate into multiple cells and tissues like epithelial cells of liver, lung, gastrointestinal tract and skin.[38] In addition to hematopoietic stem cells (HSC) in the bone marrow which is the most extensively studied adult stem cell, mesenchymal stem cells (MSC), which reside in tissues, have the ability to differentiate into both hematopoietic lineages like adipocytes,[39] osteoblasts,[40] and endothelial cells as well as into non-hematopoietic lineages like cardiac and skeletal muscle, chondrocytes,[41] neurons,[42] myocytes and hepatocytes.[43] While bone marrow stem cells do migrate to injured sites, there are stem cells which reside permanently in many organs and are known as "tissue stem cells."[44, 45] They can regenerate the organ that they reside in but when put elsewhere can differentiate into various lineages. Examples of tissue stem cells are the cells residing in the hair follicles, isthmus of the gastrointestinal tract and the corneal limbus.[44]

Numerous approaches have been be used to combine stem cells and tissue engineering. Stem cells harvested *ex vivo* can be locally implanted at the diseased site or genetically engineered cells can be injected systemically for a global effect. Stem cells are injected directly at the site and allowed to grow into the desired tissue. Many a times, genetically manipulated cells are also injected to bring about a specific outcome. In fact, clinical trials have been conducted for the MSC administration in the treatment of diseases like osteogenesis imperfecta,[46, 47] and also to enhance bone marrow transplant engraftment.[48] Guided tissue regeneration can be achieved using 3D porous scaffolds. Such scaffolds serve as templates for the surrounding cells to infiltrate into the scaffold and grow into a desired tissue. Quite often, surface modification of these implants can yield better control on the cellular response.[1, 49]

1.4 Deterrents to Stem Cells in Tissue Engineering

Although a lot of effort has been placed on combining stem cells and tissue engineering, it is not without its share of problems. ESCs have been mired in controversies and its application curtailed by ethical considerations. In addition, they have safety issues and can

potentially lead to neoplasia.[44] Although there are comparisons with ESCs, a lot of questions still remain unanswered. For example, do subsequent cell divisions alter the cell's ability to change fate? How safe are such reprogrammed cells? How can we control the fate of such cells *in vivo*? In addition the long-term safety of this cell type is not clear at this point. Considering the deterrents to the application of ESCs and iPSCs, the capabilities of adult stem cells to remodel tissues and organs has been explored. Although safer than ESCs, they have lower differentiation capacity. Also, their extraction procedures from bone marrow are very painful. Subcutaneous adipose tissue has also been shown to be an abundant source of adult stem cells, although such cells can not be obtained from all patients. In addition, the procedures involved to recover adipose stem cells are still traumatic and painful.[50] Finally, the tedious extraction procedures followed by their prolonged in *vitro* culture time makes their application a very cumbersome process. In addition to the problems encountered in the use of stem cells, getting the cells to infiltrate the scaffold matrix is a totally different story. Plausibly, because cells interact with the surface, getting the cells inside the scaffolds requires a favorable cue from within the scaffold.

1.5 Development of Orchestrated Stem Cell-based Regeneration (OSCeR)

My early work focused on devising strategies to modulate the inflammatory responses elicited by biomaterial implants. The influence of implant surfaces modified with chemical functional groups like –OH, -COOH, -CH2 on inflammatory response was studied.[1] Although surface functionality can redirect the cellular responses, it is still not sufficient to boost tissue regeneration. Since we were aware that wound healing responses occur daily in the body, we thought that it would be advantageous to induce or to replicate the regenerative process *in viv*o. To explore this possibility, we hypothesize that tissue scaffolds can be modified to trigger the recruitment and differentiation of autologous stem cells. We term this strategy "Orchestrated Stem Cell-based Regeneration (OSCeR)." To achieve this, firstly we identify, characterize and try to develop a better understanding of the cell recruitment pattern and behavior around an

implant. We then develop a novel OSCeR scaffold that will preserve and deliver bioactive cytokines over time. Subsequently, these scaffolds are applied to clinically relevant challenges like vascular graft production and bone tissue engineering. The aims are summarized as follows.

Specific Aim 1 Spontaneous recruitment and differentiation of stem cells surrounding biomaterial implants

Stem cells are immensely popular in regenerative tissue engineering, but a major challenge is its source.[20-25] Challenged by the ethical considerations associated with ESCs, the yet to be realized potential of iPSCs and the cumbersome procedures associated with adult stem cell extraction, isolation, expansion and differentiation strategies, alternate approaches are mandated. Autologous stem cells are well established to be the best cells for stem cell therapy, although large number of autologous stem cells is hard to obtain. Our preliminary studies showed that while a large number of inflammatory cells are recruited in and around a biomaterial implant, a large number of cells that were uncharacterized were also recruited. Is there a pattern behind their recruitment? Are these multipotent stem cells? Do they respond to certain signals, like those from inflammatory cells? If they are indeed stem cells, can we engineer their behavior and take advantage of their plasticity? *The data in this aim is part of a manuscript titled "Induced Localized Recruitment and Differentiation of Autologous Stem Cells in Mice" which is currently submitted to the journal Stem Cells.*

Specific Aim 2 Develop Novel OSCeR Scaffolds for Directing Stem Cell Homing

The second aim details an approach for fabricating and testing a novel system that can preserve the bioactivity and deliver cytokines and growth factors. Polymeric tissue engineering scaffolds prepared by conventional techniques like salt leaching and phase separation are greatly limited by their poor biomolecule-delivery abilities. Conventional methods of

incorporation of various growth factors, proteins and/or peptides on or in scaffold materials via different cross linking and conjugation techniques are often tedious and may affect scaffold physical, chemical, and mechanical properties. To overcome such deficiencies, a novel two-step porous scaffold fabrication procedure has been created in which protein [bovine serum albumin (BSA) and gelatin] microbubbles were used as porogen and growth factor carriers. Such scaffolds will be characterized and tested for their ability to serve as cytokine delivery systems and suitability for *in vivo* studies. A major part of the data has been published in a manuscript *"Novel Polymeric Scaffolds Using Protein Microbubbles as Porogen and Growth Factor Carriers" published in Tissue Engineering Part C vol.16; issue 1; pages 23-32.*

Specific Aim 3 Direct the Differentiation of Recruited Stem Cells for Specialized Tissue Regeneration

In clinical practice, the treatment of posttraumatic skeletal conditions such as delayed unions, non-union, malunion, and other problems of bone loss are challenging. In many cases, adjunctive measures such as bone-grafting or bone transport are required to stimulate bone-healing and fill bone defects. Based on aims 1 and 2, in the final aim we try to apply the novel OSCeR scaffolds in bone tissue engineering using a cranial defect model. Stem cells are recruited to the scaffold that bridges the cranial defect and the healing and osteogenic activity at the site is evaluated.

In addition, we also try to lay the groundwork for a new strategy to produce synthetic small diameter vascular grafts (SDVGs). Although synthetic grafts like Dacron or ePTFE met with a fair amount of success as large blood vessel grafts, they failed as small blood vessels. This was because of their inadequate blood compatibility and inability to prevent coagulation of blood along with thrombosis in low shear environment which is encountered in small blood vessels.[51] Although PLLA and PLGA are commonly used for various tissue engineering applications, they do not have the same mechanical properties as actual blood vessels.

Recently, a new elastomeric material cross linked urethane-doped polyester (CUPE) which matches a biological blood vessel in mechanical properties has been developed.[52] In addition, they have very good biocompatibility and hemocompatibility which makes them attractive for *in vivo* vascular graft engineering. To meet the challenge of thrombosis, increasing evidence suggests that endothelialization of the vascular graft lumen may prevent coagulation and thrombosis.[51, 53, 54] We evaluate the potential of using erythropoietin (Epo) – a potent pro-angiogenic growth factor – along with small diameter vascular grafts made out of a new elastomeric material, cross linked urethane-doped polyester (CUPE), which matches a biological blood vessel in physical and mechanical properties.

CHAPTER 2

BIOMATERIAL IMPLANT AND AUTOLOGOUS STEM CELL INTERACTIONS

2.1 Introduction

Although considered inert, biomaterial implantation is typically associated with inflammatory responses and also fibrosis. The spontaneous adsorption and denaturation of fibrinogen on implant surfaces was found to be a major factor.[55] Many methods have been developed to alter fibrotic reactions. For example, dexamethasone releasing rods have been developed to reduce fibrotic reactions in implant surrounding tissue.[56] Some studies have proposed coating implantable medical devices with anti inflammatory drug releasing systems.[57, 58]

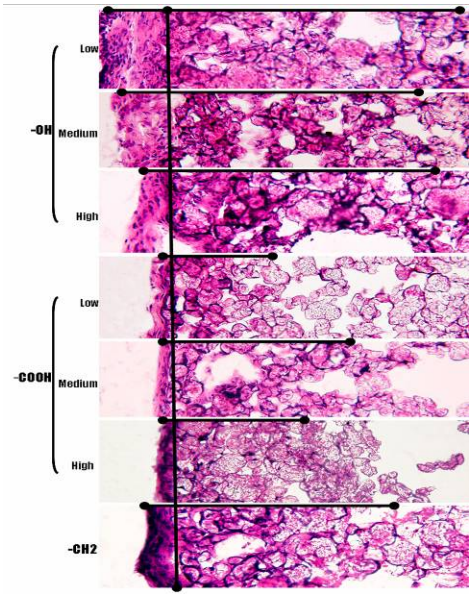

Figure 2.1 Implant-induced tissue responses were assessed based on capsule thickness and cellular infiltration. Polypropylene microspheres with –OH and –COOH functionalities at low, medium and high densities and control microspheres with $–CH_2$ functionality were subcutaneously injected in to Balb/C mice. H&E stain of subcutaneous tissue 2 weeks post implantation shows the tissue reaction to different surface functionalities. Left pointed indicators (●——) show the trend followed by capsule thickness while right pointed indicators (——●) depict the extent of cell infiltration in to the implant across functional groups (Magnification 20x). (From Nair, et al., [1])

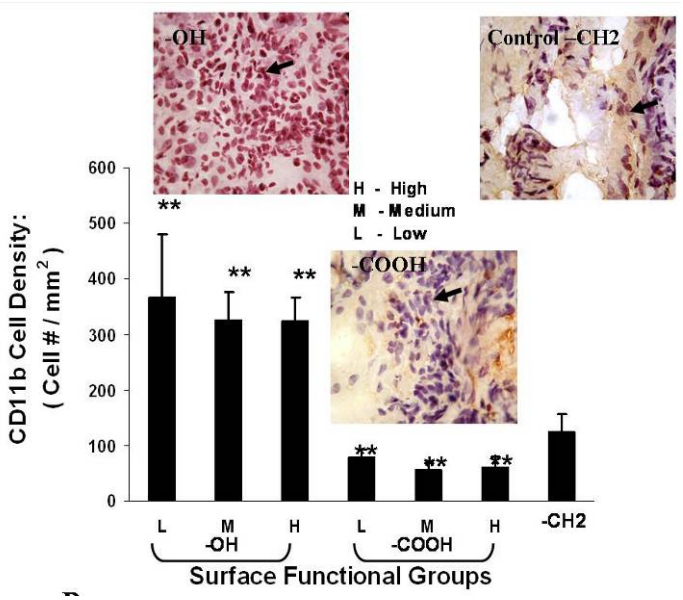

Figure 2.2 IHC analyses of recruitment of CD11b+ inflammatory cells. Functional groups influenced this recruitment but varying the density had no significant effect. (From Nair, et al., [1])

We had conducted studies that aimed to alter the biomaterial-mediated fibrotic reactions. Specifically, one such study involved functionalizing implant surfaces with various chemical groups.[1] It was found that while various chemical groups on the implant surface did affect fibrotic reactions, the functionalization density had no bearing on the reactions as shown in figures 2.1 and 2.2. Thus, there is a link between inflammatory and fibrotic responses.

2.2 Hypotheses

Hypothesis 1: Biomaterial implant-mediated tissue responses prompt the recruitment of autologous stem/progenitor cells.

Hypothesis 2: Autologous stem/progenitor cells recruited around an implanted biomaterial are multipotent.

2.3 Materials and Methods

2.3.1 Identification of Stem and Progenitor Cells In Ascites

In the search for a better source of autologous stem cells, our preliminary studies have suggested that a detectable population of non-inflammatory cells exist at the site of biomaterial implantation. To characterize these cells completely, drawing from earlier studies employing wound chambers, we fabricated modified wound chambers made out of poly (l-lactic acid) (PLLA). We collected the cells that accumulated in the ascites and characterized them using flow cytometry and *in vitro* differentiation studies.

2.3.2 Modified Wound Chamber

High-molecular weight poly (L-lactic acid) (PLLA, 137 kDa), was obtained from Birmingham Polymers (Birmingham, AL, USA) and 1,4-dioxane was purchased from Aldrich (Milwaukee, WI). To mimic biomaterial-mediated cellular responses, PLLA tubes (inner diameter of 2 mm) were produced for this investigation. Briefly, Teflon rods (2mm diameter) were dip coated with PLLA (10 % w/v) in 1, 4-dioxane and frozen. Such tubes were then lyophilized for three days to extract the solvent, yielding PLLA tubes. Such tubes (length 1.5 cm) were punched with holes using an 18 gauge needle and sterilized in 70% ethanol and exposed to UV light.

2.3.3 In Vivo Implantation of Wound Chamber

For wound chamber studies, two PLLA tubes (1.5 cm long, 3 mm inner diameter) per animal, were implanted in the dorsal subcutaneous space of Balb/c mice. Three days post-implantation, wound fluid was aspirated using a 3 cc syringe with an 18 gauge needle. Cells were counted and aliquoted into two groups: for *in vitro* differentiation studies and for FACSArray analysis.

2.3.4 FACSArray Analysis of Cells In Wound Chamber Ascites

The phenotypic determination of cell types was carried out using flow cytometric method. Briefly, cells were fixed in cold ethanol and resuspended in PBS containing 1% FBS.

Cell aliquots (5 x 10^5 cells / 200 µl) were incubated with mAbs against the following: (1) MSC: SSEA4+/CD45-; CD73+/CD105+/CD90+/CD45-; (2) HSC: Lin-/Sca-1+/ckit+; (3) Inflammatory cells: CD11b+ and CD45+. Flow cytometry was performed using a FACS Array and FACSCalibur (BD Biosciences, CA, USA) and data was analyzed using BD CellQuest (BD Biosciences, CA, USA).

2.3.5 In Vitro Differentiation of Cells From Wound Chamber Ascites

Cells aspirated from the PLLA tubes were centrifuged and resuspended in DMEM with 20% fetal bovine serum (FBS) and 1% antibiotics (100 U penicillin and 100 µg streptomycin) at 37^{o}C with 5% CO_2. Non-adherent cells were removed and the attached cells provided with more media. Cells maintained in DMEM with 20% FBS and antibiotics served as control. When the cells reached almost 50% confluence, differentiation agents were added and cells analyzed as follows. To test the osteogenic potential, cells were incubated with DMEM + 10% FBS and 100 nM dexamethasone, 10 mM β-glycerolphosphate and 0.05 mM 2-phosphate-ascorbic acid. Cell differentiation into an osteogenic lineage was determined using Alizarin Red staining for calcified deposits.[59] To test the chrondrogenic potential, chondrogenic differentiation condition consisted of DMEM supplemented with 10% FBS, 1% antibiotics, 10 ng/ml transforming growth factor-β, 100 ng/ml Insulin-like growth factor-1 (IGF-1) and 10 nM dexamethasone. Alcian blue staining for sulfated glycosaminoglycans was performed to determine chondrogenic differentiation.[59] To test the adipogenic potential, cells were incubated with DMEM supplemented with 10% FBS and 1% antibiotics supplemented with 0.5 mM isobutylmethylxanthine, 100 nM IGF-1, 1 µM dexamethasone and 200 µM Indomethacin for 3 weeks. Media was fully changed every 3 days and cells evaluated after 3 weeks in culture. Oil Red staining which stained lipid filled vacuoles in the adipogenic differentiated cells was performed.[59] Cells maintained in DMEM with 10% FBS and antibiotics served as control.

2.3.6 Microsphere Synthesis

Various forms of biomaterials were used in this investigation. Specifically, N-isopropyl acrylamide (NIPAm) microspheres with an average size of 1 µm were synthesized using a free radical precipitation polymerization method as described earlier,[60] and HPC microspheres with an average size of 6 µm were synthesized using modified precipitation polymerization techniques described earlier.[61, 62] PLLA microspheres were synthesized according to a modified precipitation method with an average size of 15 µm.[63] Polypropylene microspheres, of uniform 35 micron diameter, were obtained from Polysciences, Inc (Warrington, Pa).

2.3.7 Evaluation of Stem Cell Recruitment In Response To Various Microsphere Implants

To determine the relationship between foreign body reactions and stem cell recruitment, microspheres made of HPC, NIPAm, PLLA and PP were used in the study. For that, 1.0 ml of microspheres (2 mg/ml) was implanted subcutaneously *via* 27 gauge needle in the Balb/C mice (male, 20 g body weight).[1, 49] After implantation for 7 days sufficient time for both inflammatory cells and stem cell responses), the animals were sacrificed and implant and surrounding tissue were isolated for histological analyses.

2.3.8 Study The Recruitment Kinetics of Inflammatory Cells and Stem Cells

To determine the cell recruitment pattern, HPC microspheres were used in the study. For that, 1.0 ml of microspheres (2 mg/ml) was implanted subcutaneously *via* 27 gauge needle in the Balb/C mice (male, 20 g body weight). After implantation for different periods of time (1, 2, 4, 7 and 14 days), the animals were sacrificed and implant and surrounding tissue were isolated for histological analyses.

2.3.9 Effect of Anti-inflammatory Drug Dexamethasone on Stem Cell Recruitment

The influence of implant-associated inflammatory responses on stem cell recruitment was assessed using anti-inflammatory agent, dexamethasone. Briefly, HPC microspheres were immersed in dexamethasone (1 mg/ ml) or saline (as control) and then implanted

subcutaneously in mice for 1 week. At the end of the studies, implant and surrounding tissue were recovered for histological analyses.

2.3.10 Role of Inflammatory Cytokines In Stem Cell Recruitment

Protein antibody microarray analysis was performed to compare the inflammatory cytokine profiles in tissue surrounding microspheres triggering different extent of tissue responses using mouse cytokine antibody array III (Raybiotech, Norcros, GA) following manufacturer's instruction. Briefly, 30 slices of tissue sections from HPC/tissue (strong inflammatory response) and NIPAm/tissue (weak inflammatory responses) were used to extract proteins produced by cells adjacent to the implants. Eluted proteins (50 microgram/sample) were used in the mouse cytokine antibody array III. The image analysis of the slide was then carried out using Axon GenePix 4000B microarray scanner (Molecular Devices, Sunnyvale, CA). The ratio of relative expression was calculated after subtraction of the background intensity and comparison with the positive controls (biotin-conjugated protein available on the slides). The fluorescence ratio for each spot was further processed using macros in EXCEL to identify cytokines/growth factor with a ratio of 2.0 or above (up-regulated cytokines) or a ratio of 1.0 or below (down-regulated cytokines) with respect to the control values.

2.3.11 Histological Evaluation of Inflammatory and Stem Cell Recruitment

All histological evaluations were carried out using frozen section technique. All implants and surrounding tissues were frozen in OCT compound (Polysciences Inc., Warrington, PA) and then sectioned into 6 µm tissue using a Leica Cryostat (Leica Microsystems, Wetzlar, Germany). To assess the tissue responses to microsphere implants, some of these slides were stained with hematoxylin and eosin (H & E) as described in our earlier studies. [1, 49]For assessing the extent of inflammatory cell, stem cells, or osteogenic responses, immunofluorescence analyses were carried out on some slides following established procedures.[1, 49] Specifically, immunofluorescence analyses were used to quantify the density of implant associated inflammatory cells (CD11b+); hematopoietic stem cells (Lin-/Sca-

1+/ckit+), and mesenchymal stem cells (CD105+/Stro-1+/SSEA4+/CD45-/CD34-/CD56-). DAPI staining was done to locate the cell nuclei.

2.3.12 Scaffold Fabrication

PLLA scaffolds were fabricated using salt leaching technique following established techniques.[64] Briefly, PLLA was dissolved in chloroform at 10% (w/v). The PLLA polymer solution was then added evenly over a Petri dish. Sodium chloride (porogen weight fraction of 90%, sieved at 150–250 mm) was then spread evenly on PLGA solution with continuous stirring in a fume hood until the solvent–polymer solution became pasty. After 72 h, the scaffold was placed under vacuum to complete solvent evaporation overnight. For the salt-leaching process, all scaffolds were submersed in distilled water and placed on an orbital shaker at 100 rpm. The water was changed every 30 min at room temperature until chlorides could not be detected by addition of 0.1M silver nitrate. After salt leaching, the scaffolds (3-4mm thick) were dried and cut into square pieces 5mm in length. The scaffolds were then sterilized by submersion in 70% ethanol. After 24 h, the ethanol was exchanged by submerging the scaffolds in phosphate buffered saline (PBS) and orbital shaking three times for 5 to 10 min. Scanning electron microscopy (SEM) was used to observe the cross-sectional morphology of the 3D PLGA scaffolds. The scaffolds were freeze fractured to expose the cross-section. Briefly, the scaffolds were immersed in liquid nitrogen and then cut using a sharp blade along their cross-sections. The scaffold specimens were sputter coated with silver before observation using a Hitachi S3000N scanning electron microscope (Hitachi High Tech Inc., Tokyo, Japan). PLLA scaffolds were soaked in bone morphogenetic protein -2 (BMP-2)

2.3.13 In Vivo Tracking of Injected Stem MSCs In A Scaffold

Isolation of BM MSCs was carried out following established procedures. Briefly, both the femurs of donor Balb/c mice (12 to 20-weeks old) were excised cleaned to remove the adherent muscle tissue. Bone marrow cells were obtained by inserting a syringe needle (25-gauge) and flushing with DMEM containing 20% FBS. The cells were dispersed and suspended

with the same medium for several times. These cells were plated onto 25-cm^2 plastic flasks (containing $1x10^6$ to $2x10^6$ marrow cells) with 8ml complete medium, and incubated in a fully humidified system containing 95% air and 5% CO_2 at 37^oC. After 3 days (by when cells had attached) the non-adherent cells were discarded. When primary stem cells formed a cell layer in culture flasks, the cells were subcultured into 75-cm^2 plastic flasks by using 0.025% trypsin. The cells were passaged two times. When the cells reached confluence, medium was replaced with fresh culture medium with 5μM concentration of Kodak X-Sight imaging agent (Rochester, NY) in each well-plated and cultured at 37^oC for 24 hours. Cells were then washed with PBS twice to remove excess imaging agent. Mesenchymal stem cell migration toward implanted PLLA microspheres was assessed as follows. After ventral skin depilation and anesthesia, 0.5 ml of PLA microspheres (2 mg/ml) was injected subcutaneously on the lower back-side of Balb/c mice (12 to 20 weeks old) following sterile techniques. After 24hours, X-Sight labeled stem cells ($3x10^6$/0.2ml) were injected via a 25-gauge syringe needle intravenously (IV) through the dorsal tail vein in mice. After implantation for different periods of time, stem cell distribution was then imaged by using Kodak *In Vivo* Multispectral Image System FX (configured for 760nm excitation, 830nm emission, 45s exposure, 8x8 binning, f-stop 2.5, 120mm field of view) and followed by with X-ray image capture to determine stem cells fluorescence intensity, and stem cell migration. The overall fluorescence intensity images of abdomen and implantation sites vs. time ware analyzed by using Kodak *In-vivo* imaging system at various time points. The high resolution images were captured based on the fluorescent signals emitted by the X-Sight imaging agents. Also, since bone and soft tissues differentially absorb X-rays, a projection of the mouse's anatomical structure was created on the phosphor screen. The software of overlay fluorescence and X-ray images of the mice injection with/without implantation were designed in our laboratory, which demonstrated the expected co-localization and the precise localization of the labeled cells distribution at various times under the same condition.

2.3.14 In Vivo Osteogenic Differentiation of Recruited Stem Cells On Scaffolds

To study the differentiation of recruited autologous stem cells in a tissue engineering scaffold, PLLA scaffolds soaked with 1 µg/ml BMP-2 was implanted on the back of Balb/c mice. Scaffolds without BMP-2 served as control. The animals were sacrificed after 8 weeks and the implant was recovered for histological analyses.

2.4 Results

2.4.1 FACSArray Analysis of Wound Chamber Ascites Cells

It is well established that foreign body reactions are accompanied with the accumulation of inflammatory cells. To determine the cell types in the biomaterial implantation site, ascites were collected from 3-5 day PLLA tube implants and then analyzed using flow cytometry method. As expected, we found that the wound fluid contains many CD45+ (27.5 ± 5.7 %) and CD11b+ (42.9 ± 4.9 %) and inflammatory cells (Figure 2.3 A and B respectively). Rather surprisingly, our analyses also revealed that small numbers of MSC (CD73+/CD105+/CD90+/ CD45-) (0.60 ± 0.29 %) (Figure 2.3 C-D) and HSC (Lin-/Sca-1+/c-kit+) (0.22 ± 0.07 %) (Figure 2.3 E-F) present in the ascites.

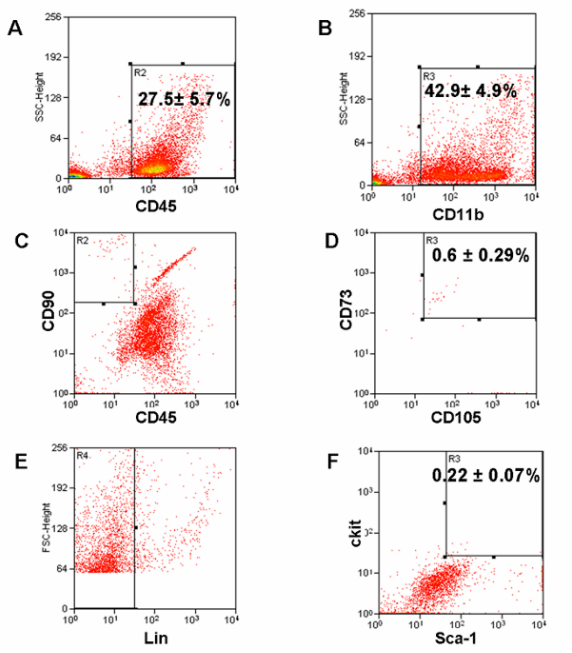

Figure 2.3 Characterization of cells in wound fluid aspirates using flow cytometry analyses. In wound fluid aspirates, the majority of cells were inflammatory in nature based on (A) CD45+ and (B) CD11b+ expression. The wound fluid also contained some number of (C-D) mesenchymal stem cells (CD73+/CD105+/CD90+/CD45-) along with (E-F) hematopoietic stem cells (Lin-/Sca1+/c-kit+).

2.4.2 In Vitro Differentiation of Wound Chamber Ascites Cells

To assess their multipotency, the ascites' stem cells were cultured in the presence of various differentiation cocktails. While the control cells showed an undifferentiated morphology (Figure 2.4 A), after 10 days in osteogenic differentiation medium, Alizarin Red staining showed the presence of calcified deposits indicative of osteogenic activity (Figure 2.4 B). Both adipogenic and chondrogenic differentiation medium treated cells showed adipogenic activity (Figure 2.4 C) based on Oil Red staining, and chondrogenic activity based on Alcian Blue staining (Figure 2.4 D) by day 14. This indicates that ascites' stem cells could differentiate into mesenchymal lineages *in vitro*.

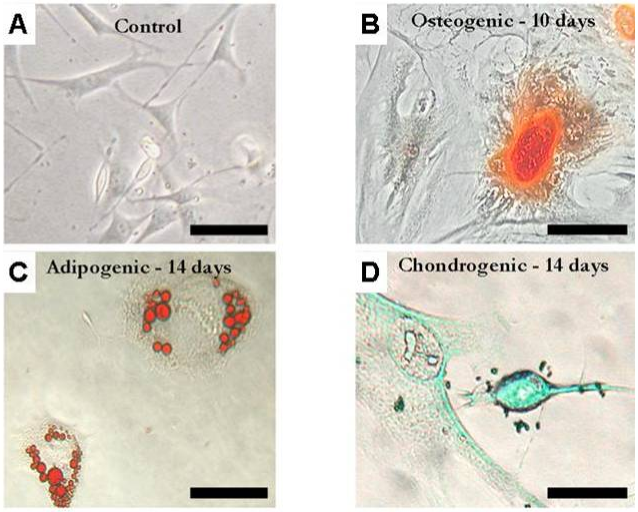

Figure 2.4 Plastic adherent cells from such aspirates were treated with various specific differentiation medium. (A) Control untreated cells remained largely undifferentiated. At various time points post-treatment cells were stained with (B) Alizarin Red for osteogenic (day 10); (C) Oil Red for adipogenic (day 14) and (D) Alcian Blue for chondrogenic activity (day 14). Magnification: 400X; Scale bar = 20 µm.

2.4.3 Recruitment of Stem Cells In Response To Different Types of Biomaterials

While studying the mechanisms of implant-mediated tissue responses, we accidentally discovered that, in addition to inflammatory cells, stem cell-like cells can also be found adjacent to the biomaterial implants. Specifically, by analyzing the tissue responses to subcutaneously implanted salt leached PLGA scaffolds for 2 weeks in Balb/c mice, we found that a thick fibrotic capsule had formed around the implant, as shown by the arrows in figure 2.5 A. The scattered presence of cells was found inside the scaffold (Figure 2.5 B). Using immunofluorescence (IF), we have identified that many of the implant-associated cells are inflammatory cells (CD11b+). However, many non-inflammatory cells (CD11b-) were also recruited to the implantation sites. Since we observed stem cells in the wound fluid is it possible that implants, in general, attract stem cells? To determine the causative factors and better understand the phenomenon, we implanted different types of microspheres. Microspheres were chosen for this study, as they provide maximum surface area for cells to interact. The implant tissue was analyzed at various time points and the cell types were characterized. Different materials were then compared at 1

week, to determine the effect of implant chemistry on cell recruitment. An anti-inflammatory agent was administered to block the inflammatory response in order to study its effect on stem cell recruitment.

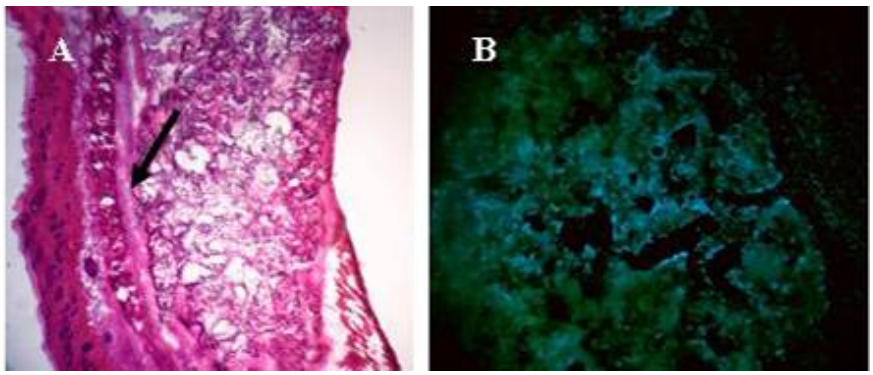

Figure 2.5 Implantation of a scaffold for 2 weeks showed the presence of a thick fibrotic capsule (arrows) around the implant (A). DAPI staining showed the presence of cells inside the implant (B).

2.4.4 Stem Cell Recruitment Around Various Microsphere Implants

Although stem cells were found in the ascites from the wound chamber, it was not clear whether some of these stem cells resided in or surrounding biomaterial implants. Furthermore, it has not been determined whether biomaterials triggering different tissue responses would prompt varying extent of stem cell recruitment. To find the answer, microspheres made of PLLA, NIPAm, PP and HPC were implanted for 7 days (sufficient time for both inflammatory cells and stem cell responses) and then histologically analyzed. As expected, different materials were found to prompt varying degree of inflammatory response which, upon quantification showed that NIPAm evoked the lowest inflammatory response (almost 3X lower than PP group) (Figure 2.6).

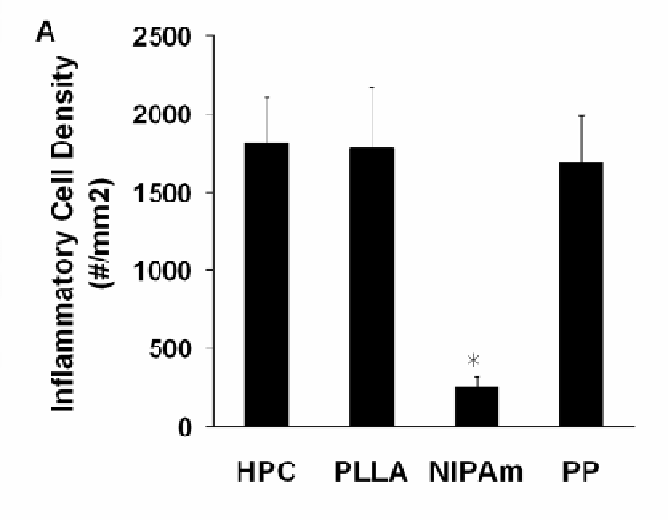

Figure 2.6 Cells accumulate in the tissue around different microsphere implants (HPC, PLLA, NIPAm, and PP). Based on the expression of inflammatory cell surface markers cells were quantified over a period of 7 days.

Importantly, we observed more MSCs (with different sets of markers, including CD105+/CD45-/CD34-/CD56-, Stro-1+/CD45-/CD34-, and SSEA4+/CD45-) in high inflammatory PP group (top panel) than low inflammatory NIPAm group (lower panel) (Figure 2.7 A). Similar trend was also found in the recruitment of (Lin-/Sca-1+/ckit+) (Figure 2.7 B).

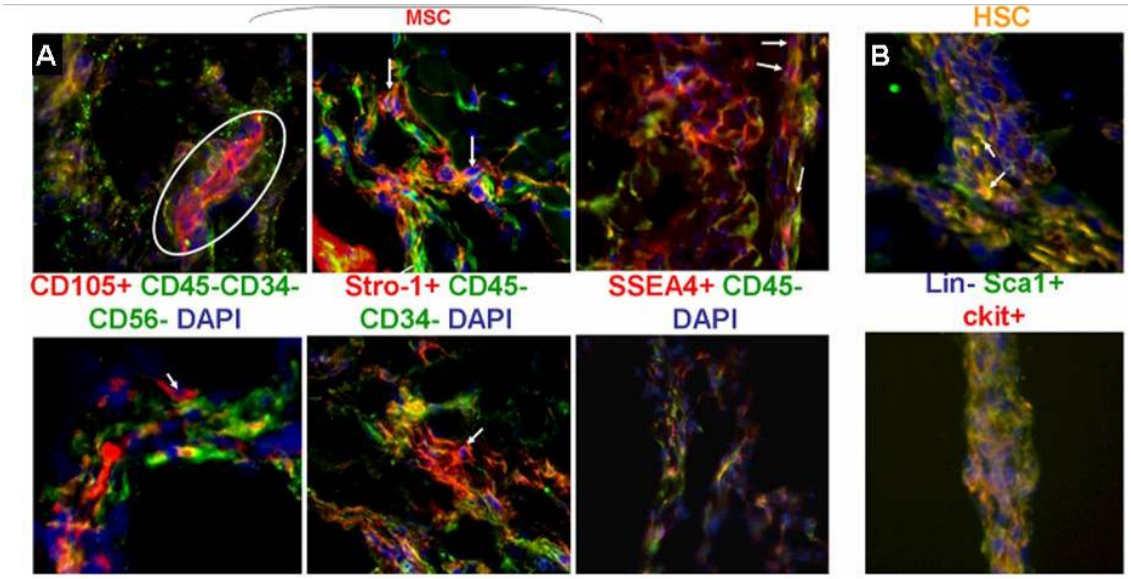

Figure 2.7 Histological staining of: (A) MSCs (with varying sets of markers including CD105+/CD45-/CD34-/CD56-, Stro1+/CD45-/CD34- and SSEA4+/CD45-) surrounding proinflammatory PP materials (top panel) vs. NIPAm materials (lower panel). Arrows indicate the MSC uniquely expressing red color (signifying positive marker expression). (B) HSCs (Lin-/Sca1+/c-kit+) adjacent to PP materials (top panel) and NIPAm materials (lower panel). Arrows indicate the HSC expressing Sca-1 and c-kit and lacking expression of lineage markers. Images mag 200X.

The cell numbers of MSCs (Stro1+/CD45-/CD34-/CD56-) and HSCs were quantified and compared among different groups of test materials (Figure 2.8). As shown in figure 2.7 A and B respectively, the number of MSCs and HSCs in the high inflammatory PP group (215.64 ± 89.78 and 297.3 ± 32.25 respectively) was significantly higher than the low inflammatory NIPAm group (60.29 ± 13.01 and 65.49 ± 2.37 respectively).

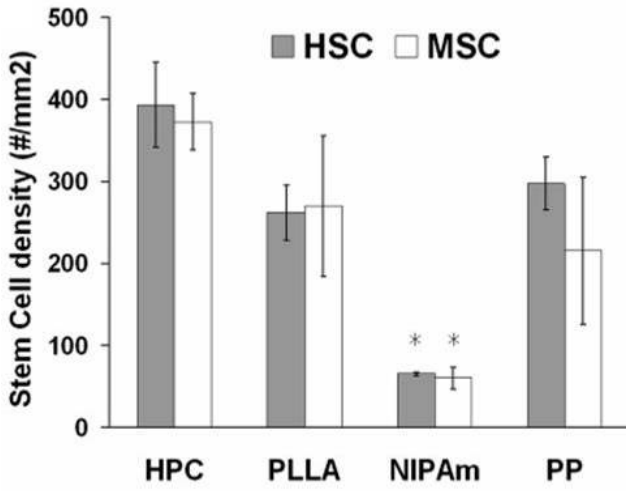

Figure 2.8 Quantification of density of MSCs and HSCs surrounding different implants. Data are mean ± SD. Significance of PLLA, NIPAm, PP vs. HPC; * p< 0.05.

Since pro-inflammatory materials were found to recruit more stem cells, we further analyzed the relationship between the percentages of recruited inflammatory cells (CD11b+), MSCs (Stro1+/CD45-/CD34-/CD56-) and HSCs among all test materials using linear regression (Figure 2.9 A & B). Very interestingly, we found good relationship between the inflammatory cells and HSCs (Figure 2.9 A) and between inflammatory cells and MSCs (Figure 2.9 B).

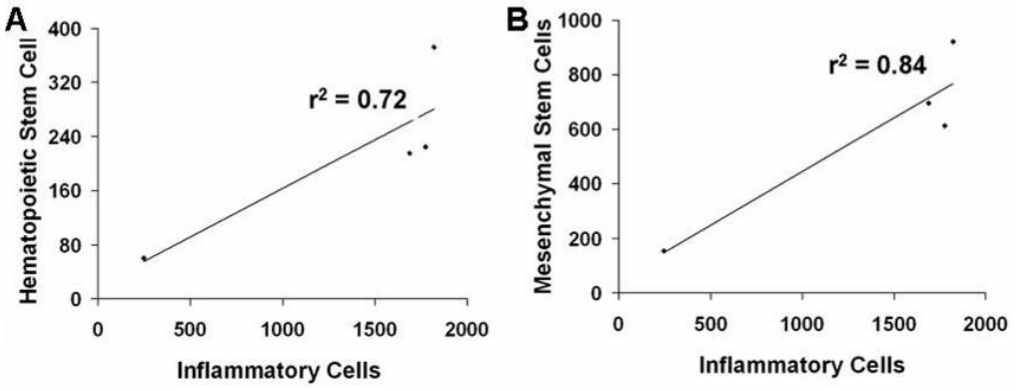

Figure 2.9 Determination of the relationship between inflammatory responses and stem cell recruitment by linear regression between the density of recruited inflammatory cells and MSCs and HSCs respectively among all materials.

2.4.5 Recruitment Kinetics of Stem Cells In Response To Inflammation

The interesting relationship between inflammatory cells and stem cells warranted the study of kinetic responses between these two types of cells. For that, we quantified the presence of various cell types around the subcutaneous HPC microsphere (which prompt intermediate cellular responses) implanted over a period of time (0, 2, 4, 7, and 14 days) (Figure 2.10 A-C). As anticipated and in agreement with earlier findings in biomaterial-mediated inflammatory responses, the percentages of CD11b+ inflammatory cells (Figure 2.10 A) around the implant tissue increased until around day 4 (~ 35%) after which the percentage declined sharply to ~10% on day 14. Differing from inflammatory cell responses, stem cell numbers peaked by day 7 (Figure 2.10 B). We found that the proportion of MSCs surrounding biomaterial implants continued increasing with time (at least until 14 days) while the percentage of HSCs reached plateau around 4 days and stayed at the same level during the rest of this study (Figure 2.10 C).

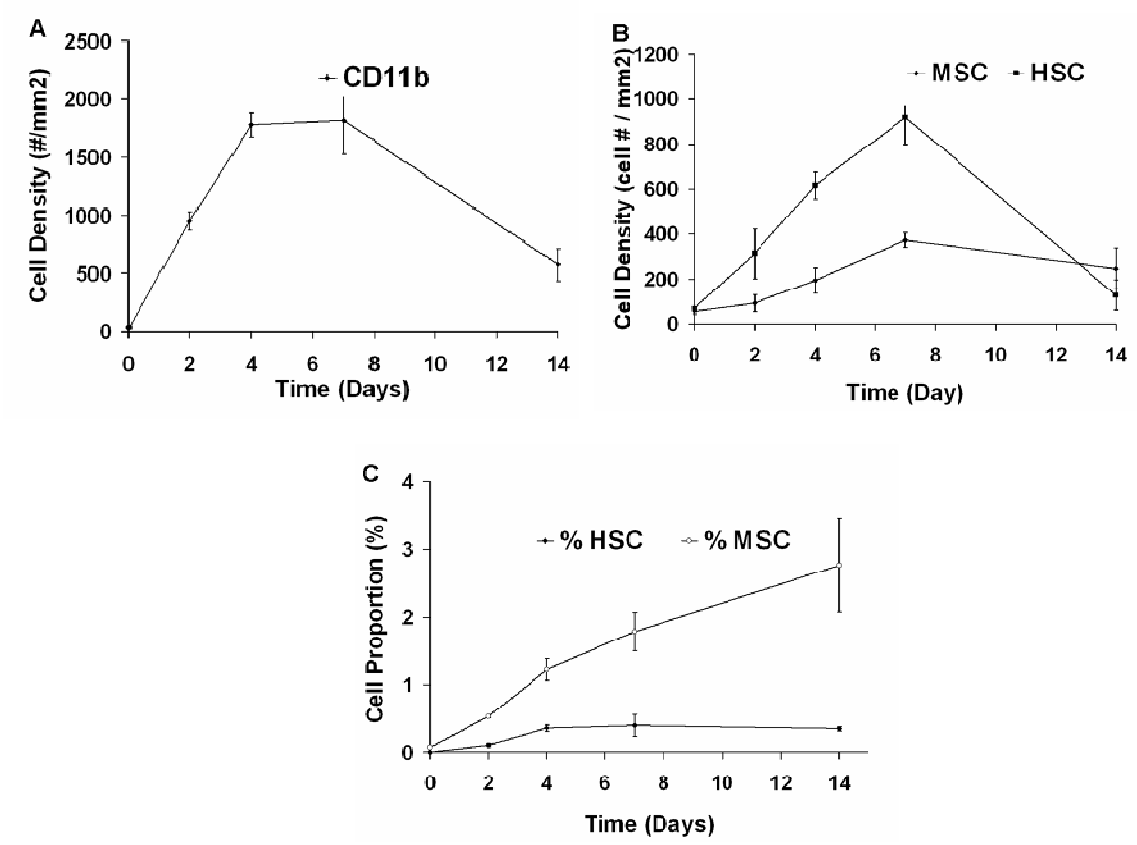

Figure 2.10 Kinetic study of microsphere implant-mediated cell recruitment and the treatment of anti-inflammatory agent on cell responses. Quantitative analysis of (A) CD11b+ inflammatory cell number, (B) MSCs (Stro1+/CD45-/CD34-/CD56-) and HSCs (Lin-/Sca1+/c-kit+) and (C) proportion of MSCs and HSCs recruited to the implantation sites. Data are mean ± SD.

2.4.6 Effect of Inflammatory Stimulus Suppression On Stem Cell Recruitment

Our results so far support the idea that inflammatory responses influence stem cell recruitment. To test this assumption, we studied the effect of blocking the inflammatory process on stem cell recruitment. HPC microspheres were soaked in an anti-inflammatory drug, dexamethasone (DXM) (1 mg/ml) prior to subcutaneous implantation. At day 7, we found that the administration of DXM substantially reduced the fibrotic tissue reaction around the implant (Figure 2.11).

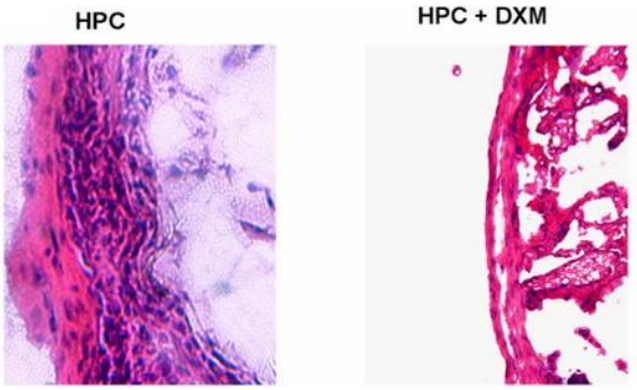

Figure 2.11 For 7-day HPC implants, some of the animals were treated with HPC soaked with anti-inflammatory drug, dexamethasone (DXM). Representative histological images of fibrotic capsular region in untreated control vs. DXM treated mice. (Mag 400 X).

There was an almost 60% decrease in cell density around the DXM coated implant (Figure 2.12 A). Specifically, there was similar reduction in the numbers of inflammatory cells based on expression of CD11b and CD45 markers after administration of DXM (Figure 2.12 B). Having seen that both overall capsular cell density and inflammatory cell density in the capsule went down after DXM administration, in support of our hypothesis, we observed ~70% reduction in the numbers of recruited stem cells (both HSC and MSC) compared to untreated controls (Figure 2.12 C).

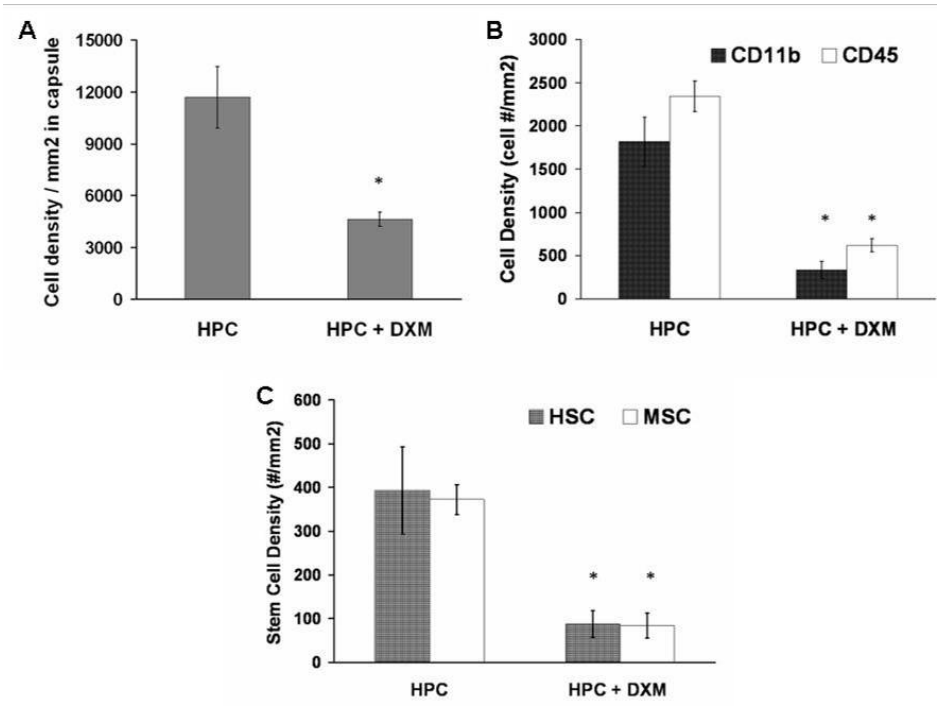

Figure 2.12 (A) Overall cell density in fibrotic capsular region in untreated control vs. DXM treated mice. (B) The localized release of DXM on the recruitment of CD11b+ inflammatory cells and CD45+ immune cells in HPC implant-bearing mice. (C) Numbers of stem cells (both HSC and MSC) in the implant tissue. Data are mean ± SD. Significance of (HPC+DXM) vs. HPC; * $p < 0.05$

2.4.7 Role of Inflammatory Chemokines In Stem Cell Recruitment

Although many inflammatory cytokines/chemokines have been linked to stem cell migration, the molecular mechanism(s) and signals required for implant-mediated stem cell homing is mostly undetermined. To identify the potential inflammatory cytokines mediating stem cell buildup, we compared the inflammatory cytokine profiles in tissue surrounding HPC implants (with most inflammatory cells and stem cells) vs. NIPAm implants (with the least cells) (Table 2.1). Interestingly, our results have shown that a very high upregulation of pro-inflammatory cytokines like Macrophage Inflammatory Protein-1α (MIP-1α) (13X) and MIP-2 (14X) was seen in HPC implants as compared with NIPAm. In addition, a high expression of several pro-inflammatory cytokines like Monocyte Chemotactic Protein (MCP-1) (7X), MIP-1γ (3X), is seen in the HPC implant group as compared with NIPAm. It should be noted that MIP-1γ (8X), MIP-2 (23X) was

observed in the HPC implant group as compared to normal skin (no implant). Tissue Inhibitor of Metalloproteinase-1 (TIMP-1) which is a pro-fibrotic cytokine has a ~41X increase in expression in the HPC implant group as compared to normal skin which did not receive any implants and an 11X increase compared to the least inflammatory NIPAm group. It must be noted that a few pro-inflammatory cytokines like Tumor Necrosis Factor–α (TNF-α), RANTES, Granulocyte Colony Stimulating Factor (G-CSF) and Interferon-γ (IFN-γ) were not significantly up-regulated.

Table 2.1 Inflammatory Cytokine Expression in the Tissues Surrounding HPC Microsphere Implant Group (Strong Stem Cell Response) Compared With NIPAm Microspheres (Weak Stem Cell Response) After 7 Days

	Expression			Expression	
Protein	Upregulated	Downregulated	**Protein**	Upregulated	Downregulated
Axl	1.93		KC	3.62	
BLC	3.70		Leptin		0.83
CD30		0.58	Leptin R		0.94
CD30L		0.67	LIX	1.42	
CD40	3.30		L-Selectin		0.36
CRG-2		0.51	Lymphot-actin		0.72
CTACK	1.09		MCP-1	11.48	
CXCL16	2.36		MCP-5	1.17	
Eotaxin	2.11		M-CSF	1.15	
Eotaxin-2	1.99		MIG	1.43	
Fas Ligand		0.27	MIP-1α	19.76	
Fractalkine		0.43	MIP-1γ	7.53	
GCSF		0.82	MIP-2	23.49	
GM-CSF		0.77	MIP-3β		0.88
IFNγ		0.75	MIP-3α		0.88
IGFBP-3		0.48	PF-4	4.17	
IGFBP-5	2.23		P-Selectin	1.76	
IGFBP-6	12.10		RANTES	1.75	
IL-1 beta		0.56	SCF		0.68
IL-10		0.98	SDF-1α		0.61
IL-12 p40/p70	1.26		sTNF RI	2.00	
IL-12 p70	1.10		sTNF RII	3.01	
IL-13	1.02		TARC		0.70
IL-1α		0.66	TCA-3	1.55	
IL-2		0.43	TECK		0.38
IL-3		0.62	TIMP-1	41.26	
IL-3Rβ		0.44	TNFα	1.24	
IL-4	1.01		TPO	1.18	
IL-5	1.56		VCAM-1	2.64	
IL-6	1.23		VEGF	2.07	
IL-9	1.32				

2.4.8 Osteogenic Differentiation of Autologous Stem Cells In Scaffolds

Our previous studies have found that biomaterial implants prompted acute inflammatory responses and followed with the accumulation of stem cells. Since these recruited multipotent stem cells can be differentiated into different types of cells *in vitro*, we thus assumed that, with localized release of differentiation agent, recruited MSCs can be directed to form specialized cells and tissue.

2.4.9 Differentiation of Recruited Autologous Stem Cells Into A Specific Lineage

Our previous studies have found that biomaterial implants prompted acute inflammatory responses and followed with the accumulation of stem cells. Since these recruited multipotent stem cells can be differentiated into different types of cells *in vitro*, we thus assumed that, with localized release of differentiation agent, recruited MSCs can be directed to form specialized cells and tissue. To test this hypothesis, we used porous PLLA scaffolds loaded with bone morphogenetic protein-2 (BMP-2), an osteogenic differentiation agent. We first determined whether PLLA scaffolds were able to recruit stem cells. After implantation of PLLA scaffolds for 2 days, near-infrared (NIR) fluorophore (X-sight) labeled MSCs were transplanted into animals *via* tail vein injection. As expected, we found that substantial numbers of transplanted MSCs were found around the implant site (shown in dotted circle) within 24 hours of stem cell injection (Figure 2.13).

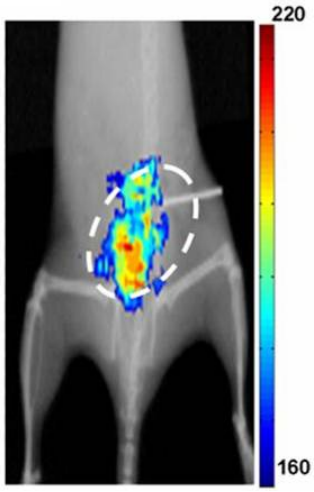

Figure 2.13 PLLA scaffold implants mediated stem cell recruitment and osteogenic responses. *In vivo* image of 2-day scaffold-implanted mice transplanted with X-sight labeled bone marrow derived MSCs for 24 hours. The material implantation site is shown in dotted circle.

The effect of localized release of BMP-2 on inducing stem cells' osteogenic responses was subsequently tested using both PLLA and PLLA-BMP-2 scaffolds implanted for a period of 8 weeks. As evidenced by the histological staining for osteocalcin expression, with BMP-2 scaffolds having enhanced expression of osteocalcin which is indicative of the osteoblast function and activity at the site (Figure 2.14 A). By quantifying fluorescence intensity, we find an 18X increase in osteocalcin expression in BMP-2 scaffolds as compared to controls (Figure 2.14 B). Calcified deposits were also found to substantially increase in the BMP-2 treated scaffolds as compared to controls based on von Kossa staining (Figure 2.15 A) and Alizarin Red (Figure 2.15 C). The quantitative assessment of the area distribution of the calcified deposits showed that a significant increase in calcification in BMP-2 scaffolds as compared to

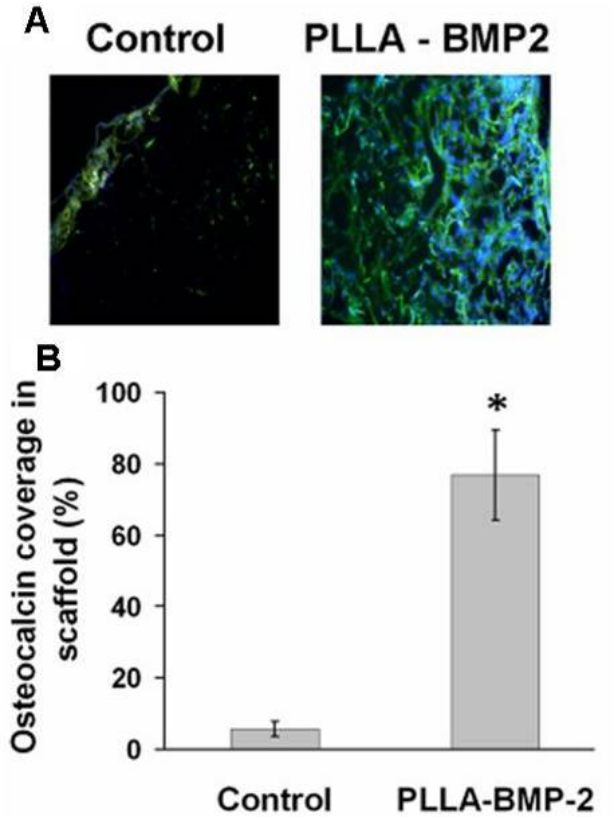

Figure 2.14 Long-term (8 weeks) osteogenic responses to PLLA scaffolds with or without BMP-2 implanted in the subcutaneous cavities. (A) Osteocalcin expression in BMP-2 soaked scaffold was determined by immunofluorescence staining using antibodies against osteocalcin. DAPI was used to counterstain the nuclei. (B) Quantitative assessment of osteocalcin distribution over the scaffold area. Images mag 200X. Significance of (PLLA+BMP-2) vs. Control; Data are mean ± SD. * $p < 0.05$.

controls based on von Kossa stain (Figure 2.15 B; 5X greater) and based on Alizarin Red staining (Figure 2.15 D; 4X greater). These results support our original hypothesis that biomaterial implants prompt the homing of autologous stem cells and the recruited stem cells can be turned into specialized cells/tissue with proper localized stimulation.

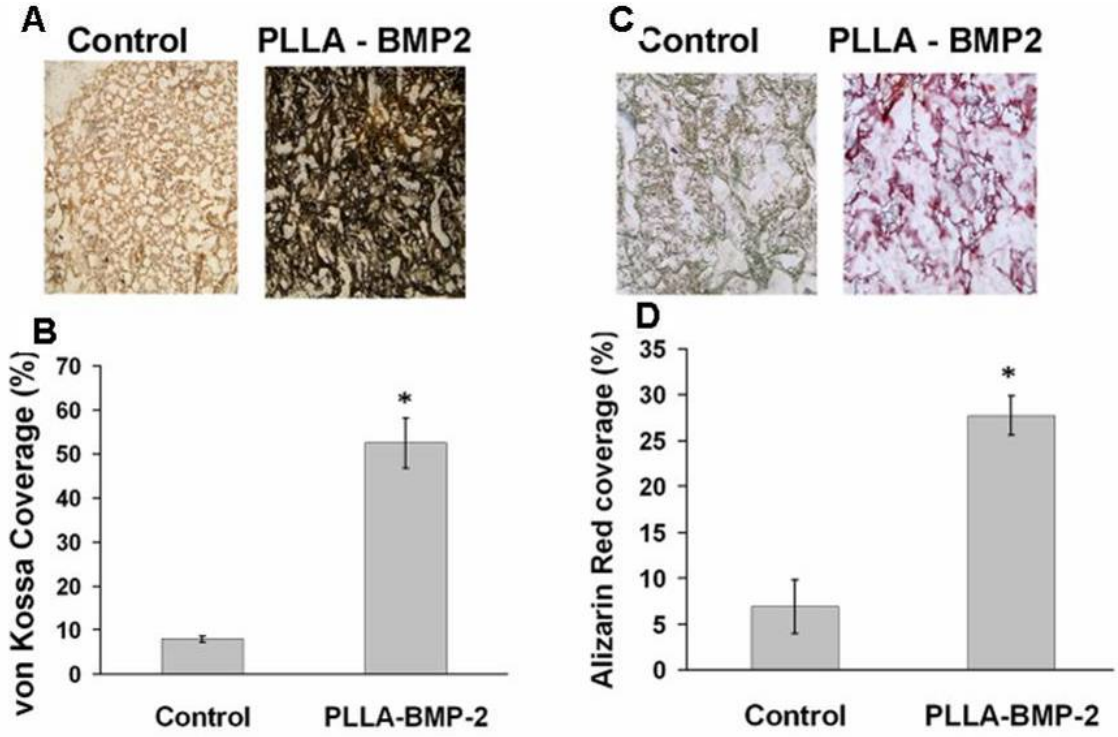

Figure 2.15 Histological images of calcium deposits and quantitative assessment of calcium distribution based on von Kossa staining (A & B respectively); Alizarin Red S staining (C & D respectively) of BMP-2 soaked vs. control salt leached PLLA scaffold. Images mag 200X. Significance of (PLLA+BMP-2) vs. Control; Data are mean ± SD. * $p < 0.05$.

2.5 Discussion

Despite the tremendous potential shown by stem cells in treatment of diseases and regenerative tissue engineering,[65-67] it has quite a few drawbacks. Firstly, there is a lack of safe and reliable sources for large numbers of stem cells. Secondly, transplanted allogenic stem cells often exert immune reactions,[18, 19] which may eventually lead to their death.[19, 68] Wound healing responses promote the recruitment of MSCs/HSCs, and both groups of cells have been shown to participate in tissue regeneration.[69-71] It, thus, would be highly desirable if biomaterial implants were to be developed to direct autologous stem cell responses to resemble those in wound healing reactions. This can have profound implications from a regenerative medicine standpoint and this has been the driving force behind this work. This study supports that implantation of a biomaterial can trigger localized inflammatory responses

and indirectly recruit multipotent autologous stem cells to the implantation site. Their subsequent behavior could then be controlled so as to yield a desired outcome.

PLLA was used to fabricate the wound chambers as it is a commonly used FDA approved biomaterial for fabricating tissue engineering vascular grafts and many other types of scaffolds. The implantation of PLLA tubes was found to prompt the influx of cells (mainly monocytes and other peripheral blood cells) into the chamber lumen within 24-48 hours. This observation agreed well with a previous study that employed wound chambers.[72] Interestingly, we found that cells expressing MSC and HSC markers were present in the ascites along with inflammatory cells for at least 2 weeks. The selection of markers for MSCs, especially in tissue is highly debatable. As such based on an extensive search of available literature, [73-77] and expert opinion *[Drs. Arnold Caplan at Skeletal Research Center - Cleveland, Robert Pignolo at University of Pennsylvania School of Medicine, Jim Middleton at Keele University - UK, Kim O'Connor at Tulane University and Pranela Rameshwar at UMDNJ - New Jersey Medical School]* a set of markers was short-listed. For flow cytometry, cells positive for CD73, CD105, CD90 and negative for CD45 were identified as multipotent MSCs. Based on the expression of markers Sca-1 and c-kit and negative expression for Lineage markers HSCs were identified as in earlier publications.[78-80] To include multiple antibodies in tissue immunofluorescence staining, expression of a positive marker (tagged red) was analyzed against a group of negative markers (tagged green). It is generally accepted that MSCs lack expression of CD45, CD34 and CD56 markers.[73-76] However, they are positive for CD105, Stro-1 and very recently it was found that cells expressing SSEA4+ and CD45- cells are multipotent MSCs.[16, 20, 81] In fact there have been studies of late that have shown that SSEA-4 is a marker for primitive MSCs in both murine and human bone marrow.[20, 82] It should be noted that such multipotent stem cells could not be found in the "untreated" tissue or the animals which did not receive an implant. The expression of Stro-1, which is a characteristic

surface antigen, found on bone marrow derived MSC was quantified to indicate the source of MSCs.

We are aware that the cell surface markers are not sufficient to determine the function of recruited stem cells. As a true test of their “plasticity”, it is desirable to show that these cells can, not just express these progenitor cell markers, but also adhere to plastic and differentiate into various lineages under the appropriate conditions.[75, 76] We were able to use various specific differentiation cocktails and induce lineage specific differentiation of the cells into osteogenic, adipogenic and chondrogenic lineages. Our qualitative results agree with stem cell differentiation studies in which wound chamber-derived MSCs were differentiated into various lineages.[59] This further supports previous observations that the collections of cells that are recruited in response to a wound or injury include stem cells.

This study has demonstrated that microsphere implants with varying degree of pro-inflammatory properties also trigger different extent of MSCs recruitment. By analyzing tissue responses to materials prompting varying degrees of inflammatory responses, we found that there was a good relationship between stem cell and inflammatory cell recruitment. It is well established that material surface properties affect the extent of inflammatory responses.[1, 49] However, the influence of implant material properties on the recruitment of autologous stem cells has not been studies thus far. Interestingly, we found that the administration of anti-inflammatory drug – dexamethasone – curtailed not only inflammatory cell responses but also stem cell homing. The recruitment of stem cells is likely to be triggered by inflammatory products, since inflammatory cell numbers achieved their maxima 3 days before stem cells. This observation also agrees well with previous studies which have found that inflammatory responses play a role in stem cell homing.[65, 83, 84] The results from this work also support the idea that the localized biomaterial-mediated inflammatory responses could be used as a controlled means to elicit autologous stem cell recruitment. Our findings agree well with

previous studies which showed reduced MSC and neural stem cell proliferation following anti-inflammatory drug administration.[85, 86]

So as to understand the mechanism behind the recruitment of autologous stem cells in response to inflammatory stimuli, we analyzed the expression of various cytokines around the pro-inflammatory HPC implant group and compared it with the least inflammatory NIPAm group and the possible role they could have played in recruiting stem cells. The increase in production of several inflammatory cytokines, including MCP-1, MIP-1α, MIP-1 γ and TIMP-1 supports the pro-inflammatory nature of HPC microsphere implants. It is well established that CC chemokines like MCP-1 (CCL2) and MIP-1α prompt the migration of monocyte/macrophages. [87-89] It must also be noted that some pro-inflammatory cytokines TNF-α, RANTES, G-CSF and IFN-γ showed down-regulation. Although the exact mechanism governing this is not clear, it is possible that certain conditions in the milieu around the implant could play a role in down-regulation of these cytokines. In light of this finding, it must be noted that in recent studies, many of these chemokines have been found to participate in the recruitment of stem cells. For example, MIP-1α is found to mobilize hematopoietic progenitors.[90, 91] MCP-1 has been shown to be a potent chemoattractant for bone marrow stem cells, especially MSC.[92] In addition, increased production of Vascular Endothelial Growth Factor (VEGF), Vascular Cell Adhesion Molecule-1 (VCAM-1) and Platelet Factor 4 (PF4) may contribute to the enhanced stem cell recruitment based on the following observations. VEGF has been shown to play an important role in the recruitment and reactions of bone marrow derived MSC and HSC. [93] VCAM-1 has been shown to mediate the transmigration of stem cells through endothelial cells. [91] PF4 was found to enhance HSC recruitment *via* the adhesion of HSC to endothelial cells.[94, 95] Interestingly, we also observed a slightly decreased expression of IFN-γ. The reduction of IFN-γ may be correlated with MSC recruitment, since an earlier study showed that in the presence of MSCs, IFN-γ production is reduced.[96] Taking all this in to consideration, our findings indicate that the release of inflammatory chemokines and growth factors play an

important role in autologous stem cell recruitment. This can be harnessed to play a vital role in tissue regeneration strategies.

A mainstay of tissue regeneration applications are tissue scaffolds. However, lack of reliable sources of stem cells, tedious cell isolation and culture procedure, and poor tissue integration after transplantation hinders their success.[2, 71] So far we found that multipotent stem cells, both HSC and MSC are recruited in response to biomaterial implantation. Current studies reveal that inflammatory responses are required for stem cell homing. However, certain chemokines, such as stromal derived growth factor-1 α (SDF-1 α), have been shown to promote stem cell homing without exerting inflammatory reactions.[97] In the presence of inflammatory products, recruited stem cells often form scar or soft tissue.[98, 99] However, when exposed to cell differentiation agents, recruited stem cells can be induced for form specialized cells and tissue. This concept is tentatively proven by our results that recruited MSCs showed signs of osteogenic differentiation in the scaffold matrix releasing BMP-2, a potent osteogenic differentiation agent. Our finding that stem cells recruited in response to a biomaterial implants do not lose their ability to differentiate is important as it can be successfully used for a wide range of *in situ* stem cell therapy and tissue engineering applications. In such scenarios, biomaterial implant can be made in different forms (spheres, gel or scaffold) to release a variety of agents able to differentiate stem cells into different lineages. By implanting such materials in or nearby diseased or injured tissue, autologous stem cells can be homed and then turned into specialized cells for *in situ* tissue regeneration without the cell recovery and handling problems currently associated with stem cell therapies and tissue engineering applications.

CHAPTER 3

DEVELOPMENT OF NOVEL ORCHESTRATED STEM CELL-BASED REGENERATION (OSCeR) SCAFFOLDS FOR DIRECTING TISSUE REGENERATION

3.1 Introduction

Scaffold design is a crucial aspect that dictates the success of tissue engineering. Tissue engineering scaffolds play a critical role in tissue engineering by acting as a temporary tissue construct or building block for cell accommodation, proliferation, and differentiated function as well as serving as three dimensional templates for neotissue/organ formation.[100] To create such temporary structure for cell growth, degradable polymeric materials, such as poly (L-lactic acid) (PLLA) and poly (l-lactic-co-glycolic acid) (PLGA), are commonly used and have been extensively researched.[5, 100] In addition, many procedures have been developed for the preparation of porous matrices such as solvent casting/particulate leaching, emulsion freeze drying, gas foaming and thermally induced phase separation.[6, 101-103] These methods allow us to produce a series of scaffolds with desired porosity and different physical/mechanical properties. However, most scaffolds fail to attract and grow a large number of cells mostly due to the lack of a suitable growth environment. Table 3.1 lists commonly used scaffold fabrication techniques along with their merits and demerits.

To improve cell seeding and growth, substantial progress has been made in recent years by either coating the scaffold with different adhesive proteins like laminin, fibronectin, fibrin, collagen and vitronectin,[10, 104] or soaking the scaffold with various growth factors like insulin-like growth factor, transforming growth factor-β, platelet derived growth factor, fibroblast growth factor via spontaneous adsorption or covalent linking.[10-12] These additional treatments improved cell growth, although such enhancements were often limited and short-lived. It is also possible that common growth factor:scaffold conjugation processes may alter the

morphological and physical strength of the scaffold. Thus, there is an urgent need on the development of new scaffold fabrication technique in which a variety of growth factors can be embedded and released for a prolonged period of time.

Quite a few studies have reported that growth factor loaded nanoparticles are able to release a variety of growth factors for a long period of time.[105] Despite impressive research progress, such growth factor eluting particles may not be adopted as part of the porous scaffold fabrication processes. The main hurdle is that growth factors can be easily denatured or inactivated by organic solvents used for scaffold fabrication.[106, 107] Studies have also shown that scaffolds soaked in growth factors have a characteristic high burst release in the first 1-2 days. This occurs since most of the growth factor is bound to the surface, instead of being embedded inside the scaffold.[13]

Table 3.1 Scaffold Fabrication Techniques – Advantages and Limitations [103]

Technique	Advantage	Limitation
Fiber weaving	• Easy process. • High porosity.	• Poor structural stability.
Fiber bonding	• High porosity.	• Poor mechanical strength. • Residual organic solvent. • High processing temperature hinders biomolecule incorporation.
Solvent casting and particulate leaching	• High porosity. • Large pores. • Crystallinity can be tailored.	• Very thin membranes • Poor mechanical strength. • Residual solvent. • Immunogenic remnant salt. • No biomolecule incorporation
Membrane lamination	• 3-D structures	• Poor mechanical strength. • Limited pore-connectivity. • Residual solvent.
Gas Foaming	• High porosity.	• Poor pore-interconnection. • Residual solvent and salts.
Thermally Induced Phase Separation	• Highly porous. • Incorporation of biomolecules • No loss of activity. • Good solvent extraction.	• Small pore size. • Difficult to control internal scaffold architecture.

Polymeric tissue engineering scaffolds prepared by conventional techniques like salt leaching and phase separation are greatly limited by their poor biomolecule-delivery abilities.

Conventional methods of incorporation of various growth factors, proteins and/or peptides on or in scaffold materials via different cross linking and conjugation techniques are often tedious and may affect scaffold physical, chemical, and mechanical properties. In this light we considered protein microbubbles which are widely used in medical applications. It should be noted that protein MB have been widely used in the field of ultrasound imaging as a contrast agent,[108] and gene delivery vehicles.[109, 110] Our preliminary work focused on testing the hypothesis that scaffolds can be fabricated using protein microbubbles. For our early studies we successfully tested bovine serum albumin (BSA) and gelatin microbubbles for its suitability in fabricating scaffolds with open pores by combining it with phase separation technique.

3.2 Hypotheses

Hypothesis 1: Protein microbubbles can preserve the bioactivity of growth factors loaded in scaffold.

Hypothesis 2: A desirable cellular response can be elicited by protein microbubble scaffolds.

3.3 Material and Methods

3.3.1. Fabrication and Testing of BSA Microbubble (MB) Scaffolds

75:25 Poly (d, l-lactic-co-glycolic acid) PLGA with a molecular weight of 113 kDa was purchased from Medisorb (Lakeshore Biomaterials, Birmingham, AL). The solvent 1, 4-dioxane was purchased from Aldrich (Milwaukee, WI), Bovine Serum Albumin (BSA) Sigma (St Louis, MO) and Coomassie blue was purchased from EMD Biosciences (Darmstadt, Germany). Masson's trichrome kit was purchased from Sigma (St Louis, MO).

3.3.2. Preparation of BSA MB and Insulin-like Growth Factor Loaded MB

IGF-1 was chosen as model growth factor, since it stimulates fibroblastic 3T3 cell proliferation.[111-113] BSA MB were produced based on an established procedure.[108] Briefly, 5% w/v solution of Bovine Serum Albumin (BSA) was overlaid with nitrogen gas. The mixture was sonicated using a probe sonicator (Ultrasonix, Bothell, WA) at 20 kHz for 10 seconds. This procedure resulted in the formation of nitrogen gas filled MB which were surrounded by a BSA

protein shell. The MB were transferred to glass tubes and kept at 4^{o}C. To observe the physical structure of microbubbles, a small droplet of the microbubble was placed on a glass slide and then imaged under a microscope (Leica, Wetzlar, Germany). The microbubble size distribution was determined using the images and NIH ImageJ.[114] To synthesize IGF-1 loaded MB (labeled as MB-IGF1), IGF-1 (500 ng/ml) solution was mixed with BSA solution prior to sonication under nitrogen gas as described earlier.

3.3.3. Fabrication of Porous MB Scaffolds, Salt Leached and Phase Separated Scaffolds

BSA microbubble embedded porous scaffold (labeled as MB scaffold) was produced based on a modified phase separation procedure. In our pilot studies, different concentrations of BSA (5, 10, 20, 50% w/v) were used to synthesize the MB and different loading amounts (1:1, 1:2) of MB were added into various concentrations of polymer solution (5, 7.5, 10% w/v). Such MB-polymer mixtures were phase separated at various temperatures (0, -20, -196)^{o}C. The technique was optimized based on the information obtained from these studies and in this work, 7.5% w/v PLGA was dissolved in 1,4-dioxane by vortexing for about 20 minutes till the polymer completely dissolved in the solvent. The polymer solution was then mixed with the BSA MB (5 % w/v BSA) or water (as negative control) in a ratio of 1:1. After gentle agitation for 3 minutes at room temperature, the polymer/solution mixtures were then quenched in liquid nitrogen to induce phase separation. The solidified scaffolds were then lyophilized for 48 hours at 0.03 mBar vacuum in a Freezone 12 lyophilizer (Labconco, Kansas City, MO, USA). As comparison, conventional phase separated scaffolds and salt leached scaffolds were also synthesized as described earlier.[6, 64] For producing IGF-1 loaded MB embedded scaffolds, IGF1-loaded MB (MB-IGF1, MB manufactured in the presence of 500 ng/ml IGF1) were used as porogens. To directly test the influence of MB on IGF-1 release, some phase separated scaffolds were soaked in 500 ng/ml IGF-1 at 4℃ overnight and these IGF1-soaked scaffolds were used in some studies as controls.

3.3.4. Scaffold Characterization

To determine the potential contribution of BSA MB in creating porosity in scaffold, a staining method was developed to visualize the location of BSA bubbles following scaffold fabrication procedure. For that, variously manufactured scaffolds were immersed with freezing medium Tissue-Tek OCT (Sakura FineTek, Torrance, CA, USA) and then placed under vacuum at -70 kPa, for 15 minutes to facilitate the perfusion of the freezing medium through the pores of the scaffold. After freezing overnight, the scaffolds were sectioned in a cryostat (Leica CM1850, Leica Microsystems, Wetzlar, Germany) and collected on poly (L-lysine) treated slides. To visualize MB distribution, 10µm scaffold sections were obtained and then stained with Coomassie brilliant blue solution (0.1% w/v of Coomassie blue dye, 45% w/v methanol, 45% w/v water and 10% w/v acetic acid) for 4 min. Destaining to remove unbounded dye was accomplished by dipping the sections in destaining solution (10% w/v methanol, 10% w/v acetic acid and 80% w/v water).[2, 6] The slides were observed under a Leica microscope (Leica, Wetzlar, Germany) equipped with a CCD camera (Retiga EXi, Qimaging, Surrey BC, Canada). Surface morphology of the cross sections of the scaffolds (60 µm thickness) was also observed using a Hitachi 3000N Scanning Electron Microscope (Hitachi High Tech Inc, Tokyo, Japan). The porosity of the scaffolds was determined by ethanol displacement method based on a published procedure.[115] Mechanical testing was conducted with an MTS Insight 2 machine fitted with a 500 N load cell. The samples were cut into square discs (6.3 mm width x 6.5 mm thickness). The deflection rate was adjusted to 2 mm/min. Samples were compressed to 10% strain. The Young's modulus was calculated from the initial slope of the curve. [52]

3.3.5. In Vitro Testing of MB Scaffolds

For *in vitro* cell growth study, square sections (1 cm x 1 cm x 1 cm) of both phase separated scaffold and the protein microbubble (MB) scaffolds were soaked in ethanol for few minutes followed by multiple washes with sterile PBS. Scaffolds were seeded with 3T3 cells ($5x10^5$/sample in DMEM media with 10% fetal calf serum and 1% antibiotics) using a dynamic

cell seeding technique (n=4).[64] The cell-seeded discs were then supplemented with DMEM and placed in a new culture well in an incubator under 37^{o}C and 5% CO_2. After culturing for 7 days, the cell viability and proliferation on the scaffolds was determined using a MTS assay.[64]

3.3.5.1 To test ability of MB to protect and preserve bioactivity of growth factor

The ability of BSA MB to protect the bioactivity of growth factor was determined using an IGF1 bioactivity assay. First, an IGF bioactivity assay was established using a 3T3 cell proliferation assay. Specifically, different concentrations (50, 200, 500 ng/ml) of IGF-1 were added to 3T3 cells plated at a density of 10,000 cells/well in 24 well tissue culture dishes and incubated for 4 days. After 4 days MTS cell proliferation assay was performed to determine the linear relationship between IGF1 concentrations and cell numbers. Our results have also shown that 500 ng/ml is the optimum concentration of IGF-1 for triggering maximum cell proliferation.

3.3.5.2 To Determine The Protective Function of MB On IGF1 Activity

IGF-1-loaded MB, MB alone and IGF alone (as negative) were exposed to 1,4-Dioxane and lyophilized. The dry residuals were resuspended in 1 ml DMEM. The residual IGF1 bioactivity was then determined as described above.

3.3.5.3 To Assess The Release of Bioactive IGF1 From Scaffold

MB-IGF-1 scaffolds and IGF-1 soaked phase separated scaffolds were incubated at 37^{o}C with 1 ml DMEM which served as release media. At various time intervals (12hrs, 1, 2, 3, 4, 5, and 6 days), the incubated media was collected for bioactivity assay and fresh media was then added. At the end of the study, the extent of IGF1 bioactivity in media was determined using IGF1 bioactivity assay.

3.3.6. In Vivo Evaluation of MB Scaffolds

To evaluate the *in vivo* biocompatibility, square sections (1 cm length x 1 cm breadth x 1 cm thickness) of salt leached, phase separated control, and MB scaffolds were implanted in the dorsal subcutaneous region of BALB/c mice (25gm body weight) from Harlan (Indianapolis, IN). After implantation for 7 days, the animals were sacrificed and the tissue explanted. The

tissue responses to scaffold implants were then analyzed histologically. Animals were cared for in compliance with protocols approved by the Institutional Animal Care and Use Committee (IACUC) at the University of Texas at Arlington.

3.3.7. Histological Analyses

All tissue samples were frozen sectioned into 10 □m thick sections using a Leica Cryostat (CM1850) (Leica Microsystems, Wetzlar, Germany). To assess the extent of gross inflammatory responses to the implants, some of the tissue sections were stained with haematoxylin and eosin (H&E). Microscopic images of H&E stained slides were used to assess the extent of implant-mediated fibrotic responses by measuring the extent of fibrotic tissue thickness. To assess the bioactivity of the released IGF-1, some of the tissue sections were stained with Masson's Trichrome blue in which nuclei stains blue-black and collagen stains blue.[1, 116] The relative intensity of trichrome blue was determined using the Measure RGB feature in NIH ImageJ and was expressed in arbitrary units per square mm.[114]

3.3.8. Evaluation of The Potential of Gelatin MB OSCeR Scaffolds For Tissue Regeneration

While BSA MB scaffolds were able to preserve the bioactivity of loaded growth factor, it was not able to attract a lot of cells *in vivo* and *in vitro*. Gelatin has been shown to be conducive to cell growth and its extensive use in food, pharmaceutical and medical purposes due to its biosafety makes it very attractive for the development of OSCeR scaffolds. In addition, we have successfully synthesized stable gelatin MB in our early stage studies. 75:25 Poly (d, l-lactic-co-glycolic acid) PLGA with a molecular weight of 113 kDa was purchased from Medisorb (Lakeshore Biomaterials, Birmingham, AL), solvent 1, 4-dioxane from Aldrich (Milwaukee, WI) and gelatin from Sigma (St Louis, MO).

3.3.9. Synthesis of Gelatin Microbubbles

Gelatin microbubbles (MB) will be synthesized using 10% (w/v) gelatin using similar procedure as study 3.3.1.

3.3.10. Fabrication and Comparison of Gelatin MB OSCeR Scaffolds with BSA MB And Salt Leached Scaffolds

Using the same procedure as in study 3.2.2.2, gelatin MB OSCeR scaffolds will be fabricated. Characterization of such scaffolds under SEM and determination of porosity will be done as in study 3.2.2.3. This data will be compared with the porosity and mechanical strength of BSA MB and salt leached scaffolds.

3.3.11. In Vitro Comparative Assessment of Gelatin MB OSCeR Scaffold With BSA MB and Salt Leached Scaffolds

For *in vitro* cell growth study, 3T3 cells were seeded on square sections (1 cm x 1 cm x 1 cm) of gelatin MB OSCeR scaffold, BSA MB and salt leached scaffolds as detailed in study 3.2.2.4. After culturing for 7 days, the scaffolds were stained with CFDA-SE stain as previously described,[64] and imaged under the microscope.

3.4 Results

3.4.1 Characterization of BSA MB

BSA MB were synthesized and then used as growth factor carrier and tissue scaffold porogen. Following sonication, one ml of BSA solution usually generated 0.8 ml of MB. The synthesized MB observed under the microscope revealed a core-shell structure (Fig 3.1 A) and had a size range of 100 to 150 μm (Fig 3.1 B). The protein shell coupled with the low diffusivity nitrogen gas ensured that the MB are stable at room temperature and can be stored at 4^{o}C for up to 2 hours. The supplement of insulin-like growth factor-1 (IGF) in the process allowed the production of IGF-loaded MB. IGF-loaded MB exhibited similar morphology and size distribution as control BSA MB.

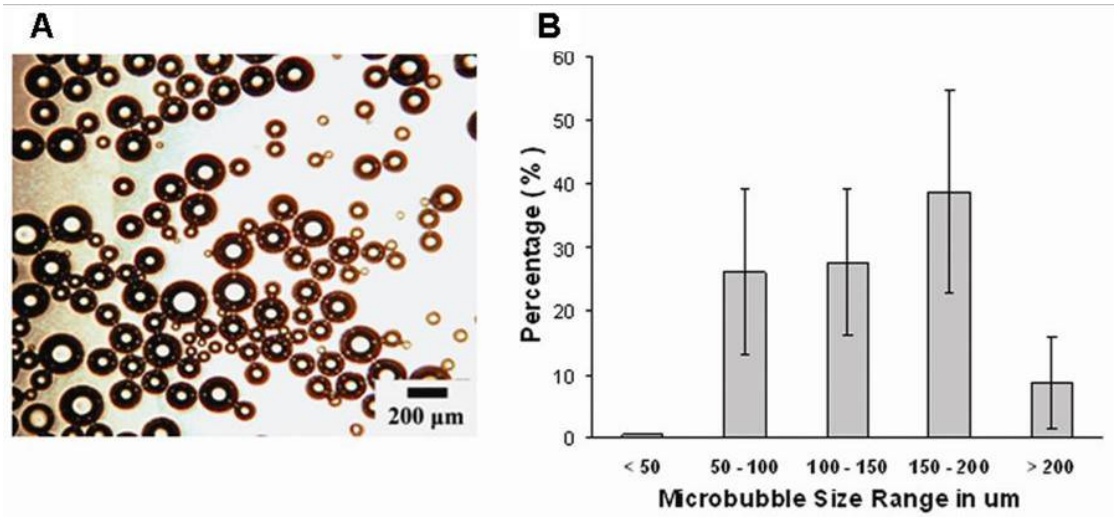

Figure 3.1 Microbubbles were placed on glass slides and observed under a light microscope (A). Optical images of the protein microbubbles were used to determine the size range distribution of the microbubbles (B). (Mag 100X; Scale bar 200 µm).
(Image from Nair et al., [2])

3.4.2 Characterization of BSA MB Embedded Scaffolds

By observing the cross sections of the MB embedded PLGA scaffolds under the SEM, we found that, without the addition of MB, phase separated scaffold shows porous structure with pore sizes ranging 10 to 30 µm (Fig 3.2 A and 3.2 B). MB embedded scaffolds (MB) are also highly porous. However, the pore sizes of MB scaffold were much larger ranging from 100 to 150 µm (Fig 3.2 C and 3.2 D). The interconnectivity of these pores in MB scaffold was very high, since a closer look at the microbubble loaded scaffolds showed a honeycomb-like structure with the presence of large interconnected pores (Fig 3.2 D).

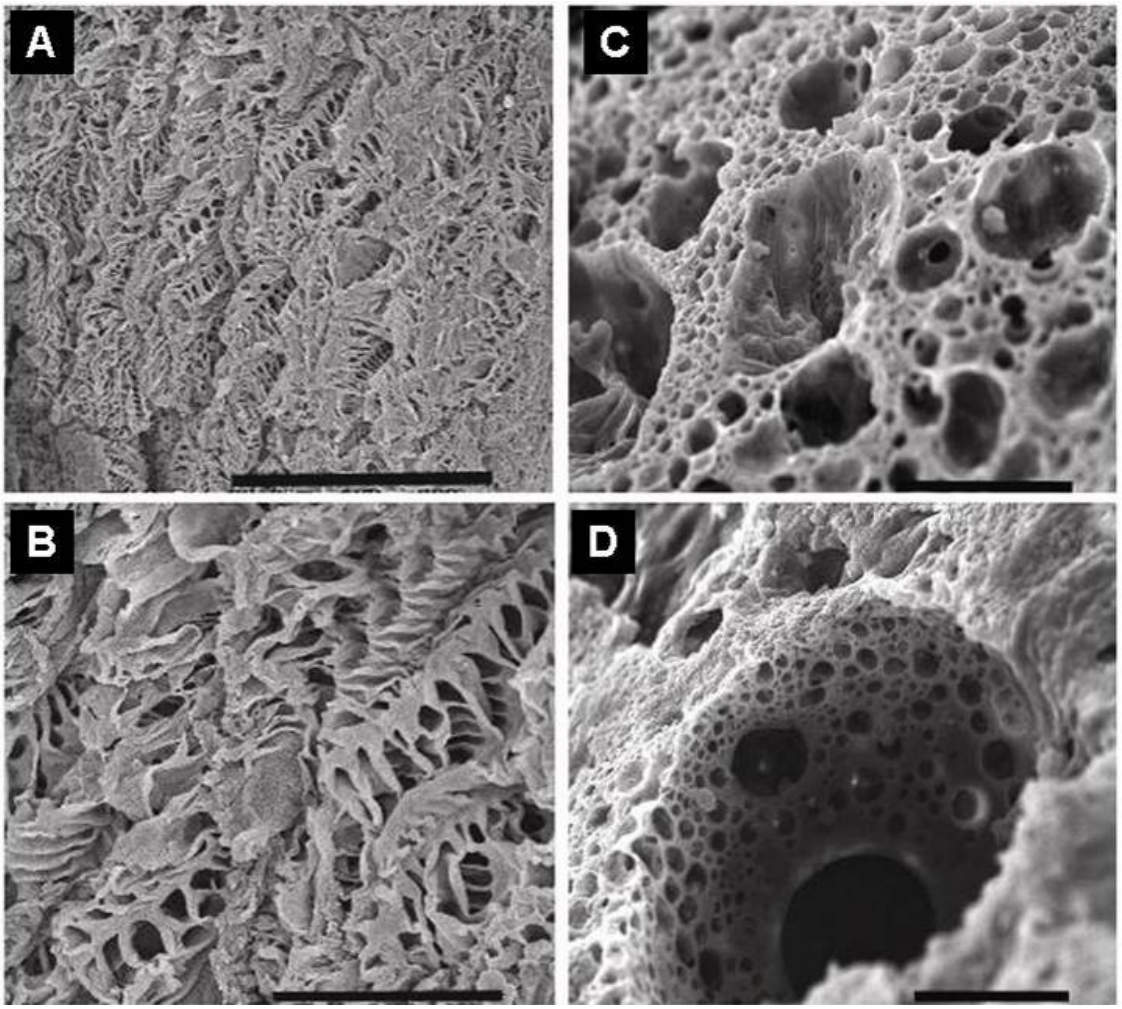

Figure 3.2 Scanning electron microscopy (SEM) analysis shows the porous structures of control phase separated scaffold with small pores in lower (A) and higher magnifications (B). On the other hand, BSA MB scaffold showed large pores and honeycomb-like pore-wall structure in lower (C) and higher (D) magnifications. (Scale bars = 100 μm). (Image from Nair et al., [2])

Under the SEM, consistent with surface morphology, control phase separated scaffolds showed an internal microporous structure in the range of 10 to 20 μm (Fig 3.3 A) and BSA MB-embedded scaffold showed the presence of large pores measuring around 100 to 200 μm (Fig 3.3 B). To further determine the role of MB in scaffold porosity, the distribution of MB in scaffolds was visualized using Coomassie Blue stain, which labels the protein with dark blue color. Indeed, almost all of the walls of large pores stained positive with Coomassie Blue stain (Fig 3.3 D). As expected, such localized Coomassie Blue stain could not be found in control

scaffold as no protein was added during the fabrication (Fig 3.3 C). These results support our idea that BSA MB can be used as porogens to create homogenous large-sized pore distribution throughout tissue scaffold.

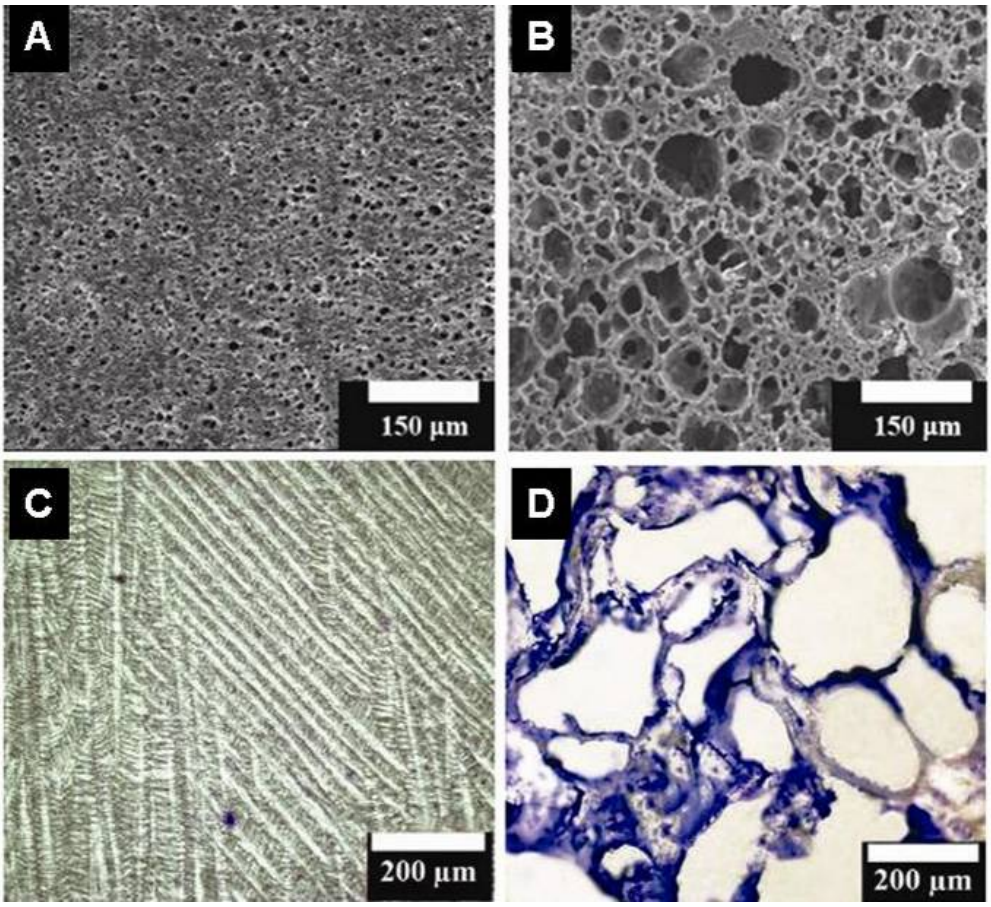

Figure 3.3 The cross section images of phase separated scaffold in the presence or absence of BSA microbubbles (MB). The morphology of control phase separated scaffolds (A) and BSA MB scaffolds (B) were observed under the SEM. To visualize the distribution of the MB in scaffold, scaffold sections were stained with Coomassie blue and observed under an optical microscope. Control phase separated scaffolds (C) MB-embedded scaffolds (D). (Mag 200X). (Image from Nair et al., [2])

3.4.3 Porosity and Mechanical Strength of BSA MB Embedded Scaffolds

To allow cell growth and tissue transplantation, it is critical that the MB-embedded scaffold have high porosity and good mechanical strength. We found that the porosity of the microbubble loaded scaffolds was comparable to that of the control phase separated scaffolds

(almost 92%) (Fig 3.4 A). These results suggest that the increase of pore size does not affect the overall porosity of the scaffold. However, large pore size may weaken the mechanical strength of the scaffold as seen in the compressive strength analysis of microbubble-embedded scaffolds compared to controls (Fig 3.4 B).

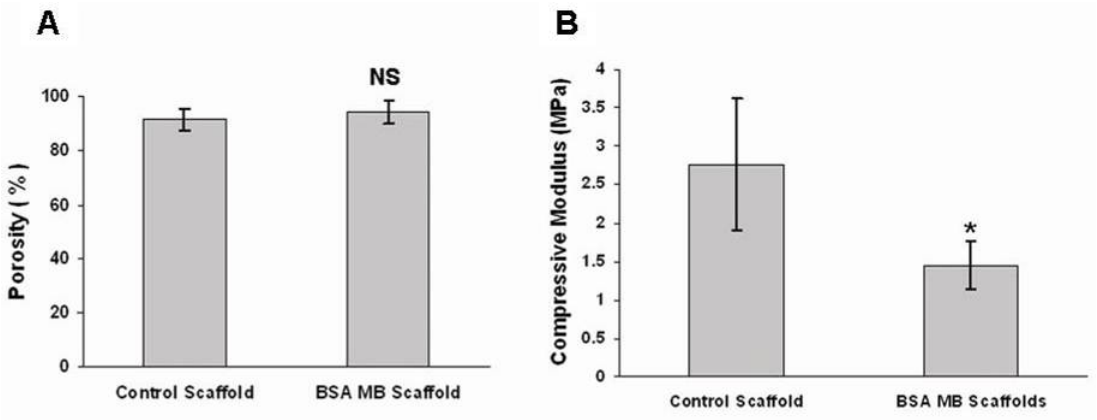

Figure 3.4 Physical and mechanical characterization of MB-embedded scaffolds. The porosity of the scaffolds was determined by ethanol displacement method and compared with control phase-separated scaffolds (A). Mechanical strength of MB-embedded scaffolds was compared with control phase separated scaffolds using a MTS mechanical tester (B). * $p < 0.05$ (Image from Nair et al., [2])

3.4.4 In Vitro Evaluation of BSA MB Embedded Scaffolds

Although BSA MB have been shown to be very biocompatible and have low cell cytotoxicity, it is not clear whether scaffold fabrication procedure would affect the biocompatibility and cell compatibility of BSA MB. To find the answer, both phase separated scaffolds and MB embedded scaffolds were seeded with 5×10^5 3T3 cells/scaffold and the proliferation of seeded cells on different scaffold was then determined. Surprisingly, we found that the incorporation of BSA MB in fact enhanced the cell proliferation by almost three times as compared with the control scaffolds (Fig 3.5).

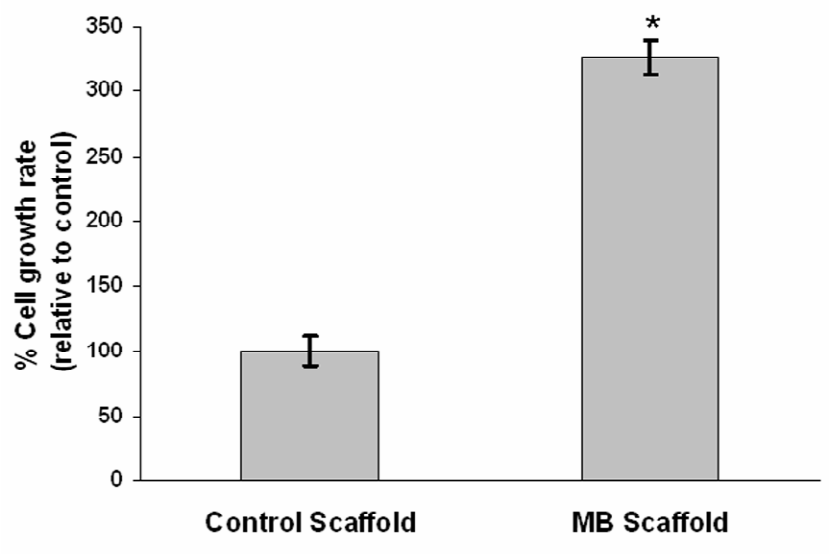

Figure 3.5 Growth rate of 3T3 cells on phase separated scaffold and microbubble-embedded scaffold (MB scaffold). Cells were grown on phase separated scaffolds (Control) and MB scaffolds for 7 days and percentage cell growth rates were determined relative to control. *p<0.05 (Image from Nair et al., [2])

3.4.5 In Vivo Evaluation of BSA MB Embedded Scaffolds

Using mice subcutaneous implantation model, the tissue compatibility of MB-embedded scaffolds was compared with two commonly used scaffolds - salt leached scaffolds and phase separated scaffolds made of the same materials. In agreement with earlier observations, prominent fibrotic tissue formation was found surrounding salt leached (Fig 3.6 A) and phase separated scaffolds (Fig 3.6 B). However, there was a significant reduction in the fibrotic tissue reaction elicited by the MB-embedded scaffolds (Fig 3.6 C). The statistical analyses confirmed our observations (Fig 3.6 D).

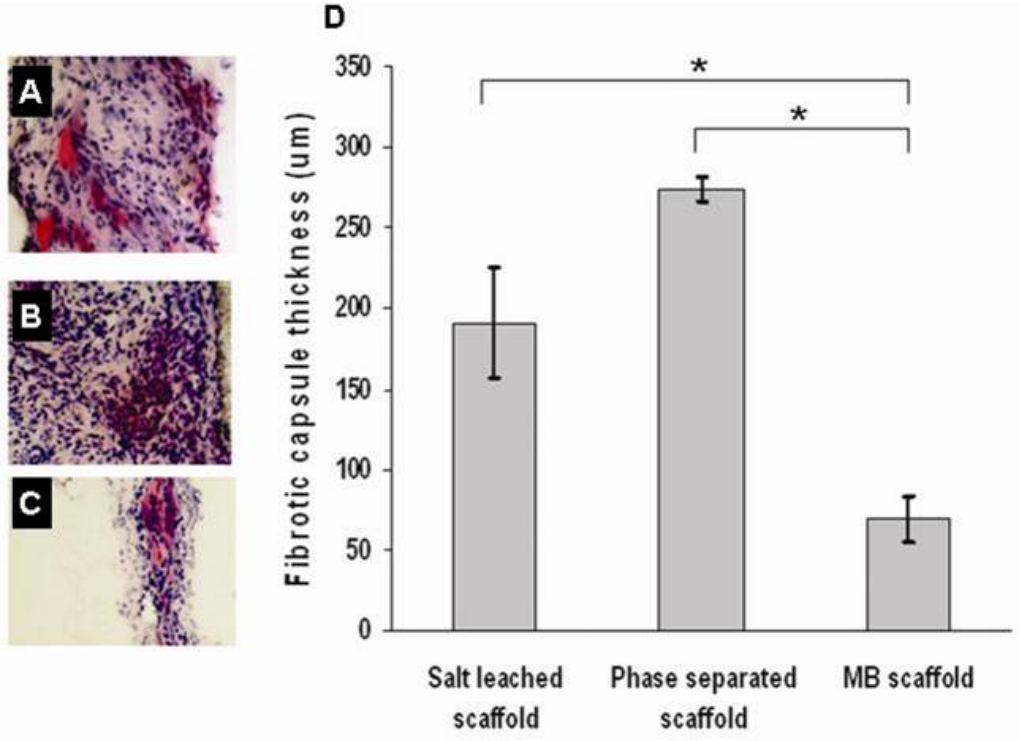

Figure 3.6 *In vivo* histological analysis of fibrotic tissue reactions surrounding MB scaffolds (A) compared to salt leached (B) and phase separated scaffolds (C). All images were taken at 200X magnification with scaffold toward the right edge of the tissues. Fibrotic capsule thickness measured using NIH ImageJ were quantified to reflect the extent of implant-mediated tissue responses (D). * $p<0.05$ (Image from Nair et al., [2])

3.4.6 Retention of IGF-1 Bioactivity by BSA MB

MB have been used to sheath growth factors and genetic materials from the inactivation of host enzymes and protein antagonists. We thus assumed that MB may be able to embed growth factors in scaffold and also protect their bioactivity from solvent denaturation during scaffold fabrication process. To test this hypothesis, IGF-1 was used as a model protein and a cell culture bioassay was established to determine the bioactivity of IGF1. We first determined whether MB can shield the growth factor from organic solvent inactivation. For that, scaffold fabrication process. To test this hypothesis, IGF-1 was used as a model protein and a cell culture bioassay was established to determine the bioactivity of IGF1. We first determined whether MB can shield the growth factor from organic solvent inactivation. For that, solutions of

IGF-1, BSA MB, and BSA MB loaded with IGF-1 (MB-IGF-1) (500 ng/ml) were added to organic solvent 1,4-dioxane, frozen and lyophilized. Post lyophilization, DMEM media was added to each group and then used in IGF-1 bioassays. As expected, IGF-1 alone lost almost all its bioactivity after being exposed to solvent. Solvent-incubated MB exerted minimal cell - proliferation activity (Fig 3.7 A). Most importantly, IGF-1 shelled in MB was found to retain most of its bioactivity (before vs. after solvent exposure: 500 ± 5 ng/ml vs. 150 ± 10 ng/ml). These results support our hypothesis that MB shield loaded growth factors from solvent inactivation.

3.4.7 In Vitro Release Curve of Bioactive IGF-1

We further determined whether growth factor releasing scaffold can be made using MB embedded scaffold fabrication technique. IGF-1 coated phase separated scaffold were used as negative control. Both groups of scaffolds were incubated with DMEM media with daily changes of fresh media. The bioactivity of IGF-1 in the collected media was then determined based on cell proliferation assay (Fig 3.7 B). In the case of IGF-1 coated scaffold, most of IGF-1 release occurred before day 1 and then dropped sharply. By day 3, there was almost no bioactive IGF-1 release from scaffold. On the other hand, MB-IGF-1 embedded scaffold showed a prolonged release of IGF-1 for at least 6 days. These results demonstrate that MB can be used to fabricate growth factor releasing scaffold.

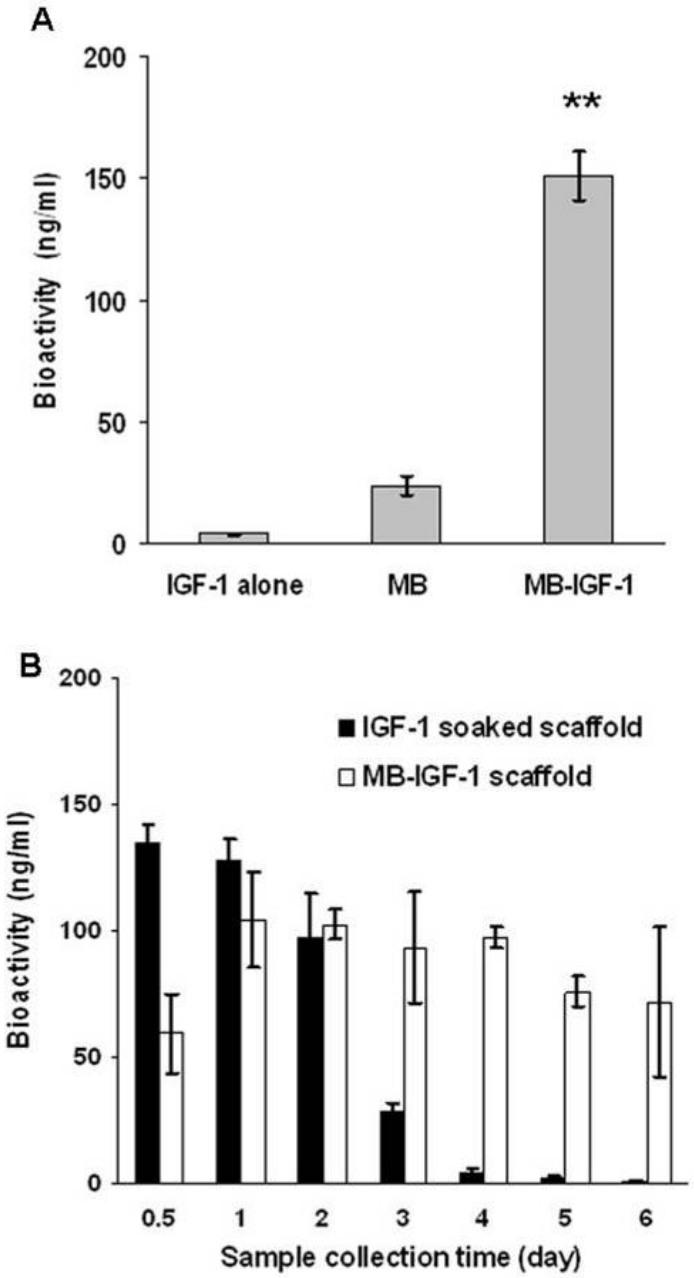

Figure 3.7 IGF-1 bioactivities of variously treated samples were measured based on cell proliferation assay. The effect of solvent on IGF-1 bioactivity was determined using solvent pre-exposed IGF-1 alone, MB alone and MB-IGF-1 as explained in methods. (Significance vs. MB control; ** $p < 0.01$) (A). The bioactivity of released IGF-1 from MB-IGF1 scaffolds and IGF-1 soaked scaffolds at different time points was assessed as shown in (B). (Image from Nair et al., [2])

3.4.8 In Vivo Bioactivity of IGF-1

Further studies were carried out to assess the effect of MB-IGF-1 embedded scaffold on tissue responses using a mice subcutaneous implant model. Since IGF-1 has been shown to enhance fibroblast proliferation and collagen production, the *in vivo* bioactivity of IGF-1 was assessed by histologically analyzing the extent of collagen production surrounding scaffold implants. The capsule region around the salt leached (Fig 3.8 A) and phase separated scaffold (Fig 3.8 B) showed sparse collagen formation after implantation for 1 week while low degree of collagen was found surrounding the MB scaffolds (Fig 3.8 C). However, as anticipated, the MB-IGF1 scaffolds (Fig 3.8 D) showed a well formed band of collagen around the implants. The quantitative analysis of the collagen deposition (based on intensity of collagen blue stain) confirmed the visual observations (Fig 3.8 E). These results clear demonstrated the ability of MB-IGF1 scaffold to release bioactive IGF-1 and to affect the surrounding tissue responses.

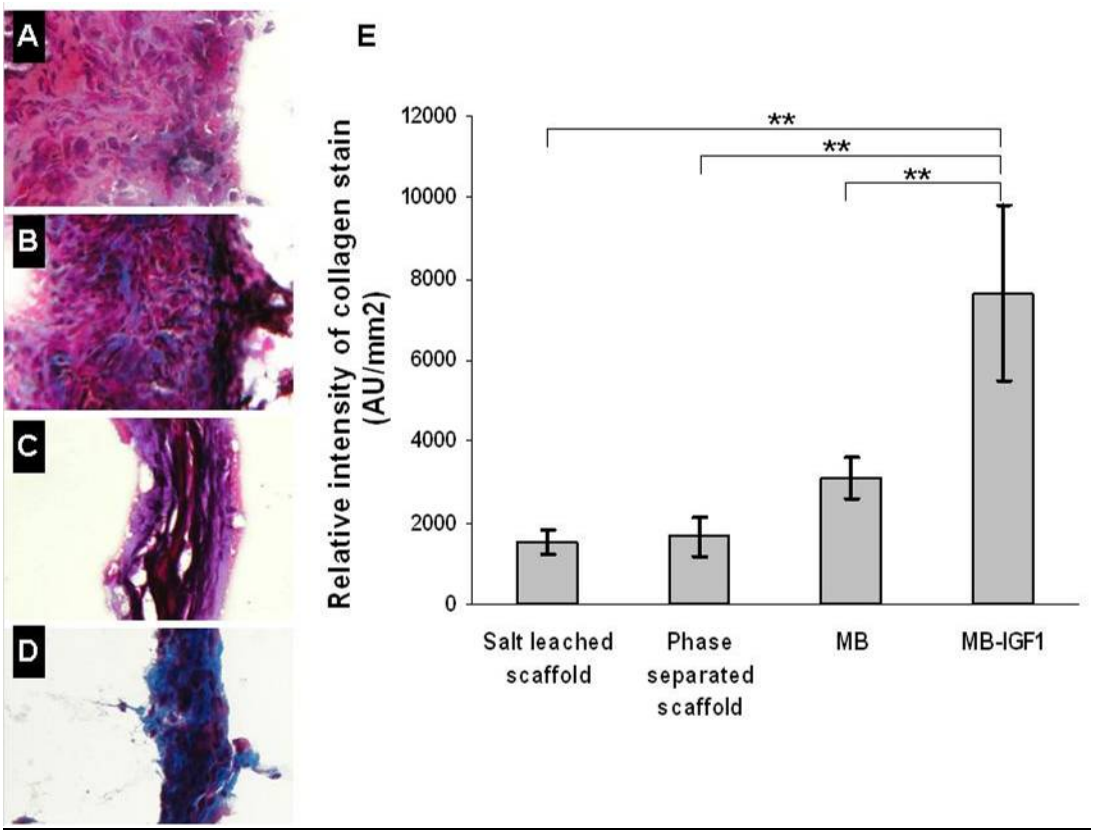

Figure 3.8 *In vivo* bioactivity of IGF-1 was determined based on collagen production. Tissue sections were histologically analyzed using Masson's trichrome blue staining (collagen stain) wherein, the blue coloration indicates presence of collagen (scaffold is to the right of fibrotic tissue). The fibrotic capsule around salt leached (A), phase separated scaffold (B) and MB scaffolds (C) were compared with MB-IGF1 scaffolds (D). All images were taken at a magnification of 200X. The quantitative analysis of collagen deposition was done based on intensity of blue color using NIH ImageJ. **p<0.01

3.4.9. Characterization of Gelatin MB OSCeR Scaffold

The synthesized gelatin MB observed under the microscope revealed a core-shell structure (Figure 3.9) and had a size range of 60 to 70 µm. The protein shell coupled with the low diffusivity nitrogen gas ensured that the MB are stable at room temperature and can be stored at 4^{o}C for up to 2 hours.

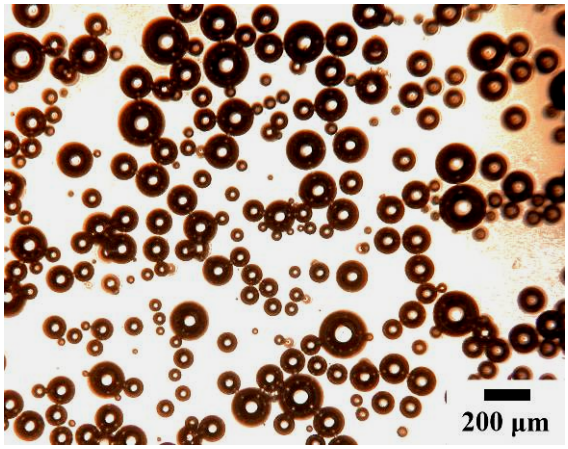

Figure 3.9 Optical micrograph of gelatin microbubbles observed under the microscope had an average size of 30 µm.

Similar to the BSA MB scaffold, as compared to the phase separated microporous scaffold controls (Figure 3.10 A), the gelatin MB OSCeR scaffolds showed the presence of larger pores with pore sizes almost 150 to 200 µm (Figure 3.10 B). Closer look at the scaffolds confirmed this observation (Figure 3.10 C).

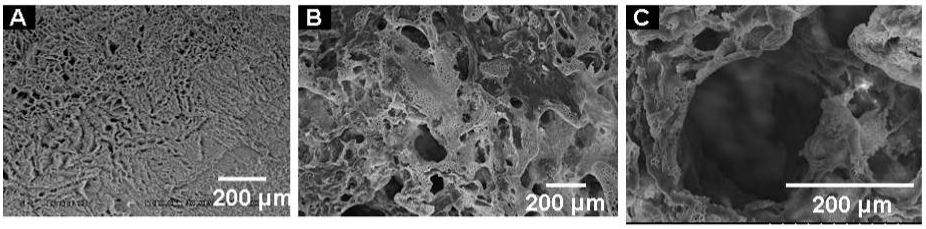

Figure 3.10 Compared to phase separated scaffold controls which showed a microporous structure (A) gelatin MB scaffolds showed larger pores in low magnification (B) and high magnification (C).

As earlier, Coomassie Blue staining showed the deposition of the blue dye along the pores in the gelatin MB OSCeR scaffold matrix, as compared to control scaffold, indicating the role of gelatin MB in pore formation (Figure 3.11).

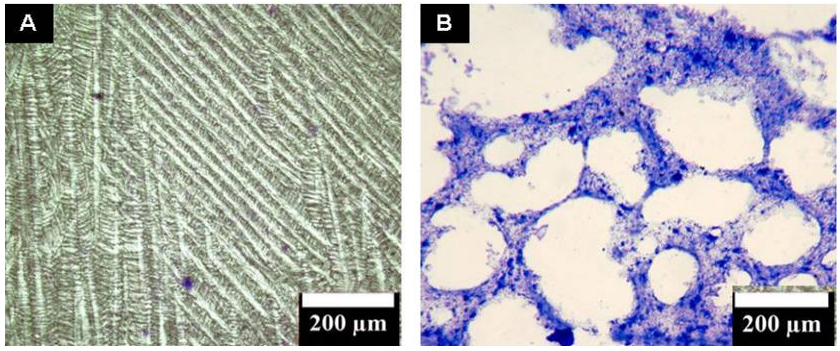

Figure 3.11 Control scaffolds without MB did not stain blue (A); Coomassie blue staining within the gelatin MB scaffolds indicated localization of gelatin protein within the matrix. (Mag 200X)

Porosity of the scaffolds was determined by ethanol displacement method as described earlier.[115] The comparison of porosity between gelatin MB OSCeR scaffold, BSA MB scaffold and salt leached scaffold showed that there was no significant difference between the scaffolds (Figure 3.12). This indicates that regardless of the method, the overall porosity is not compromised.

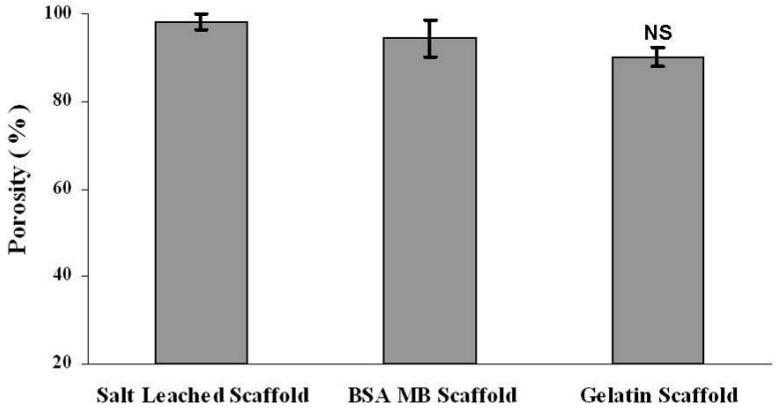

Figure 3.12 Comparison of the porosity of gelatin MB scaffolds with Salt leached and BSA MB scaffolds showed that there was no significant difference between the scaffolds.

3.4.10. In Vitro Evaluation of Gelatin MB Scaffold

The cell interaction with the scaffolds was studied over 7 days wherein 3T3 cells were seeded on gelatin MB scaffolds along with salt leached and BSA MB scaffolds. Gelatin MB

scaffolds (Figure 3.13 B) provided a more favorable surface for cell attachment followed by salt leached scaffolds (Figure 3.13 A) and then BSA MB scaffolds (Figure 3.13 C).

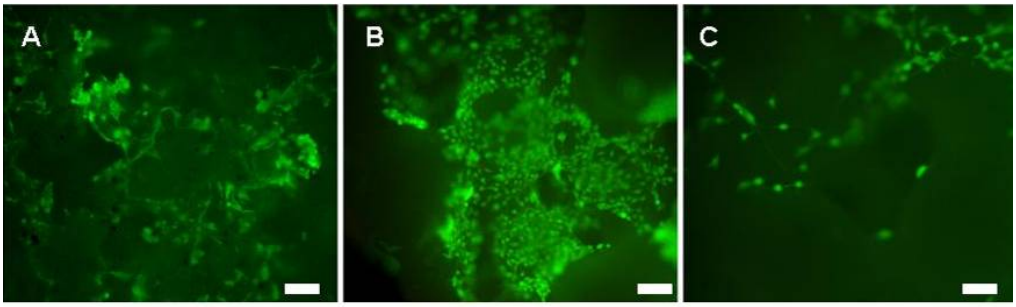

Figure 3.13 3T3 cells were seeded on salt leached scaffolds (A), gelatin MB scaffolds (B) and BSA MB scaffolds (C). Cells showed greater affinity to gelatin MB scaffolds as compared with salt leached and BSA MB scaffolds. (Scale bar 100 µm; Mag 100X)

3.4.11 In Vivo Suitability of Gelatin MB OSCeR Scaffold

Subcutaneously implanted gelatin MB OSCeR scaffolds (Figure 3.14 B) were histologically analyzed and compared with salt leached (Figure 3.14 A) and BSA MB scaffolds (Figure 3.14 C). The extent of inflammatory response was assessed based on the thickness of fibrotic capsule around the scaffold (Figure 3.14 D). Gelatin MB OSCeR scaffolds showed intermediate capsule thickness suggesting moderate inflammatory response, with salt leached scaffolds eliciting the highest and BSA MB scaffolds the least. Cell infiltration in the scaffold matrix was assessed by quantifying the cell numbers inside the scaffold based on DAPI staining. As expected, BSA MB scaffolds showed the least cell infiltration. Interestingly, gelatin MB OSCeR scaffolds showed the maximum cell infiltration inside the scaffold as compared to even salt leached scaffold (Figure 3.14 E). This finding validates our hypothesis that gelatin can prove conducive for cell infiltration.

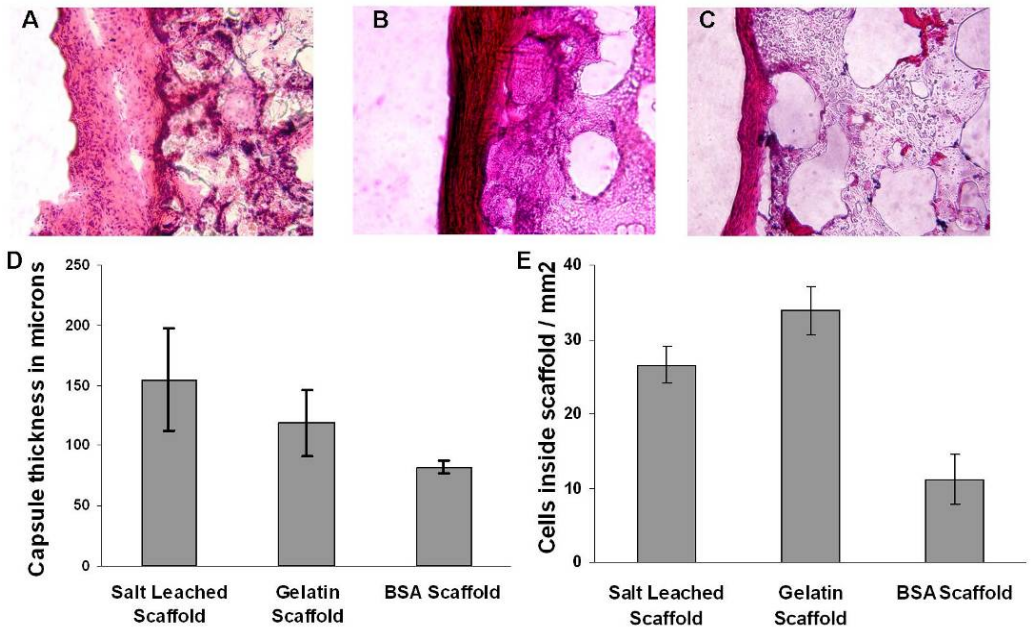

Figure 3.14 *In vivo* evaluation of gelatin MB scaffolds to serve as OSCeR scaffolds. Salt leached scaffolds (A) and BSA MB scaffolds (B) served as controls for the *in vivo* comparison with gelatin MB scaffolds (C). Quantification of the extent of fibrotic reaction elicited by the scaffolds (D) and cell infiltration inside the scaffold (E). Mag 200X Data expressed as mean ± SD.

3.5 Discussion

Ensuring the bioactivity of growth factors and other biomolecules delivered by scaffolds is one of the major hurdles in tissue engineering.[117, 118] This challenge arises primarily due to the incompatibility between proteins and organic solvents used in fabricating scaffolds. Using nitrogen gas filled protein MB as porogen, a novel scaffold fabrication technique has been established here to produce porous and growth factor releasing scaffold. Their suitability to serve as OSCeR scaffolds has also been assessed.

For fabricating MB-embedded scaffold, phase separation technique was used since the technique yields scaffolds with high porosity and interconnectivity albeit with small pores.[6] MB were found to be stable at low temperature and could be lyophilized and then resuspended.[108] Our studies have shown that MB are easy to synthesize and incorporate in scaffold. It should be noted that MB are stable at room temperature possibly due to the superior

stability of protein coating around the bubble as suggested by earlier studies.[108] In addition, earlier studies have shown that nitrogen gas with low diffusivity has been used commercially (in Imagent, AF0150) to stabilize the MB.[119] The stability of MB may be further improved using lower diffusivity gases like sulfur hexafluoride and perfluorocarbons.[120]

The overall porosity of the MB embedded scaffolds was comparable to scaffolds fabricated using other techniques.[6, 101, 102] However, the porosity of microbubble embedded scaffold can be easily engineered by altering the polymer concentration and volume ratio between polymer solution and MB. We noticed that the mechanical strength of the MB scaffolds is slightly weaker than control scaffolds. Although the main cause of such mechanical property change is yet to be determined, the large pores created by MB are likely to be the reason. The cross-sections of microbubble scaffolds showed a honeycomb-like pore wall structure with large pores (100-150 μm) differing from smaller sized pores (10 to 20 μm) found in the control phase separated scaffold. The small sized pores are formed by dioxane crystals formed during the quenching process.[102] The larger pores can possibly be attributed to the protein MB based on several lines of evidence. First, the large pore size and MB have similar size range (100-150 μm in case of BSA MB and 50 to 70 μm in case of gelatin MB). Second, large pores coincide with Coomassie blue protein staining,[6] indicating that large pores are co-located with MB. Third, protein MB-embedded scaffolds possess high cell seeding affinity which is a typical property found on BSA coated scaffolds.[121]

Using an *in vivo* implantation model, BSA MB scaffolds were found to be more tissue compatible than salt leached and phase separated scaffolds with similar porosities. The improved tissue compatibility is likely to be associated to the presence of MB for the following reasons. First, BSA has been shown to block or limit unfavorable protein adsorption/denaturation which is thought to be a major initiating step in the inflammatory response.[122] Second, albumin coating has been shown to reduce inflammatory responses to tissue scaffolds and polymeric materials.[122, 123] At the same time a comparative study

between gelatin MB scaffolds, BSA MB and salt leached scaffolds showed that gelatin with intermediate inflammatory response allowed for the greates cell infiltration inside the scaffold matrix. This suggests that gelatin MB scaffolds are good candidates to serve as OSCeR scaffolds.

Further studies have revealed that MB can not only be used as porogen but also as a growth factor carrier. Although MB have been shown to protect proteins and activity of genetic material,[109] the ability of MB to protect the bioactivity of growth factors during scaffold fabrication procedure had not been determined. In fact, our *in vitro* studies have shown that the bioactivity of IGF1 was preserved when embedded in MB. Furthermore, growth factor releasing scaffold can be made following similar scaffold fabrication process with growth factor-loaded MB. This two-step process enables fabrication of variety of growth factor eluting scaffolds which is substantially simple and versatile compared to commonly used loading methods.[10]

This MB scaffold fabrication technique provides a unique opportunity to explore the effect of a wide variety of growth factors in different tissue engineering application, tissue regeneration and wound healing processes. Specifically, erythropoietin (Epo) has been shown to enhance endothelial progenitor cell (EPC) differentiation both *in vitro* and *in vivo*,[124] and also early stage endochondral ossification.[125] Such growth factor loaded scaffolds can also be used for bone tissue engineering (requires pore sizes of 100-150 μm).[126] We believe that further studies and developments of this novel fabrication technique may lead to the development of more cell and biocompatible tissue engineering products. Assimilation of all this information supports the assumption that MB (both BSA and gelatin) embedded scaffolds can serve as OSCeR scaffolds.

CHAPTER 4

EXPLORATION OF OSCeR TECHNIQUES IN CREATING BONE AND VASCULAR TISSUE IN MICE

4.1 Introduction

Our studies have found that stem cells can be recruited around a biomaterial implant in the peritonea as well as in subcutaneous space. Quite a few studies have met with fair amount of success in cellularizing scaffolds, but its culmination into functional tissues is yet to be realized. Since more work needs to be done to utilize this phenomenon, strategies focused at differentiating the recruited autologous stem cells into a specific phenotype need to be developed. In our studies until now, we have found that multipotent autologous stem cells are recruited around an implant. These cells could be differentiated *in vitro* and *in vivo* into specific lineages, by delivering suitable differentiation agents. We have also developed a novel scaffold fabrication technology that can be used for fabricating Orchestrated Stem Cell-based Regeneration (OSCeR) scaffolds, delivering a growth factor or cytokine with preserved bioactivity. In this aim, we make use of the phenomenon of spontaneous recruitment of autologous stem cells around a biomaterial implant for two clinically relevant applications – namely, bone tissue engineering and vascular tissue engineering.

4.2 Bone Tissue Engineering

More than 6 million bone fractures occur every year, and a significant number of such fractures experience impaired healing and nonunions.[127, 128] If left untreated, the patient's day to day activities can be severely impaired. Bone can heal without scar formation, but this regenerative process falls short in patients with large lesions and defects and impaired wound

healing, which mandates clinical intervention.[129] Among the various treatment alternatives discussed in chapter 1, autografts are in short supply and associated with donor site morbidity and infection; allografts have concerns of disease transmission and host response; while artificial materials like metal alloys necessitate the removal of adjacent bone. In addition they have concerns of friction and wear debris at the prosthetic – bone interface.[130] These limitations mandate the development of tissue engineering strategies to facilitate bone regeneration.

Many bone tissue engineering strategies involve the use of biomaterials in the form of scaffolds or particles. Regardless of the biomaterial form, the success of osteogenic tissue regeneration using biomaterials relies on several factors. Firstly, the biomaterial should be biocompatible and processable into a 3-D shape. Secondly, it should be osteoconductive and thirdly, it should degrade into non-toxic products. Additionally, it should have large enough porosity to facilitate cell ingrowth and support cell proliferation and differentiation.[131] Natural polymers like collagen,[132] chitosan,[133] alginate,[134] and silk,[135] have been considered for bone grafts, but they have very poor mechanical properties. Calcium phosphate ceramics, like β-tricalcium phosphate and hydroxyapatite, have good osteoconductivity but their mechanical properties are found lacking.[131] Polymeric biomaterials are advantageous, in the sense that they are more flexible than ceramics. Their mechanical strength and degradation can be controlled by careful selection of materials. Poly(propylene fumarate) which is often used has biocompatible degradation products and has good load bearing properties often is found lacking when it comes to cortical bone related applications.[136] Frequently studied bone tissue engineering polymers include poly (α-hydroxy esters) such as PLLA, PGA and PLGA have all been approved by the FDA and are capable of delivering growth factors and facilitating cell growth.

A lot of research is being done on growth factors and delivery mechanisms that can maintain their activity. Some of the key cytokines involved in bone formation is transforming

growth factor-β (TGF- β) which is an abundant mitogen in the human bone extracellular matrix. It plays a vital role in cell growth and differentiation during developmental stages and also in tissue repair.[137] It belongs to the superfamily TGF which also includes BMPs. BMPs are low molecular weight glycoproteins and include more than 40 types. BMPs are synthesized in the cells as a precursor and some studies have found that a high dose of BMP-2 can induce progenitor cells to differentiate into osteoblasts.[138] *In vitro*, BMP-2 by itself is found to be highly osteo-inductive. Its use has shown positive in ectopic and orthotopic bone generation in rodent,[139] rabbit, [140] and canine models.[141] It is also known that fibroblast growth factors (FGFs), insulin-like growth factors (IGFs), platelet derived growth factors (PDGFs) and epidermal growth factors (EGFs) stimulate MSC differentiation into osteoblasts.[142] However, what is significant are a few recent findings which have established that angiogenesis is essential for osteogenesis.[128] Vascular endothelial growth factor (VEGF) is one of the key agents that promotes angiogenesis.[143] PLGA scaffolds were employed for the controlled release of VEGF and platelet derived growth factor (PDGF). This dual release was capable of forming a well developed vascular network than release of one factor alone.[144] Similar studies were done, wherein gelatin microparticles were used to release VEGF and BMP-2. This study found that such dual cytokine releasing systems were capable of bridging a critical size defect in rats.[128] Interestingly, quite a few studies of late have shown that delivering multiple cytokines, like angiogenic and osteogenic together, has a more pronounced effect on bone tissue engineering.[128, 130, 145, 146] Since bone is a highly vascularized tissue, it is plausible that angiogenesis might have a major role to play in bone regeneration by supporting MSC and osteoblasts. Vascular endothelial growth factor (VEGF) has been used in the past and serves as a very good angiogenesis inducing agent. A previous study showed that VEGF and BMP-2 delivery at an ectopic site using collagen gels resulted in increased capillary density and bone formation over 3 weeks as compared to BMP-2 alone.[147] However, the efficacy of such strategy in a critical size defect *in vivo* was not examined.[128] In a more recent study, a similar

strategy was adopted for rat calvarial critical size defect.[128] Also, there was no emphasis on positively harnessing stem cells which could have potentially changed the outcome of the study for better. In this light, it must be mentioned that Erythropoietin (Epo) is a cytokine which shares genetic and functional homologies with VEGF.[125] Quite similar to VEGF, it is proangiogenic and acts by VEGF and nitric oxide (NO)-dependent pathways. In fact it was found that Epo treatment was associated with VEGF and endothelial Nitric Oxide Synthase (eNOS) detection around 7 to 14 days after bone fracture contributing to ossification.[148] Epo-Receptor expression goes up in the early stages following bone injury and goes down upon treatment with Epo. Our recent findings on the presence of progenitor cells in the peritoneum that showed pro-angiogenic signs bolsters our justification for the use of Epo for the subsequent studies.

However, there are some problems with existing strategies. Most of these problems stem from the breakdown of the biomaterial implant, debris, lack of cellularization and detachment of cells. Hence, recent strategies have revolved around the use of transplantation of stem cells in the biomaterial scaffold. For example, osteoblasts and embryonic stem cells have been used along with polymeric scaffolds for bone regeneration studies.[149, 150] Mesenchymal stem cells have also been cultured on scaffolds and differentiated into an osteogenic phenotype *in vitro*.[151-153] However, these studies require the cumbersome isolation, time consuming *in vitro* culture and differentiation of stem cells. In this light our, studies (Specific Aim 1 - Chapter 2) have shown that multipotent autologous stem cells can be recruited around a biomaterial implant in the form of both scaffolds and microspheres. In addition, we also found that delivering a differentiation agent could differentiate these cells into an osteogenic lineage within the scaffolds over 8 weeks.

Significant progress has been made in regenerative bone tissue engineering in various areas. Briefly, it has been shown that PLGA was more suitable for attachment and osteogenic differentiation of osteoprogenitor cells.[154, 155] Drawbacks with existing strategies have necessitated the use of growth factors and proteins. However, such osteoinductive factors

cannot be delivered directly as the protein might become unstable and lose their bioactivity.[156] Studies have found that scaffolds decorated with natural extracellular matrix (ECM) materials such as collagen, gelatin, glycosaminoglycans and self-assembling peptides direct preferable osteogenic responses.[14, 151] A few studies have found that gelatin is a preferred material for growth factor and cytokine release for various reasons. Gelatin which is derived from the hydrolysis of collagen is identical in composition to collagen and is mechanically tough.[157] It evades concerns of immunogenicity and pathogenicity associated with collagen. [117, 157-160] Hence, based on our results from Chapter 3 - Specific Aim 2, OSCeR scaffolds seemed like a suitable candidate to serve as a growth factor carrier.

4.2.1 Hypothesis

OSCeR scaffold loaded with suitable angiogenic and osteogenic growth factors can aid osteogenesis in a critical size defect.

4.2.2 Materials and Methods

4.2.2.1 Materials

75:25 Poly (d, l-lactic-co-glycolic acid) PLGA with a molecular weight of 113 kDa was purchased from Medisorb (Lakeshore Biomaterials, Birmingham, AL). The solvent 1, 4-dioxane was purchased from Aldrich (Milwaukee, WI), gelatin was purchased from Sigma. Erythropoietin (Epo) was purchased from Cell Sciences (Canton, MA) and BMP-2 from R&D Systems (Minneapolis, MN). OsteoSense 800 was purchased from VisEn Medical (Woburn, MA).

4.2.2.2 Fabrication of OSCeR Scaffolds

OSCeR scaffolds were fabricated using the similar published procedure as in chapter 3 using gelatin microbubbles.[2] Various scaffold groups were fabricated using the gelatin Epo microbubbles loaded with combinations of growth factors. The groups were: Epo, BMP-2 and Epo + BMP-2.

4.2.2.3 Critical Size Defect and Animal Model

While our aim has been to make the strategy developed in this study applicable to bone defect in general, we have used a critical size defect in the skull of mice as a model to test our strategy. The critical sized defect model was selected as it allows us to noticeably identify the effect of treatment.[128, 130, 161] Surgical repair of skull defects remains a challenge for craniofacial surgeons. It leads to headaches and delay in mental development of young children. There is very limited published data available concerning the management of such deformities.[162]

Our selection of a murine model is because mouse models have been well established to study body's reactions to implanted biomaterials. Moreover, the skull of the mice resembles that of new-born babies and infants and hence can serve as a good model to study the translatability of this technique into clinical correction of craniofacial defects. Finally, to mimic responses in human, there is no lower species suitable for these studies.

Balb/c mice were anesthetized using isoflurane inhalation. Following anesthesia, a linear scalp incision was made from the nasal bone to the occiput and full thickness flaps elevated. The periosteum overlying the calvarial bone was completely resected. A trephine was used to produce a 3 mm craniotomy defect centered on the superior sagittal sinus. The wound was irrigated with phosphate buffered solution (PBS) continuously while drilling. The calvarial disk was removed carefully so as to avoid injury to the underlying dura or brain. The PLGA scaffolds cut to the dimensions of the defect were placed in the defect. Untreated cranium, wherein no scaffold was placed at the size defect served as control. The skin was sutured over the implant using 5-0 Vicryl suture. Animals were then placed in the recovery cages, kept warm and closely observed till recovery from anesthesia. To avoid damage to the implant from other animals, each implanted mouse was housed individually. The surgical procedure usually took

20 minutes per animal and the animals were cared for 4 weeks. At the end of 4 weeks, the osteogenic activity was monitored followed by histological analyses.

4.2.2.4 *In Vivo* Monitoring of Osteogenic Activity Using OsteoSense 800

A balance between osteoblast and osteoclast activity indicates normal development and maintenance of the skeleton. A major indicator of osteogenic activity is the formation of hydroxyapatite (HA), which is the major mineral product of osteoblasts. Detection of HA is, thus, an indicator of osteoblast activity. Near Infrared (NIR) light (700 to 900 nm) has deep photon penetration, low background autofluorescence and is advantageous for *in vivo* imaging of various targets.

OsteoSense 800 (ex/em 760/830, 45s exposure, 8x8 binning, f-stop 2.5, 120mm field of view) is a near infra-red (NIR) dye that can bind with high affinity to HA. The dye was administered by local subcutaneous injection (0.1 nM / 50 µl) 24 hours before imaging using a Kodak *In Vivo* Imaging system. After 24 hours, the animals were euthanized by carbon monoxide inhalation. The cranium was resected and stripped clean of brain tissue from below. The cranium was rinsed with PBS and imaged using the *in vivo* imaging system. Both fluorescence images of the defect as well as X-ray images were captured. Fluorescent images were overlaid on white light image. Optical density was quantified from the X-ray image. In addition, the HA activity based on OsteoSense intensity was correlated to the bone density based on X-ray.

4.2.2.5 Histological Analyses

Following *in vivo* imaging, the cranium was decalcified as follows. The cranium was washed with PBS for 3 times and then immersed in 10% EDTA solution with agitation at room temperature for 2 days. EDTA solution was changed every 6 hours. Thereafter, the tissues were rinsed with distilled water for 3 times and dried using blotting paper. The implants were then embedded in OCT and cryosectioned. Masson's trichrome blue was performed to determine collagen formation in which nuclei stains blue-black and collagen stains blue.[116] The relative

intensity of trichrome blue was determined using the Measure RGB feature in NIH ImageJ and was expressed in arbitrary units per square mm.[114] Osteoblast activity was immunohistochemically confirmed by osteocalcin formation and osteopontin formation.

4.2.3 Results

4.2.3.1 Monitoring Osteoblast Activity and Osteogenesis

Based on fluorescence intensity of OsteoSense 800, *in vivo* image analysis revealed that while there was very low indication of HA and almost no bridging of the defect in the untreated control, all the treatment groups showed signs of HA and some partial bridging of the defect (Figure 4.1 top and middle panel). In particular, quantitatively Epo treatment resulted in a significant increase in HA which indicates osteoblast activity. It was interesting to note that although significant compared to untreated control, the indications for HA in case of BMP-2 and Epo + BMP-2 was lower than Epo alone (Figure 4.1 bottom panel). Correlation of osteoblast activity based on intensity of OsteoSense and optical density based on X-ray imaging showed a high correlation, almost 0.8789, between the two (Figure 4.2).

4.2.3.2 Histological Assessment of Osteogenesis

Masson's Trichrome Blue staining was done on cranial cross-sections and the distribution of collagen in the OSCeR scaffold was visualized (Figure 4.3). The untreated control shows no bridging of the 3 mm gap (Figure 4.3 A). As compared to control, Epo loaded OSCeR scaffolds (Figure 4.3 B) showed collagen fibers within the scaffold. BMP-2 loaded (Figures 4.3 C) and Epo + BMP-2 loaded (Figures 4.3 D) showed moderate collagen fiber deposition. NIH ImageJ was used to quantify the collagen intensity based on blue staining. While it was found that BMP-2 exhibited significantly higher collagen staining than untreated control, both Epo and Epo + BMP-2 had much higher collagen fiber deposition than BMP-2 alone (Figure 4.3 E).

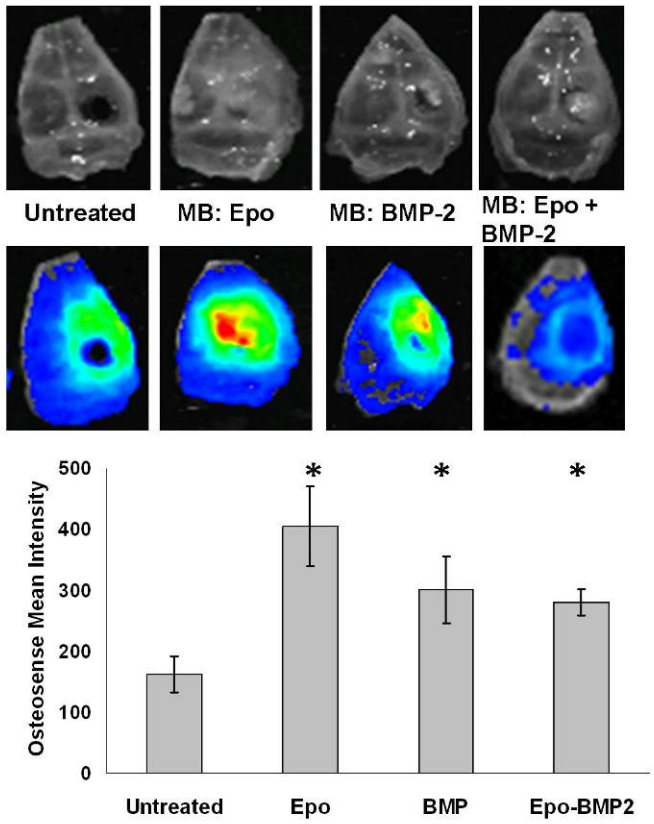

Figure 4.1 Hydroxyapatite (HA) production was determined using OsteoSense 800 (a NIR probe) that binds to HA. *In vivo* imaging system, used to scan the explanted cranium 24 hours after probe administration, showed the white light images (top panel) and the fluorescence images (middle panel). Quantitative comparison of mean intensity of OsteoSense 800 is shown (bottom panel).

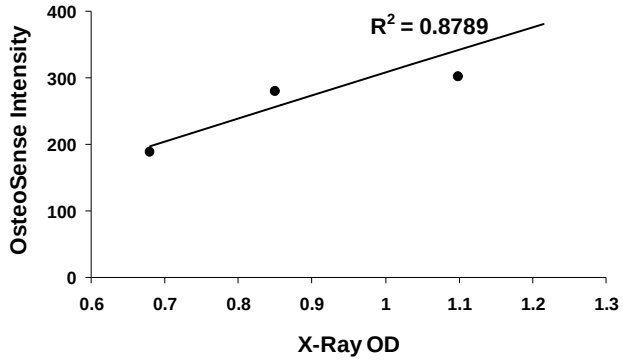

Figure 4.2 The OsteoSense 800 intensity, indicative of HA formation, was plotted against the optical density from the X-ray images and the regression coefficient calculated.

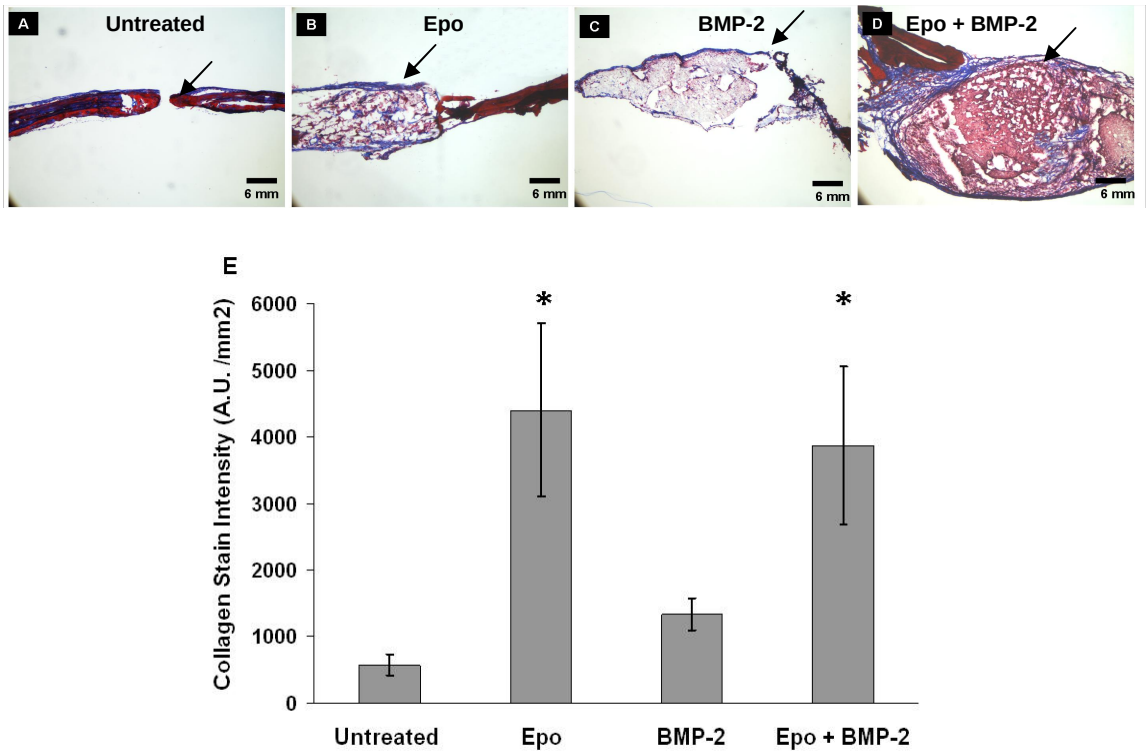

Figure 4.3 Masson's trichrome blue staining for collagen showed the untreated cranial defect showing no bridging of the gap (A). Epo (B), BMP-2 (C) and Epo + BMP-2 (D) loaded OSCeR scaffold groups are shown. Quantitative analysis of collagen staining was done as shown (E). (Mag – 100X)

As shown in figure 4.4 (upper panel), intensity of osteocalcin stain in untreated control was the least as compared to Epo, BMP-2 and Epo + BMP-2. Similarly, osteopontin formation was assessed. As with osteocalcin, osteopontin (figure 4.4 middle panel) also showed a similar trend, in that untreated control had the lowest intensity compared to Epo, BMP-2 and Epo + BMP-2. Also interesting to observe was the occurrence of blood vessels in the collagenous fibrotic tissue between the cranium and the Epo + BMP-2 scaffold (Figure 4.5).

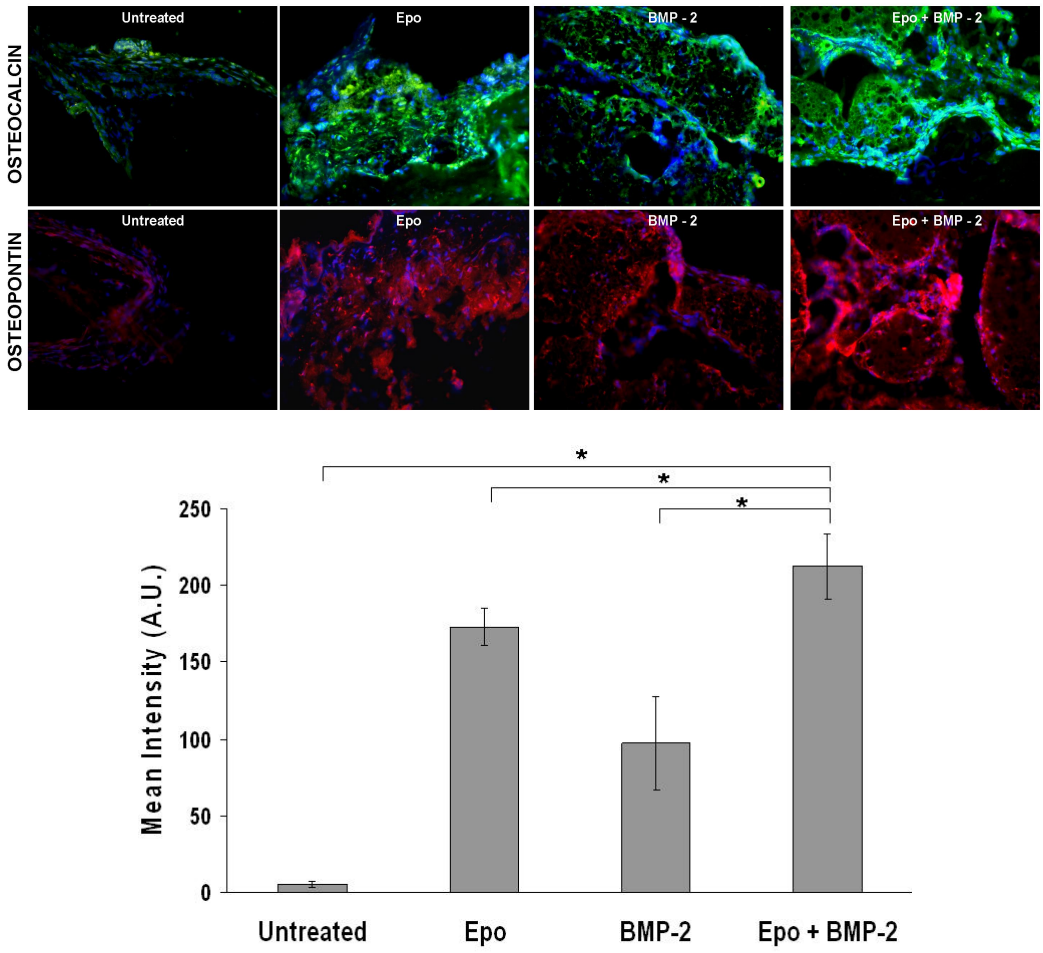

Figure 4.4 Osteocalcin (green – upper panel) and osteopontin (red – middle panel) formation in untreated control was compared with those treated with Epo, BMP-2, and Epo + BMP-2. (Mag 400X). Quantitative comparison of intensity of osteopontin staining is shown (lower panel). *p < 0.01

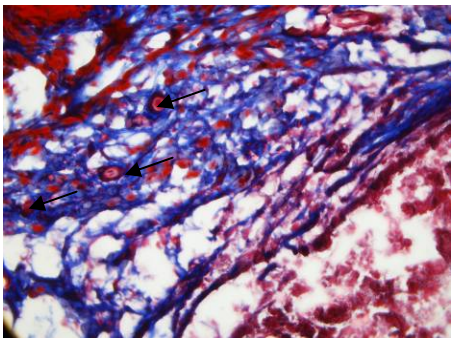

Figure 4.5 Blood vessels in the fibrotic tissue between the Epo + BMP-2 scaffold and the cranium (shown by arrows) (Mag 400X)

4.3 Vascular Tissue Engineering

Over the years, tremendous progress has been made in tissue engineering in general. However, the development of small diameter vascular grafts (SDVGs) for the treatment o cardiovascular diseases has encountered limited success. The main reasons are the poor mechanical properties and the poor blood compatibility. Dr. Jian Yang's group in UTA has recently successfully developed a novel degradable cross linked urethane-doped polyester (CUPE) with excellent physical and mechanical characteristics for use as SDVGs. To improve the blood compatibility of the CUPE tubes, increasing evidence suggests that endothelialization of the inner lumen of SDVGs would greatly improve their blood compatibility. Despite of the plethora of strategies available for enhancing endothelialization, almost all approaches have failed due to the inability to obtain sufficient autologous endothelial cells and prolonged *in vitro* cell isolation/culture.

Another clinically relevant condition that we try to find a solution for is cardiovascular disease. It remains a lethal disease, the treatment of which often involves the patients receiving coronary artery bypass graft making it among the most expensive conditions treated.[163] Autologous mammary and saphenous vein grafts are plagued by problems of unavailability and painful surgical procedures.[51, 164] Although synthetic grafts like Dacron or ePTFE met with a fair amount of success as large blood vessel grafts, they failed as small diameter vascular grafts (SDVGs). This was because of their inadequate blood compatibility and inability to prevent coagulation of blood along with thrombosis in low shear environment which is encountered in small blood vessels.[51] For that, surface conjugation of anticoagulants, such as heparin, has been used to improve the blood compatibility of vascular grafts. However, the short life-span of the anticoagulants *in vivo* substantially limits the effectiveness of anticoagulant coating. Currently, endothelialization of the vascular graft lumen has been shown to be the most effective approach to prevent coagulation and thrombosis.[51, 53, 54] Though autologous cells

are tolerated well than allogenic and xenogenic endothelial cells, it is difficult to obtain large number of autologous endothelial cells. The common source of the endothelial cells is from liposuction. Unfortunately, liposuction procedure can only been done on a small number of patients. Furthermore, the isolation and seeding of liposuction-derived endothelial cells in SDVGs is a time-consuming and expensive process.

It is now understood that the reasons for failure of existing grafts is the low compatibility and poor mechanical properties which leads to blood coagulation and thrombosis in low shear environments encountered in small blood vessels.[51] To meet the challenge of thrombosis, increasing evidence suggests that endothelialization of the vascular graft lumen may prevent coagulation and thrombosis.[51, 53, 54] Three popular means of endothelialization are (1) migration and co-option of pre-existing endothelial cells from adjacent vasculature, (2) recruitment of circulating endothelial progenitor cells from bone marrow, or (3) differentiated stem cells isolated from patients via liposuction. Since the graft surfaces are exposed to endothelial progenitor cells and, potentially, a variety of immune cells, it is an enormous challenge to create an environment that will allow endothelial progenitor cells (EPCs) accumulation and to produce endothelialized surfaces *in vitro*. In addition, most of the current approaches require the isolation and then culture of EPCs on vascular graft for a few weeks prior to transplantation As a result of these limitations, *in vitro* tissue engineering (involving cell isolation and culture *in vitro*) produces limited success despite of intensive research efforts.[165, 166] Recently, a new elastomeric material crosslinked urethane-doped polyester (CUPE) which matches a biological blood vessel in mechanical properties has been developed.[52] In addition, they have very good biocompatibility and hemocompatibility which makes them attractive for *in vivo* vascular graft engineering. Since vasculogenesis is a normal wound healing process,[167] it is possible that vasculogenesis can be induced to regenerate autologous graft *in vivo*.

Over the years, numerous studies have focused on the role of chemokines in angiogenesis and vasculogenesis. Some chemokines like Vascular Endothelial Growth Factor

(VEGF),[168] Stromal Derived Factor -1alpha (SDF-1α),[97] and Erythropoietin (Epo) [124, 169] have been implicated in stem cell, including EPCs, mobilization and differentiation. Our preliminary studies showed that Epo was potent in recruiting progenitor cells around the implant in the peritoneal and subcutaneous space. A previous study also showed that Epo treatment improves cardiac function and increased myocardial expression of VEGF, which in turn correlates with the neovascularization.[124, 170]

The peritoneum was chosen as the implantation site for our study for multiple reasons. Firstly, it has been found that biomaterial implantation in the peritoneum is associated with recruitment of a variety of cells including stem and progenitor cells.[78] Second, we have found, through our preliminary studies using peritoneal implantation of CUPE, that endothelial progenitor cells (EPCs) and endothelial cells (ECs) are found. Thirdly, studies using subcutaneous implantation sites have not been highly successful.[171-173]

4.3.1 Hypothesis

Vascular graft lumen can be endothelialized using OSCeR technology to spontaneously recruit endothelial progenitor cells.

4.3.2 Materials and Methods

4.3.2.1 Fabrication of CUPE Biphasic SDVGs

CUPE was synthesized as previously published by Dr. Yang's group in the journal Biomaterials.[52] The biphasic CUPE SDVG was prepared based on a previously published technique.[174, 175] The SDVG had a non-porous phase that was created by dip-coating a glass rod (outer diameter 3 mm) in 3% (w/w) CUPE0.9 in 1,4 – dioxane. The prepolymer coated rods were air-dried for 12 hours and subsequently cross-linked for 12 hours in an oven at 80^0C. The porous phase was prepared by mixing salt (150 to 250 µm) with CUPE0.9 in 1,4-dioxane in a 1:9 w/w ratio. After solvent evaporation, the paste was filled into a tubular mold (inner diameter 6 mm). The prepolymer coated rods were inserted into the tubular mold concentrically.

The construct was air-dried and polymerized at 80^0C for 4 days. Salt was leached out and the SDVG was allowed to swell in ethanol – water (50% w/w) and demolded from the rod.

4.3.2.2 Erythropoietin Coated Conduits

From our preliminary studies, we were able to establish that a concentration of 500 IU Erythropoietin (Epo), when coated in the SDVG lumen can help recruit endothelial progenitor cells (EPCs) and endothelial cells (ECs). Biphasic SDVGs were coated with Epo via spontaneous adsorption and implanted in the peritoneal space of Balb/c mice for 1 and 2 weeks. Uncoated CUPE SDVGs served as control.

4.3.2.3 Histological and Immunohistological Analysis

At the end of the study the animals were sacrificed and the SDVGs recovered for histological and immunofluorescence analysis. SDVGs were sectioned and analyzed using H&E and immunofluorescence using Stem cell antigen-1 (Sca-1) for HSC (shown by green) and CD31 for endothelial cells and CD133 for EPCs (both shown by red). The Sca-1+ CD133+ EPCs in both CUPE-Epo and uncoated CUPE controls were quantified and compared. α-smooth muscle actin (α-SMA) was used to locate smooth muscle cells.

4.3.3 Results

4.3.3.1 *In Vivo* Studies On Epo Coated CUPE SDVGs

The SDVGs explanted after 2 weeks showed signs of cellularization (Figure 4.6). CUPE control scaffolds showed scarce cellularization (Figure 4.5 A) while Epo coated CUPE SDVGs (Figure 4.6 B) showed extensive cellularization on the exterior.

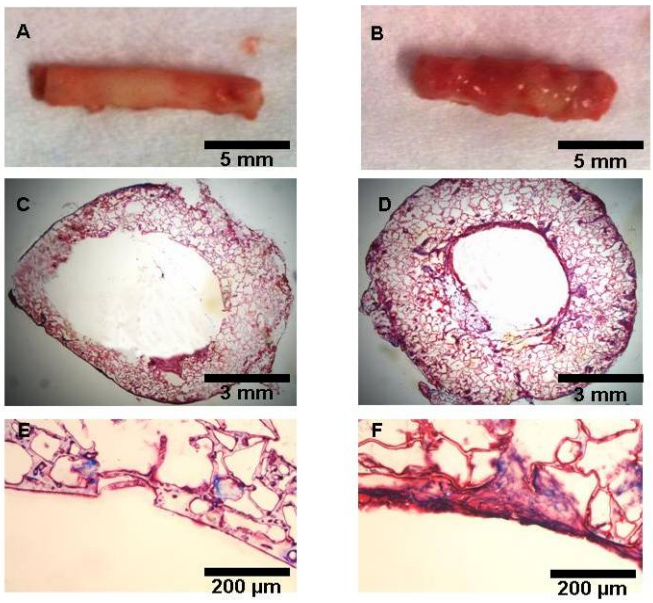

Figure 4.6 Digital image of explanted SDVGs after 2 weeks intra-peritoneal implantation; uncoated CUPE control (A) and Epo coated CUPE grafts (B). H&E stained cross-sections of uncoated controls (C- low mag; E- high mag) and Epo coated graft (D- low mag; F- high mag). (Low mag – 25 X; High mag – 200 X)

H&E stained image of control (Figure 4.6 C) vs. CUPE-Epo SDVG (Figure 4.6 D) showed barely any cells in the lumen of the control grafts, while the Epo coated grafts showed a more or less uniform coverage of cells in the lumen. A closer look at the lumen of control (Figure 4.6 E) and Epo- coated graft (Figure 4.6 F) confirms this.

Our immunofluorescence analysis showed that while uncoated controls showed almost no EPCs or ECs (Figure 4.7 A), Epo coated SDVGs had a smooth layer of EPCs (Sca-1+ CD133+ --- yellow) in the lumen by week 1 (Figure 4.7 B). By the second week there was an almost uniform coverage of ECs (Sca-1+ CD31+ --- yellow) (Figure 4.7 C) in the lumen. In addition, smooth muscle cells are seen based on α-SMA stain around the Epo-coated SDVGs (Figure 4.7 D). Quantification of the EPCs in the luminal space after 1 week showed that there was almost 3 times as many EPCs as compared to control CUPE grafts (Figure 4.7 E).

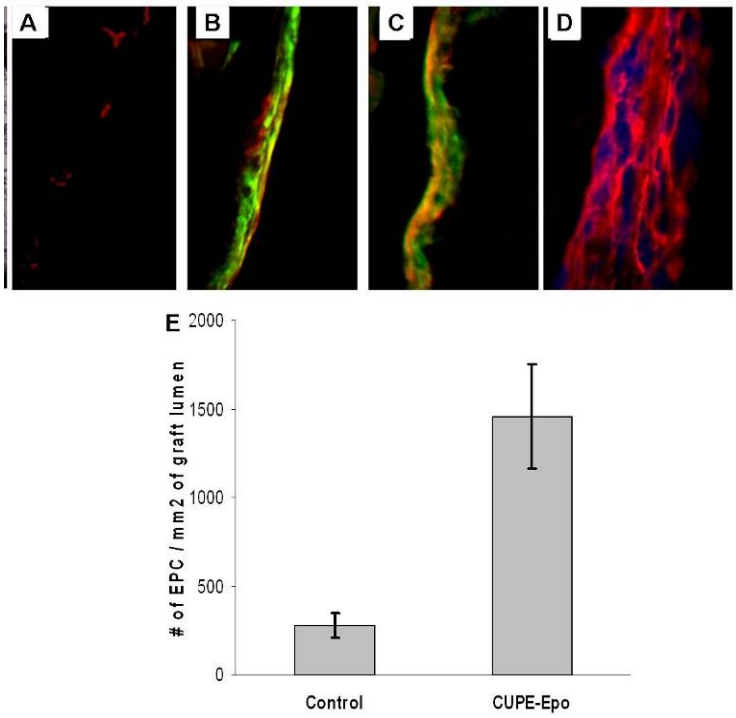

Figure 4.7 Based on immunofluorescence staining for EPCs (Sca-1+CD133+ - yellow) and endothelial cells (Sca-1+CD31+ - yellow), compared to uncoated control (A) Epo coated SDVG was endothelialized after 1 and 2 weeks (B & C respectively). Outer surface of graft covered with layers of smooth muscle cells as seen by α-SMA staining (D). EPCs in the graft lumen based on co-expression of Sca-1 and CD133 were quantified to estimate the number of EPC in recruited in the graft lumen (E).

4.4 Discussion

We applied the OSCeR strategy and our novel scaffolds to two clinically relevant conditions. For the *in vivo* bone regeneration study, we used a murine cranial defect model. It must be noted that it does resemble the skull bone of infants requiring cranioplasty. In our earlier studies in chapter 2, we found that biomaterial implantation was associated with spontaneous recruitment of autologous stem cells (both MSCs and HSCs). We were able to use this OSCeR phenomenon as a proof of concept to demonstrate the differentiation potential of the multipotent MSCs and HSCs recruited around the implant. It is also known that MSCs can differentiate into osteoblasts and osteocytes in the presence of inflammatory signals.[129, 176, 177] Hence by using our novel scaffolds delivering various cytokines we tried to enhance and

expedite the bone regenerative process. BMP-2 treatment has been a mainstay of bone regenerative studies. However, it is well understood that bone is a well vascularized tissue and hence we hypothesized that angiogenesis and thereby, pro-angiogenic conditions can play an important role in bone regeneration. Epo, a proangiogenic cytokine showed remarkable potency in recruiting mesenchymal stem cells and other progenitor cells in our preliminary studies. Importantly, it must be noted that Epo receptors are highly expressed and hence Epo has a significant impact on bone density in the first two weeks of bone injury.[125] It has also been shown to play a role in differentiating MSCs into osteoblasts.[178] Various treatment groups comprising of microbubble scaffolds loaded with Epo alone, BMP-2 alone or Epo and BMP-2 together were implanted in a 3 mm sized murine cranial defect model. OsteoSense 800 was injected locally around the cranial implantation site after 4 weeks. The bisphosphonate NIR dye binds to hydroxyapatite (HA) with high affinity and since HA is the mineral product of osteoblasts it serves as a good indicator for osteoblast activity.[179] We confirmed this by correlating the intensity from OsteoSense 800 which indicated osteoblast activity with the optical density from X-ray images; wherein, we found a strong correlation between the two parameters. Interestingly, we found that the scaffolds loaded with Epo showed very high OsteoSense 800 signal intensity, almost 2.5 times higher than untreated controls. While BMP-2 alone showed signs of HA based on the fluorescence signal, it was still lower than Epo. One plausible reason is that a lot of studies have found angiogenesis to be a precursor to osteogenesis.[128, 145] Also, Epo which shares functional and structural homologies with VEGF (another potent angiogenic cytokine) has been implicated in playing a critical role in endochondral ossification.[125] A recent study found that Epo can induce the differentiation of MSCs into osteoblasts and this could possible be the reason behind our current observations.[178] In addition, the same study suggested that Epo activates Jak-Stat signaling pathways in HSCs which leads to increased BMP-2 production and aids bone formation. Interestingly, although dual delivery of Epo and BMP-2 did not show the same effect based on our *in vivo* imaging

results, based on osteocalcin and osteopontin at the implant, it does suggest that dual delivery of Epo and BMP-2 does have some effect on osteogenic differentiation. Importantly, it must be noted that the immunofluorescence analysis was not done at the surface of the scaffold. Instead the presence of osteocalcin and osteopontin was confirmed almost half way into the scaffold. We found that Epo alone was potent as far as *in vivo* HA formation was concerned. This is in contrast to a previous study which suggested that delivering an angiogenic factor had no effect on bone formation at 4 and 12 weeks.[128] However, it must be noted that the same study found no significant difference between treatment groups at the end of 4 weeks, whereas in our studies here we have been able to see significant pro-osteogenic activity in atleast two of the treatment groups, namely Epo and Epo + BMP-2.

We performed histological and immunofluorescence analysis to analyze the internal matrix of the OSCeR scaffold. While the 3 mm sized defect in the cranium which did not receive any implant showed virtually no signs of healing, collagen matrix deposition was observed around and inside both Epo and Epo + BMP-2 scaffolds indicating bone healing and osteogenesis.[180] Interestingly, based on quantification of collagen staining intensity and distribution, there was no significant difference between Epo and Epo + BMP-2 groups, which does suggest that both the groups exerted and equally potent influence on the osteogenic differentiation of the stem cells that arrived at the implant site. Also, no adverse responses were observed around any of the groups. This observation was confirmed by the immunofluorescence analysis, wherein osteocalcin and osteopontin expression was studied and is indicative of osteogenic activity. High levels were observed for Epo + BMP-2 and Epo groups as compared to the moderate level of osteopontin in BMP-2 group. The untreated defects showed almost no activity in the gap as there was no scaffold to support the bridging of the gap. It must also be noted that we did see blood vessels around the implant site in the Epo + BMP-2 group and this finding agrees well with a recent study which found similar results when they delivered an angiogenic and osteogenic cytokine simultaneously.[128] However, it remains to

be determined whether these vessels are functional and newly formed. Our observation of BMP-2 group being significantly lower in pro-osteogenic activity emphasizes the importance of timing the delivery of the cytokines and will be given due consideration in future studies. Studies evaluating the regenerative process over 8 to 16 weeks and possibly long-term evaluation will also be conducted. The results from study will serve as a stepping stone towards future longer term studies using scaffolds, OSCeR technique and *in vivo* bone regeneration.

Another application of our OSCeR technique that we tried to explore was in cardiovascular tissue engineering. Our collaborating group, Dr. Jian Yang's Biomaterials and Tissue Engineering lab, have established a legacy of fabricating unique polymers suited for vascular graft tissue engineering. One such innovation has been CUPE, which when fabricated in the form of biphasic tubes has properties identical to native blood vessel. However, in order to make the material an effective vascular graft it was imperative that we develop strategies to alleviate concerns of thrombosis upon blood contact. One such strategy that has been widely suggested is the endothelialization of the vascular graft lumen.[51, 53, 54] The OSCeR phenomenon which is associated with stem cell recruitment around a biomaterial implant is not exclusive to the sub-cutaneous setting. It is also observed in the peritoneal space wherein, stem and progenitor cells are found around the implant.[78]

Common approaches to cellularize scaffolds rely on the artificial and limited *in vitro* techniques.[181, 182] Our lab has found that the peritoneal space serves as an abundant source of multipotent stem and progenitor cells. We employed the CUPE vascular grafts and took advantage of the OSCeR phenomenon to devise strategies to endothelialize the graft lumen. Based on our preliminary studies which found Epo to be a potent role player in stem and progenitor cell recruitment, we coated the CUPE grafts with Epo and implanted in the peritoneal space for various time points. Interestingly we found that within a week of implantation, the lumen of the CUPE grafts coated with Epo showed the presence of endothelial progenitor cells (EPCs). This agrees well with studies that have implicated Epo in EPC mobilization.[183, 184]

The fact that the EPCs were barely present in the lumen of the CUPE grafts with no Epo coating underlines the importance of the cytokine. Moreover, after 2 weeks the observation of both EPCs and endothelial cells in the lumen augurs well for future studies. A possible reason could be because Epo exerts its hematopoietic effects by stimulating the proliferation of early erythroid precursors and the differentiation of later precursors of the erythroid lineage.[185] Mature endothelial cells also express Epo receptors (Epo-R),[186] and Epo induces a proangiogenic response in cultivated mature endothelial cells by stimulation of endothelial cell proliferation, migration, endothelin-1 release, and increase in cytosolic-free calcium concentration.[187] It must be noted that merely based on appearance, the CUPE-Epo vascular grafts showed a more cellularized appearance on the exterior upon explantation after 2 weeks, as compared to the uncoated tubes. Moreover these grafts showed the presence of cells which stained positive for smooth muscle cells. Whether this was a consequence of Epo is yet to be determined.

CHAPTER 5

SUMMARY AND CONCLUSION

5.1 Summary

The ultimate goal of tissue engineering is to successfully blend the application of cells, scaffolds, signaling growth factors and bioreactor towards the therapeutic solution of a clinically relevant condition. It is imperative that we understand the behavior of cells and develop systems that can wield better control on their fate. This dissertation can be summarized as a collection of work that, firstly, brings forth a not so well understood phenomenon – that of spontaneous recruitment of multipotent stem and progenitor cells in response to a biomaterial implant. Second, we have developed a novel scaffold fabrication technique that can be used to deliver cytokines and growth factors. Importantly, the bioactivity of the released agent is preserved. Thirdly, we made use of the phenomenon of spontaneous stem/progenitor cell recruitment and applied it towards two clinically relevant conditions – bone defect and small diameter vascular graft tissue engineering. We call this process Orchestrated Stem Cell-based Regeneration (OSCeR).

The first aim focused on the phenomenon of spontaneous recruitment of stem and progenitor cells around an implant. Autologous stem cells are recognized as the best cells for stem cell therapy, although their recovery and culture is often difficult, time consuming and traumatic to the patients. To combat such challenges, we have recently uncovered that shortly after biomaterial implantation, following the recruitment of inflammatory cells, substantial numbers of mesenchymal stem cells (MSC) and hematopoietic stem cells (HSC) were recruited to the implantation sites. These multipotent stem cells could be differentiated into various lineages *in vitro*. Inflammatory signals may be responsible for the gathering of stem cells, since

there is a good relationship between biomaterial-mediated inflammatory responses and stem cell accumulation *in vivo*. In addition, the treatment with anti-inflammatory drug – dexamethasone – substantially reduced the recruitment of both MSC and HSC. When the implants were made to release an osteogenic factor - bone morphogenetic protein – 2, we found that the recruited stem cells quickly turned into osteoblasts and formed mineralized tissue in the subcutaneous soft tissue space. The results from this work in Aim 1 support that such novel implant-induced localized recruitment and differentiation of progenitor cells may permit the future development of autologous stem cell therapies without the need for tedious cell isolation, culture and transplantation.

The second aim emphasized on the development of a scaffold system that can deliver bioactive growth factors and facilitate *in vivo* tissue engineering. Polymeric tissue engineering scaffolds prepared by conventional techniques like salt leaching and phase separation are greatly limited by their poor biomolecule-delivery abilities. Conventional methods of incorporation of various growth factors, proteins and/or peptides on or in scaffold materials via different cross linking and conjugation techniques are often tedious and may affect scaffold physical, chemical, and mechanical properties. To overcome such deficiencies, a novel two-step porous scaffold fabrication procedure was created in which protein (both bovine serum albumin (BSA) and gelatin) microbubbles (MB) were used as porogen and growth factor carriers. Polymer solution mixed with MB was phase separated and then lyophilized to create porous scaffold. Interestingly, MB scaffold triggered substantially lesser inflammatory responses than salt leached and conventional phase separated scaffolds *in vivo*. Most importantly, the same technique was used to produce growth factor eluting porous scaffolds, simply by incorporating the growth factor loaded MB with polymer solution prior to phase separation. *In vitro* such scaffolds were able to promote cell growth to a much greater extent than scaffold soaked in growth factor confirming the bioactivity of the released growth factor. Furthermore, such MB-growth factor scaffolds elicited a specific response in the surrounding tissue *in vivo*.

In the third aim, this novel growth factor eluting scaffold was applied towards healing a critical size defect in the bone. Using the cranial defect model in mice, it was shown that various growth factor releasing microbubble scaffolds can be used to deliver a range of single or combination of bioactive biomolecules to substantially promote osteogenic activity in degradable scaffold. Using a similar strategy, by employing a novel polyurethane small diameter vascular graft (SDVG) developed by Dr. Jian Yang's lab, we were able to conduct early stage studies for the endothelialization of SDVG lumen.

5.2 Conclusion

Implantation of a biomaterial is associated with an inflammatory response that varies according to the material type. Interestingly we found multipotent stem and progenitor cells along with the inflammatory cells. Importantly, the extent of the inflammatory response directly affected the number of stem and progenitor cells. Such stem cells could be differentiated into various mesenchymal lineages *in vitro*. Using osteogenic differentiation as a model, we were able to differentiate the spontaneously recruited cells into an osteogenic phenotype *in vivo* within a polymeric scaffold. Considering the recent progress in tissue engineering which places a lot of emphasis on cytokines and growth factors, and the understanding that there is no efficient tool to deliver them in a highly potent form, we fabricated a novel tissue engineering scaffold that could preserve the bioactivity of the loaded cytokines and release it over time. Such scaffolds were applied to an *in vivo* cranial defect model and studies showed that the application of such cytokine-loaded scaffolds at the critical size defect showed signs of healing and bridging of the gap. In addition, we also made use of the phenomenon of spontaneous recruitment of stem and progenitor cells and using selected cytokines endothelialized the lumen of a novel small diameter vascular graft.

CHAPTER 6

FUTURE DIRECTIONS

While this study does explore the phenomenon of spontaneous recruitment of stem and progenitor cells along with inflammatory cells at the site of biomaterial implantation, it is in no way the end of the road for research in this area. In fact, the results from this study mark the beginning of more emphasis that needs to be laid in several areas. Possible directions this work could push *in vivo* tissue engineering are suggested in this chapter.

Aim 1: While we have tried to evaluate the cellular response to biomaterials in the form of microspheres and scaffolds, there could be more studies focusing on the shape of the implant materials on cellular response. The effect of surface modification techniques and coatings on stem and progenitor cell response and behavior is another aspect that could be probed. It should be noted that the use of stem cells and what qualifies as a stem cell is highly debatable. After consulting with various acclaimed stem cell researchers, the cell surface markers were selected. However, several markers are still and will be known over time and can be used to determine the type and origin of the multipotent stem cells.

Aim 2: The microbubble scaffold fabrication technique that we have devised in our lab can be potentially applied to a wide range of polymers. In fact we have successfully adapted the technique to PLLA scaffolds. This will help design scaffolds with polymers that offer various features like better mechanical strength, cell adhesion properties etc., Similarly, various proteins and combinations of proteins can also be used to synthesize the microbubbles. Such proteins can potentially elicit a varying extent of cellular response.

Aim 3: Cranial defect was selected in order to test the effectiveness of the strategy developed in aims 1 and 2. Potentially, murine cranial defect healing studies can be clinically translated to suit the craniofacial defects in newborn babies and infants. We do believe that the

study can be extended to a femoral defect model, wherein such scaffold conduits can be used to guide bone regeneration without the extensive use of external fixations and braces for a prolonged period. In addition, more emphasis will be placed on controlling the timing of cytokine delivery at the defect site.

Significant amount of effort needs to be placed on the cardiovascular tissue engineering area. What we have done here is a small step towards developing a SDVG with good *in vivo* patency. We are currently evaluating numerous strategies to deliver EPC and EC recruiting cytokines and chemokines. One way is by pre-coating the lumen with collagen prior to Epo is being evaluated. In addition, following the implantation of such SDVGs, the peritoneum will be flushed and later injected with Epo to mobilize more cells. Another strategy involves the flushing the peritoneum at various time points, concentrating the cells in the peritoneal lavage and injecting them into the SDVG lumen. We are still developing a method to incorporate our novel protein microbubble-based scaffold fabrication technique with the CUPE biphasic SDVG. This will be a major research focus for this area and our future plans could be summarized as in figure 6.1.

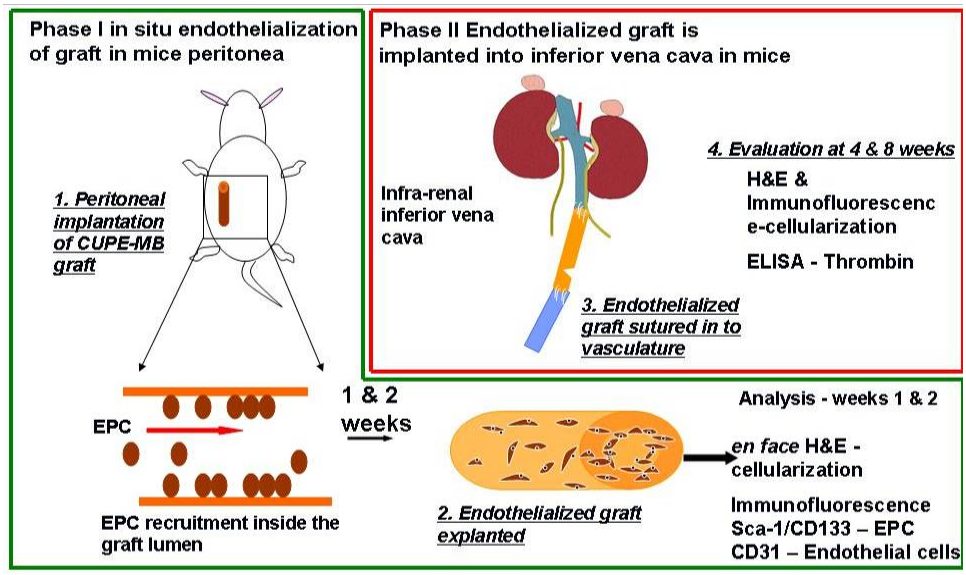

Figure 6.1 Schematic illustration of future study with CUPE-SDVG and microbubble scaffold technique.

REFERENCES

1. Nair, A., et al., *Species and density of implant surface chemistry affect the extent of foreign body reactions.* Langmuir, 2008. **24**(5): p. 2015-24.
2. Nair, A., et al., *Novel polymeric scaffolds using protein microbubbles as porogen and growth factor carriers.* Tissue Eng Part C Methods, 2010. **16**(1): p. 23-32.
3. Navarro, M. and A. Michiardi, *The challenge of combining cells, synthetic materials and growth factors to engineer bone tissue*. Tissue Engineering: Roles, Materials and Applications, ed. S.J. Barnes and L.P. Harris. 2008, New York Nova Science Publishers, Inc.
4. Lavik, E. and R. Langer, *Tissue engineering: current state and perspectives.* Appl Microbiol Biotechnol, 2004. **65**(1): p. 1-8.
5. Ho, M.H., et al., *Preparation of porous scaffolds by using freeze-extraction and freeze-gelation methods.* Biomaterials, 2004. **25**(1): p. 129-38.
6. Nam, Y.S. and T.G. Park, *Porous biodegradable polymeric scaffolds prepared by thermally induced phase separation.* J Biomed Mater Res, 1999. **47**(1): p. 8-17.
7. Ikada, Y., *Challenges in tissue engineering.* J R Soc Interface, 2006. **3**(10): p. 589-601.
8. Seitz, S., et al., *Influence of in vitro cultivation on the integration of cell-matrix constructs after subcutaneous implantation.* Tissue Eng, 2007. **13**(5): p. 1059-67.
9. Mikos, A.G., et al., *Engineering complex tissues.* Tissue Eng, 2006. **12**(12): p. 3307-39.
10. Tessmar, J.K. and A.M. Gopferich, *Matrices and scaffolds for protein delivery in tissue engineering.* Adv Drug Deliv Rev, 2007. **59**(4-5): p. 274-91.
11. Blunk, T., et al., *Differential effects of growth factors on tissue-engineered cartilage.* Tissue Eng, 2002. **8**(1): p. 73-84.
12. Mann, B.K., R.H. Schmedlen, and J.L. West, *Tethered-TGF-beta increases extracellular matrix production of vascular smooth muscle cells.* Biomaterials, 2001. **22**(5): p. 439-44.
13. Murphy, W.L., et al., *Sustained release of vascular endothelial growth factor from mineralized poly(lactide-co-glycolide) scaffolds for tissue engineering.* Biomaterials, 2000. **21**(24): p. 2521-7.
14. Spector, M., *Biomaterials-based tissue engineering and regenerative medicine solutions to musculoskeletal problems.* Swiss Med Wkly, 2006. **136**(19-20): p. 293-301.
15. Mazzini, L., et al., *Autologous mesenchymal stem cells: clinical applications in amyotrophic lateral sclerosis.* Neurol Res, 2006. **28**(5): p. 523-6.
16. Mitchell, J.B., et al., *Immunophenotype of human adipose-derived cells: temporal changes in stromal-associated and stem cell-associated markers.* Stem Cells, 2006. **24**(2): p. 376-85.
17. Romanov, Y.A., V.A. Svintsitskaya, and V.N. Smirnov, *Searching for alternative sources of postnatal human mesenchymal stem cells: candidate MSC-like cells from umbilical cord.* Stem Cells, 2003. **21**(1): p. 105-10.
18. Nauta, A.J., et al., *Donor-derived mesenchymal stem cells are immunogenic in an allogeneic host and stimulate donor graft rejection in a nonmyeloablative setting.* Blood, 2006. **108**(6): p. 2114-20.
19. Swijnenburg, R.J., et al., *Immunosuppressive therapy mitigates immunological rejection of human embryonic stem cell xenografts.* Proc Natl Acad Sci U S A, 2008. **105**(35): p. 12991-6.
20. Gang, E.J., et al., *SSEA-4 identifies mesenchymal stem cells from bone marrow.* Blood, 2007. **109**(4): p. 1743-51.

21. Li, T.S., et al., *Regeneration of infarcted myocardium by intramyocardial implantation of ex vivo transforming growth factor-beta-preprogrammed bone marrow stem cells.* Circulation, 2005. **111**(19): p. 2438-45.
22. Loebinger, M.R., S. Aguilar, and S.M. Janes, *Therapeutic potential of stem cells in lung disease: progress and pitfalls.* Clin Sci (Lond), 2008. **114**(2): p. 99-108.
23. Caplan, A.I., *Review: mesenchymal stem cells: cell-based reconstructive therapy in orthopedics.* Tissue Eng, 2005. **11**(7-8): p. 1198-211.
24. Diao, H., et al., *Improved cartilage regeneration utilizing mesenchymal stem cells in TGF-beta1 gene-activated scaffolds.* Tissue Eng Part A, 2009. **15**(9): p. 2687-98.
25. Winkler, T., et al., *Dose-response relationship of mesenchymal stem cell transplantation and functional regeneration after severe skeletal muscle injury in rats.* Tissue Eng Part A, 2009. **15**(3): p. 487-92.
26. Takahashi, K. and S. Yamanaka, *Induction of pluripotent stem cells from mouse embryonic and adult fibroblast cultures by defined factors.* Cell, 2006. **126**(4): p. 663-76.
27. Takahashi, K., et al., *Induction of pluripotent stem cells from fibroblast cultures.* Nat Protoc, 2007. **2**(12): p. 3081-9.
28. Takahashi, K., et al., *Induction of pluripotent stem cells from adult human fibroblasts by defined factors.* Cell, 2007. **131**(5): p. 861-72.
29. Liu, H., et al., *Generation of induced pluripotent stem cells from adult rhesus monkey fibroblasts.* Cell Stem Cell, 2008. **3**(6): p. 587-90.
30. Wu, Z., et al., *Generation of pig induced pluripotent stem cells with a drug-inducible system.* J Mol Cell Biol, 2009. **1**(1): p. 46-54.
31. Li, W., et al., *Generation of rat and human induced pluripotent stem cells by combining genetic reprogramming and chemical inhibitors.* Cell Stem Cell, 2009. **4**(1): p. 16-9.
32. Liao, J., et al., *Generation of induced pluripotent stem cell lines from adult rat cells.* Cell Stem Cell, 2009. **4**(1): p. 11-5.
33. Korbling, M. and Z. Estrov, *Adult stem cells for tissue repair - a new therapeutic concept?* N Engl J Med, 2003. **349**(6): p. 570-82.
34. Cohen, Y. and A. Nagler, *Umbilical cord blood transplantation--how, when and for whom?* Blood Rev, 2004. **18**(3): p. 167-79.
35. Rocha, V., et al., *Transplants of umbilical-cord blood or bone marrow from unrelated donors in adults with acute leukemia.* N Engl J Med, 2004. **351**(22): p. 2276-85.
36. Sanz, M.A., *Cord-blood transplantation in patients with leukemia--a real alternative for adults.* N Engl J Med, 2004. **351**(22): p. 2328-30.
37. Jiang, Y., et al., *Pluripotency of mesenchymal stem cells derived from adult marrow.* Nature, 2002. **418**(6893): p. 41-9.
38. Badiavas, E.V., et al., *Participation of bone marrow derived cells in cutaneous wound healing.* J Cell Physiol, 2003. **196**(2): p. 245-50.
39. Zuk, P.A., et al., *Multilineage cells from human adipose tissue: implications for cell-based therapies.* Tissue Eng, 2001. **7**(2): p. 211-28.
40. Noth, U., et al., *Multilineage mesenchymal differentiation potential of human trabecular bone-derived cells.* J Orthop Res, 2002. **20**(5): p. 1060-9.
41. Caplan, A.I., *Mesenchymal stem cells.* J Orthop Res, 1991. **9**(5): p. 641-50.
42. Sanchez-Ramos, J., et al., *Adult bone marrow stromal cells differentiate into neural cells in vitro.* Exp Neurol, 2000. **164**(2): p. 247-56.
43. Lee, K.D., et al., *In vitro hepatic differentiation of human mesenchymal stem cells.* Hepatology, 2004. **40**(6): p. 1275-84.
44. Cha, J. and V. Falanga, *Stem cells in cutaneous wound healing.* Clin Dermatol, 2007. **25**(1): p. 73-8.

45. Montesinos, J.J., et al., *Human mesenchymal stromal cells from adult and neonatal sources: comparative analysis of their morphology, immunophenotype, differentiation patterns and neural protein expression.* Cytotherapy, 2009. **11**(2): p. 163-76.
46. Horwitz, E.M., et al., *Isolated allogeneic bone marrow-derived mesenchymal cells engraft and stimulate growth in children with osteogenesis imperfecta: Implications for cell therapy of bone.* Proc Natl Acad Sci U S A, 2002. **99**(13): p. 8932-7.
47. Horwitz, E.M., et al., *Clinical responses to bone marrow transplantation in children with severe osteogenesis imperfecta.* Blood, 2001. **97**(5): p. 1227-31.
48. Koc, O.N., et al., *Rapid hematopoietic recovery after coinfusion of autologous-blood stem cells and culture-expanded marrow mesenchymal stem cells in advanced breast cancer patients receiving high-dose chemotherapy.* J Clin Oncol, 2000. **18**(2): p. 307-16.
49. Kamath, S., et al., *Surface chemistry influences implant-mediated host tissue responses.* J Biomed Mater Res A, 2008. **86**(3): p. 617-26.
50. Jang, S., et al., *Functional neural differentiation of human adipose tissue-derived stem cells using bFGF and forskolin.* BMC Cell Biol, 2010. **11**: p. 25.
51. Kim, S. and H. von Recum, *Endothelial stem cells and precursors for tissue engineering: cell source, differentiation, selection, and application.* Tissue Eng Part B Rev, 2008. **14**(1): p. 133-47.
52. Dey, J., et al., *Development of biodegradable crosslinked urethane-doped polyester elastomers.* Biomaterials, 2008. **29**(35): p. 4637-49.
53. Mitchell, S.L. and L.E. Niklason, *Requirements for growing tissue-engineered vascular grafts.* Cardiovasc Pathol, 2003. **12**(2): p. 59-64.
54. Seifalian, A.M., et al., *Improving the clinical patency of prosthetic vascular and coronary bypass grafts: the role of seeding and tissue engineering.* Artif Organs, 2002. **26**(4): p. 307-20.
55. Hu, W.J., et al., *Molecular basis of biomaterial-mediated foreign body reactions.* Blood, 2001. **98**(4): p. 1231-8.
56. Blanco, E., et al., *Local release of dexamethasone from polymer millirods effectively prevents fibrosis after radiofrequency ablation.* J Biomed Mater Res A, 2006. **76**(1): p. 174-82.
57. Hickey, T., et al., *In vivo evaluation of a dexamethasone/PLGA microsphere system designed to suppress the inflammatory tissue response to implantable medical devices.* J Biomed Mater Res, 2002. **61**(2): p. 180-7.
58. Patil, S.D., F. Papadimitrakopoulos, and D.J. Burgess, *Dexamethasone-loaded poly(lactic-co-glycolic) acid microspheres/poly(vinyl alcohol) hydrogel composite coatings for inflammation control.* Diabetes Technol Ther, 2004. **6**(6): p. 887-97.
59. Kretlow, J.D., et al., *Donor age and cell passage affects differentiation potential of murine bone marrow-derived stem cells.* BMC Cell Biol, 2008. **9**: p. 60.
60. Nguyen, K.T., et al., *Studies of the cellular uptake of hydrogel nanospheres and microspheres by phagocytes, vascular endothelial cells, and smooth muscle cells.* J Biomed Mater Res A, 2009. **88**(4): p. 1022-30.
61. Gao, J., et al., *Self-association of hydroxypropyl cellulose in water.* Macromolecules, 2001. **34**: p. 2242.
62. Lu, X.H., Z.B. Hu, and J. Gao, *Synthesis and light scattering study of hydroxypropyl cellulose microgels.* Macromolecules, 2000. **33**: p. 8698.
63. Chen, J.L., C.H. Chiang, and M.K. Yeh, *The mechanism of PLA microparticle formation by water-in-oil-in-water solvent evaporation method.* J Microencapsul, 2002. **19**(3): p. 333-46.
64. Thevenot, P., et al., *Method to analyze three-dimensional cell distribution and infiltration in degradable scaffolds.* Tissue Eng Part C Methods, 2008. **14**(4): p. 319-31.

65. Imitola, J., et al., *Directed migration of neural stem cells to sites of CNS injury by the stromal cell-derived factor 1alpha/CXC chemokine receptor 4 pathway.* Proc Natl Acad Sci U S A, 2004. **101**(52): p. 18117-22.
66. Mourkioti, F. and N. Rosenthal, *IGF-1, inflammation and stem cells: interactions during muscle regeneration.* Trends Immunol, 2005. **26**(10): p. 535-42.
67. Wang, C.H., W.J. Cherng, and S. Verma, *Drawbacks to stem cell therapy in cardiovascular diseases.* Future Cardiol, 2008. **4**(4): p. 399-408.
68. Grinnemo, K.H., et al., *Human embryonic stem cells are immunogenic in allogeneic and xenogeneic settings.* Reprod Biomed Online, 2006. **13**(5): p. 712-24.
69. Cho, K.A., et al., *Mesenchymal stem cells showed the highest potential for the regeneration of injured liver tissue compared with other subpopulations of the bone marrow.* Cell Biol Int, 2009. **33**(7): p. 772-7.
70. Kode, J.A., et al., *Mesenchymal stem cells: immunobiology and role in immunomodulation and tissue regeneration.* Cytotherapy, 2009. **11**(4): p. 377-91.
71. Moioli, E.K., et al., *Synergistic actions of hematopoietic and mesenchymal stem/progenitor cells in vascularizing bioengineered tissues.* PLoS One, 2008. **3**(12): p. e3922.
72. Bucala, R., et al., *Circulating fibrocytes define a new leukocyte subpopulation that mediates tissue repair.* Mol Med, 1994. **1**(1): p. 71-81.
73. Chamberlain, G., et al., *Concise review: mesenchymal stem cells: their phenotype, differentiation capacity, immunological features, and potential for homing.* Stem Cells, 2007. **25**(11): p. 2739-49.
74. da Silva Meirelles, L., A.I. Caplan, and N.B. Nardi, *In search of the in vivo identity of mesenchymal stem cells.* Stem Cells, 2008. **26**(9): p. 2287-99.
75. Dominici, M., et al., *Minimal criteria for defining multipotent mesenchymal stromal cells. The International Society for Cellular Therapy position statement.* Cytotherapy, 2006. **8**(4): p. 315-7.
76. Horwitz, E.M., et al., *Clarification of the nomenclature for MSC: The International Society for Cellular Therapy position statement.* Cytotherapy, 2005. **7**(5): p. 393-5.
77. Meirelles Lda, S., et al., *Mechanisms involved in the therapeutic properties of mesenchymal stem cells.* Cytokine Growth Factor Rev, 2009. **20**(5-6): p. 419-27.
78. Vranken, I., et al., *The recruitment of primitive Lin(-) Sca-1(+), CD34(+), c-kit(+) and CD271(+) cells during the early intraperitoneal foreign body reaction.* Biomaterials, 2008. **29**(7): p. 797-808.
79. Weissman, I.L. and J.A. Shizuru, *The origins of the identification and isolation of hematopoietic stem cells, and their capability to induce donor-specific transplantation tolerance and treat autoimmune diseases.* Blood, 2008. **112**(9): p. 3543-53.
80. Wong, S.H., et al., *Evaluation of Sca-1 and c-Kit as selective markers for muscle remodelling by nonhemopoietic bone marrow cells.* Stem Cells, 2007. **25**(6): p. 1364-74.
81. Gimble, J.M., A.J. Katz, and B.A. Bunnell, *Adipose-derived stem cells for regenerative medicine.* Circ Res, 2007. **100**(9): p. 1249-60.
82. Anjos-Afonso, F. and D. Bonnet, *Nonhematopoietic/endothelial SSEA-1+ cells define the most primitive progenitors in the adult murine bone marrow mesenchymal compartment.* Blood, 2007. **109**(3): p. 1298-306.
83. Benzhi, C., et al., *Bone marrow mesenchymal stem cells upregulate transient outward potassium currents in postnatal rat ventricular myocytes.* J Mol Cell Cardiol, 2009. **47**(1): p. 41-8.
84. Chavakis, E., C. Urbich, and S. Dimmeler, *Homing and engraftment of progenitor cells: a prerequisite for cell therapy.* J Mol Cell Cardiol, 2008. **45**(4): p. 514-22.

85. Chang, J.K., et al., *Effects of anti-inflammatory drugs on proliferation, cytotoxicity and osteogenesis in bone marrow mesenchymal stem cells.* Biochem Pharmacol, 2007. **74**(9): p. 1371-82.
86. Schroter, A., et al., *High-dose corticosteroids after spinal cord injury reduce neural progenitor cell proliferation.* Neuroscience, 2009. **161**(3): p. 753-63.
87. Maurer, M. and E. von Stebut, *Macrophage inflammatory protein-1.* Int J Biochem Cell Biol, 2004. **36**(10): p. 1882-6.
88. Murdoch, C. and A. Finn, *Chemokine receptors and their role in inflammation and infectious diseases.* Blood, 2000. **95**(10): p. 3032-43.
89. Suh, W., et al., *Transplantation of endothelial progenitor cells accelerates dermal wound healing with increased recruitment of monocytes/macrophages and neovascularization.* Stem Cells, 2005. **23**(10): p. 1571-8.
90. Lord, B.I., et al., *Mobilization of early hematopoietic progenitor cells with BB-10010: a genetically engineered variant of human macrophage inflammatory protein-1 alpha.* Blood, 1995. **85**(12): p. 3412-5.
91. Pelus, L.M. and S. Fukuda, *Peripheral blood stem cell mobilization: the CXCR2 ligand GRObeta rapidly mobilizes hematopoietic stem cells with enhanced engraftment properties.* Exp Hematol, 2006. **34**(8): p. 1010-20.
92. Zhang, F., et al., *Transforming growth factor-beta promotes recruitment of bone marrow cells and bone marrow-derived mesenchymal stem cells through stimulation of MCP-1 production in vascular smooth muscle cells.* J Biol Chem, 2009. **284**(26): p. 17564-74.
93. Wu, Y., et al., *Bone marrow-derived stem cells in wound healing: a review.* Wound Repair Regen, 2007. **15 Suppl 1**: p. S18-26.
94. Dudek, A.Z., et al., *Platelet factor 4 promotes adhesion of hematopoietic progenitor cells and binds IL-8: novel mechanisms for modulation of hematopoiesis.* Blood, 2003. **101**(12): p. 4687-94.
95. Zhang, J., et al., *Platelet factor 4 enhances the adhesion of normal and leukemic hematopoietic stem/progenitor cells to endothelial cells.* Leuk Res, 2004. **28**(6): p. 631-8.
96. Glennie, S., et al., *Bone marrow mesenchymal stem cells induce division arrest anergy of activated T cells.* Blood, 2005. **105**(7): p. 2821-7.
97. Thevenot, P.T., et al., *The effect of incorporation of SDF-1alpha into PLGA scaffolds on stem cell recruitment and the inflammatory response.* Biomaterials, 2010. **31**(14): p. 3997-4008.
98. Chen, L., et al., *Paracrine factors of mesenchymal stem cells recruit macrophages and endothelial lineage cells and enhance wound healing.* PLoS One, 2008. **3**(4): p. e1886.
99. Huang, Q., et al., *In vivo mesenchymal cell recruitment by a scaffold loaded with transforming growth factor beta1 and the potential for in situ chondrogenesis.* Tissue Eng, 2002. **8**(3): p. 469-82.
100. Sahoo, S., et al., *Characterization of a novel polymeric scaffold for potential application in tendon/ligament tissue engineering.* Tissue Eng, 2006. **12**(1): p. 91-9.
101. Nam, Y.S. and T.G. Park, *Biodegradable polymeric microcellular foams by modified thermally induced phase separation method.* Biomaterials, 1999. **20**(19): p. 1783-90.
102. Tu, C., et al., *The fabrication and characterization of Poly(lactic) acid scaffolds for tissue engineering by improved solid-liquid phase separation. .* Polymers for Advanced Technologies, 2003. **14**: p. 565.
103. Yang, S., et al., *The design of scaffolds for use in tissue engineering. Part I. Traditional factors.* Tissue Eng, 2001. **7**(6): p. 679-89.
104. Sales, V.L., et al., *Protein precoating of elastomeric tissue-engineering scaffolds increased cellularity, enhanced extracellular matrix protein production, and differentially regulated the phenotypes of circulating endothelial progenitor cells.* Circulation, 2007. **116**(11 Suppl): p. I55-63.

105. Eley, J.G. and P. Mathew, *Preparation and release characteristics of insulin and insulin-like growth factor-one from polymer nanoparticles.* J Microencapsul, 2007. **24**(3): p. 225-34.
106. Fransson, J., D. Hallen, and E. Florin-Robertsson, *Solvent effects on the solubility and physical stability of human insulin-like growth factor I.* Pharm Res, 1997. **14**(5): p. 606-12.
107. van de Weert, M., W.E. Hennink, and W. Jiskoot, *Protein instability in poly(lactic-co-glycolic acid) microparticles.* Pharm Res, 2000. **17**(10): p. 1159-67.
108. Klibanov, A.L., *Targeted delivery of gas-filled microspheres, contrast agents for ultrasound imaging.* Adv Drug Deliv Rev, 1999. **37**(1-3): p. 139-157.
109. Frenkel, P.A., et al., *DNA-loaded albumin microbubbles enhance ultrasound-mediated transfection in vitro.* Ultrasound Med Biol, 2002. **28**(6): p. 817-22.
110. Newman, C.M. and T. Bettinger, *Gene therapy progress and prospects: ultrasound for gene transfer.* Gene Ther, 2007. **14**(6): p. 465-75.
111. Cechowska-Pasko, M., J. Palka, and E. Bankowski, *Glucose-depleted medium reduces the collagen content of human skin fibroblast cultures.* Mol Cell Biochem, 2007. **305**(1-2): p. 79-85.
112. Froesch, E.R., et al., *Actions of insulin-like growth factors.* Annu Rev Physiol, 1985. **47**: p. 443-67.
113. Yoshinouchi, M. and R. Baserga, *The role of the IGF-1 receptor in the stimulation of cells by short pulses of growth factors.* Cell Prolif, 1993. **26**(2): p. 139-46.
114. Abramoff, M.D., P.J. Magelhaes, and S.J. Ram, *Image processing with ImageJ.* Biophotonics International, 2004. **11**: p. 36.
115. Yang, J., et al., *Fabrication and surface modification of macroporous poly(L-lactic acid) and poly(L-lactic-co-glycolic acid) (70/30) cell scaffolds for human skin fibroblast cell culture.* J Biomed Mater Res, 2002. **62**(3): p. 438-46.
116. Bryant, S.J. and K.S. Anseth, *The effects of scaffold thickness on tissue engineered cartilage in photocrosslinked poly(ethylene oxide) hydrogels.* Biomaterials, 2001. **22**(6): p. 619-26.
117. Tabata, Y., A. Nagano, and Y. Ikada, *Biodegradation of hydrogel carrier incorporating fibroblast growth factor.* Tissue Eng, 1999. **5**(2): p. 127-38.
118. Whang, K., et al., *Ectopic bone formation via rhBMP-2 delivery from porous bioabsorbable polymer scaffolds.* J Biomed Mater Res, 1998. **42**(4): p. 491-9.
119. Jakobsen, J.A., et al., *Safety of ultrasound contrast agents.* Eur Radiol, 2005. **15**(5): p. 941-5.
120. Porter, T.R. and F. Xie, *Visually discernible myocardial echocardiographic contrast after intravenous injection of sonicated dextrose albumin microbubbles containing high molecular weight, less soluble gases.* J Am Coll Cardiol, 1995. **25**(2): p. 509-15.
121. Woo, K.M., V.J. Chen, and P.X. Ma, *Nano-fibrous scaffolding architecture selectively enhances protein adsorption contributing to cell attachment.* J Biomed Mater Res A, 2003. **67**(2): p. 531-7.
122. Kurita, R., et al., *Biocompatible glucose sensor prepared by modifying protein and vinylferrocene monomer composite membrane.* Biosens Bioelectron, 2004. **20**(3): p. 518-23.
123. Tang, L. and J.W. Eaton, *Fibrin(ogen) mediates acute inflammatory responses to biomaterials.* J Exp Med, 1993. **178**(6): p. 2147-56.
124. Westenbrink, B.D., et al., *Erythropoietin improves cardiac function through endothelial progenitor cell and vascular endothelial growth factor mediated neovascularization.* Eur Heart J, 2007. **28**(16): p. 2018-27.

125. Holstein, J.H., et al., *Erythropoietin (EPO): EPO-receptor signaling improves early endochondral ossification and mechanical strength in fracture healing.* Life Sci, 2007. **80**(10): p. 893-900.
126. Maquet, V. and R. Jerome, *Design of macroporous biodegradable scaffolds for cell transplantation.* Materials Science Forum, 1997. **250**.
127. Braddock, M., et al., *Born again bone: tissue engineering for bone repair.* News Physiol Sci, 2001. **16**: p. 208-13.
128. Patel, Z.S., et al., *Dual delivery of an angiogenic and an osteogenic growth factor for bone regeneration in a critical size defect model.* Bone, 2008. **43**(5): p. 931-40.
129. Mountziaris, P.M. and A.G. Mikos, *Modulation of the Inflammatory Response for Enhanced Bone Tissue Regeneration.* Tissue Eng Part B Rev, 2008.
130. Huang, Y.C., et al., *Bone regeneration in a rat cranial defect with delivery of PEI-condensed plasmid DNA encoding for bone morphogenetic protein-4 (BMP-4).* Gene Ther, 2005. **12**(5): p. 418-26.
131. Oreffo, R.O. and J.T. Triffitt, *Future potentials for using osteogenic stem cells and biomaterials in orthopedics.* Bone, 1999. **25**(2 Suppl): p. 5S-9S.
132. Shih, Y.R., et al., *Growth of mesenchymal stem cells on electrospun type I collagen nanofibers.* Stem Cells, 2006. **24**(11): p. 2391-7.
133. Oliveira, J.M., et al., *Novel hydroxyapatite/chitosan bilayered scaffold for osteochondral tissue-engineering applications: Scaffold design and its performance when seeded with goat bone marrow stromal cells.* Biomaterials, 2006. **27**(36): p. 6123-37.
134. Awad, H.A., et al., *Chondrogenic differentiation of adipose-derived adult stem cells in agarose, alginate, and gelatin scaffolds.* Biomaterials, 2004. **25**(16): p. 3211-22.
135. Li, C., et al., *Silk apatite composites from electrospun fibers.* J Mater Res, 2005. **20**(12): p. 3211-3222.
136. Fisher, J.P., et al., *Soft and hard tissue response to photocrosslinked poly(propylene fumarate) scaffolds in a rabbit model.* J Biomed Mater Res, 2002. **59**(3): p. 547-56.
137. Bonewald, L.F. and G.R. Mundy, *Role of transforming growth factor-beta in bone remodeling.* Clin Orthop Relat Res, 1990(250): p. 261-76.
138. Wang, E.A., et al., *Bone morphogenetic protein-2 causes commitment and differentiation in C3H10T1/2 and 3T3 cells.* Growth Factors, 1993. **9**(1): p. 57-71.
139. Lutolf, M.P., et al., *Repair of bone defects using synthetic mimetics of collagenous extracellular matrices.* Nat Biotechnol, 2003. **21**(5): p. 513-8.
140. Chang, S.C., et al., *Cranial repair using BMP-2 gene engineered bone marrow stromal cells.* J Surg Res, 2004. **119**(1): p. 85-91.
141. Murakami, N., et al., *Repair of a proximal femoral bone defect in dogs using a porous surfaced prosthesis in combination with recombinant BMP-2 and a synthetic polymer carrier.* Biomaterials, 2003. **24**(13): p. 2153-9.
142. Mistry, A.S. and A.G. Mikos, *Tissue engineering strategies for bone regeneration.* Adv Biochem Eng Biotechnol, 2005. **94**: p. 1-22.
143. Geiger, F., et al., *Vascular endothelial growth factor gene-activated matrix (VEGF165-GAM) enhances osteogenesis and angiogenesis in large segmental bone defects.* J Bone Miner Res, 2005. **20**(11): p. 2028-35.
144. Richardson, T.P., et al., *Polymeric system for dual growth factor delivery.* Nat Biotechnol, 2001. **19**(11): p. 1029-34.
145. Huang, Y.C., et al., *Combined angiogenic and osteogenic factor delivery enhances bone marrow stromal cell-driven bone regeneration.* J Bone Miner Res, 2005. **20**(5): p. 848-57.
146. Kanczler, J.M. and R.O. Oreffo, *Osteogenesis and angiogenesis: the potential for engineering bone.* Eur Cell Mater, 2008. **15**: p. 100-14.

147. Kakudo, N., et al., *Immunolocalization of vascular endothelial growth factor on intramuscular ectopic osteoinduction by bone morphogenetic protein-2.* Life Sci, 2006. **79**(19): p. 1847-55.
148. Zhu, W., et al., *Localization of nitric oxide synthases during fracture healing.* J Bone Miner Res, 2002. **17**(8): p. 1470-7.
149. Brown, R.F., et al., *Growth and differentiation of osteoblastic cells on 13-93 bioactive glass fibers and scaffolds.* Acta Biomater, 2008. **4**(2): p. 387-96.
150. Cortizo, M.S., M.S. Molinuevo, and A.M. Cortizo, *Biocompatibility and biodegradation of polyester and polyfumarate based-scaffolds for bone tissue engineering.* J Tissue Eng Regen Med, 2008. **2**(1): p. 33-42.
151. Donzelli, E., et al., *Mesenchymal stem cells cultured on a collagen scaffold: In vitro osteogenic differentiation.* Arch Oral Biol, 2007. **52**(1): p. 64-73.
152. Na, K., et al., *Osteogenic differentiation of rabbit mesenchymal stem cells in thermo-reversible hydrogel constructs containing hydroxyapatite and bone morphogenic protein-2 (BMP-2).* Biomaterials, 2007. **28**(16): p. 2631-7.
153. Trombi, L., et al., *Good manufacturing practice-grade fibrin gel is useful as a scaffold for human mesenchymal stromal cells and supports in vitro osteogenic differentiation.* Transfusion, 2008. **48**(10): p. 2246-51.
154. Ignjatovic, N., et al., *Biphasic calcium phosphate coated with poly-D,L-lactide-co-glycolide biomaterial as a bone substitute.* Journal of the European Ceramin Society, 2007. **27**: p. 1589-1594.
155. Wu, Y.C., et al., *Bone tissue engineering evaluation based on rat calvaria stromal cells cultured on modified PLGA scaffolds.* Biomaterials, 2006. **27**(6): p. 896-904.
156. Fang, J., et al., *Stimulation of new bone formation by direct transfer of osteogenic plasmid genes.* Proc Natl Acad Sci U S A, 1996. **93**(12): p. 5753-8.
157. Hillig, W.B., et al., *An open-pored gelatin/hydroxyapatite composite as a potential bone substitute.* J Mater Sci Mater Med, 2008. **19**(1): p. 11-7.
158. Liu, X., et al., *Biomimetic nanofibrous gelatin/apatite composite scaffolds for bone tissue engineering.* Biomaterials, 2009. **30**(12): p. 2252-8.
159. Tabata, Y., et al., *Neovascularization effect of biodegradable gelatin microspheres incorporating basic fibroblast growth factor.* J Biomater Sci Polym Ed, 1999. **10**(1): p. 79-94.
160. Tabata, Y. and Y. Ikada, *Vascularization effect of basic fibroblast growth factor released from gelatin hydrogels with different biodegradabilities.* Biomaterials, 1999. **20**(22): p. 2169-75.
161. Winn, S.R., et al., *Tissue-engineered bone biomimetic to regenerate calvarial critical-sized defects in athymic rats.* J Biomed Mater Res, 1999. **45**(4): p. 414-21.
162. de Oliveira, R.S., et al., *Reconstruction of a large complex skull defect in a child: a case report and literature review.* Childs Nerv Syst, 2007. **23**(10): p. 1097-102.
163. Rosamond, W., et al., *Heart disease and stroke statistics--2008 update: a report from the American Heart Association Statistics Committee and Stroke Statistics Subcommittee.* Circulation, 2008. **117**(4): p. e25-146.
164. Siepe, M., et al., *Stem cells used for cardiovascular tissue engineering.* Eur J Cardiothorac Surg, 2008. **34**(2): p. 242-7.
165. Aird, W.C., *Phenotypic heterogeneity of the endothelium: II. Representative vascular beds.* Circ Res, 2007. **100**(2): p. 174-90.
166. Alsberg, E., H.A. von Recum, and M.J. Mahoney, *Environmental cues to guide stem cell fate decision for tissue engineering applications.* Expert Opin Biol Ther, 2006. **6**(9): p. 847-66.

167. Velazquez, O.C., *Angiogenesis and vasculogenesis: inducing the growth of new blood vessels and wound healing by stimulation of bone marrow-derived progenitor cell mobilization and homing.* J Vasc Surg, 2007. **45 Suppl A**: p. A39-47.
168. Asahara, T., et al., *VEGF contributes to postnatal neovascularization by mobilizing bone marrow-derived endothelial progenitor cells.* EMBO J, 1999. **18**(14): p. 3964-72.
169. Santhanam, A.V., et al., *Activation of endothelial nitric oxide synthase is critical for erythropoietin-induced mobilization of progenitor cells.* Peptides, 2008. **29**(8): p. 1451-5.
170. Klopsch, C., et al., *Intracardiac injection of erythropoietin induces stem cell recruitment and improves cardiac functions in a rat myocardial infarction model.* J Cell Mol Med, 2009. **13**(4): p. 664-79.
171. Campbell, J.H., J.L. Efendy, and G.R. Campbell, *Novel vascular graft grown within recipient's own peritoneal cavity.* Circ Res, 1999. **85**(12): p. 1173-8.
172. Kretschmer, G., et al., *[Sparks grafts as arterial substitutes in the femoro-popliteal region with a postoperative follow-up of up to 54 months].* Helv Chir Acta, 1981. **48**(1-2): p. 243-50.
173. Simmons, P., T.J. Fogarty, and J.P. Pennell, *Nineteen months clinical experience with the Sparks mandril graft.* J Am Assoc Nephrol Nurses Tech, 1975. **2**(3): p. 120-3.
174. Yang, J., et al., *Novel biphasic elastomeric scaffold for small-diameter blood vessel tissue engineering.* Tissue Eng, 2005. **11**(11-12): p. 1876-86.
175. Dey, J., et al., *Crosslinked urethane doped polyester biphasic scaffolds: Potential for in vivo vascular tissue engineering.* J Biomed Mater Res A, 2010. **95**(2): p. 361-70.
176. Heino, T.J. and T.A. Hentunen, *Differentiation of osteoblasts and osteocytes from mesenchymal stem cells.* Curr Stem Cell Res Ther, 2008. **3**(2): p. 131-45.
177. Siddappa, R., et al., *The response of human mesenchymal stem cells to osteogenic signals and its impact on bone tissue engineering.* Curr Stem Cell Res Ther, 2007. **2**(3): p. 209-20.
178. Shiozawa, Y., et al., *Erythropoietin couples hematopoiesis with bone formation.* PLoS One. **5**(5): p. e10853.
179. Zilberman, Y., et al., *Fluorescence molecular tomography enables in vivo visualization and quantification of nonunion fracture repair induced by genetically engineered mesenchymal stem cells.* J Orthop Res, 2008. **26**(4): p. 522-30.
180. Hou, L.T., et al., *Tissue engineering bone formation in novel recombinant human bone morphogenic protein 2-atelocollagen composite scaffolds.* J Periodontol, 2007. **78**(2): p. 335-43.
181. De Visscher, G., et al., *In vivo cellularization of a cross-linked matrix by intraperitoneal implantation: a new tool in heart valve tissue engineering.* Eur Heart J, 2007. **28**(11): p. 1389-96.
182. Rabkin, E. and F.J. Schoen, *Cardiovascular tissue engineering.* Cardiovasc Pathol, 2002. **11**(6): p. 305-17.
183. Heeschen, C., et al., *Erythropoietin is a potent physiologic stimulus for endothelial progenitor cell mobilization.* Blood, 2003. **102**(4): p. 1340-6.
184. Tousoulis, D., et al., *Role of inflammation and oxidative stress in endothelial progenitor cell function and mobilization: therapeutic implications for cardiovascular diseases.* Atherosclerosis, 2008. **201**(2): p. 236-47.
185. Krantz, S.B., *Erythropoietin.* Blood, 1991. **77**(3): p. 419-34.
186. Anagnostou, A., et al., *Erythropoietin receptor mRNA expression in human endothelial cells.* Proc Natl Acad Sci U S A, 1994. **91**(9): p. 3974-8.
187. Vogel, V., et al., *Effects of erythropoietin on endothelin-1 synthesis and the cellular calcium messenger system in vascular endothelial cells.* Am J Hypertens, 1997. **10**(3): p. 289-96.

BIOGRAPHICAL INFORMATION

Ashwin Nair completed his Bachelor's Degree in Instrumentation Engineering at the University of Mumbai (Bombay), India. He began work on his M.S. in Biomedical Engineering under the aegis of Dr. Liping Tang wherein he successfully devised a novel scaffold fabrication technique employing protein microbubbles. During his tenure at the Regenerative Medicine and Bioimaging lab his initial work focused on modulating the inflammatory responses to implanted biomaterials. After briefly working on nanoparticles and drug delivery systems, he worked with Dr. Tang in uncovering the phenomenon of biomaterial mediated stem cell recruitment and its dependence on inflammatory signals. He then extended his early work on scaffolds and blended it with this phenomenon to potentially apply it to clinically relevant conditions.